# REMOTE WATER QUALITY ASSESSMENT OF AN INLAND LAKE BEFORE AND DURING AN ARMED CONFLICT:

# A CASE STUDY (LAKE QATTINAH, SYRIA)

By

Lady Lee C. Dimapilis

Submitted to Central European University

Department of Environmental Sciences and Policy

In partial fulfilment of the requirements for the degree of Master of Science in Environmental Sciences, Policy and Management (MESPOM)



Supervisor: Professor Viktor Lagutov

Budapest, Hungary

2021

**Erasmus Mundus Masters Course in Environmental Sciences, Policy and Management**

# MESPOM

*This thesis is submitted in fulfillment of the Master of Science degree awarded as a result of successful completion of the Erasmus Mundus Masters course in Environmental Sciences, Policy and Management (MESPOM) jointly operated by the University of the Aegean (Greece), Central European University (Hungary), Lund University (Sweden) and the University of Manchester (United Kingdom).*



**Supported by the European Commission's Erasmus Mundus Programme**

Education and Culture

Erasmus Mundus

## Notes on copyright and the ownership of intellectual property rights



(3) For bibliographic and reference purposes this thesis should be referred to as:

Dimapilis, LLC. 2021. *Remote Water Quality Assessment of an Inland Lake before and during an Armed Conflict: A Case Study (Lake Qattinah, Syria).* Master of Science thesis, Department of Environmental Sciences and Policy, Central European University, Budapest.

## Author's Declaration

No portion of the work referred to in the thesis has been submitted in support of an application for another degree or qualification of this or any other university or other institute of learning.

**Lady Lee C. Dimapilis**

# Abstract

The long-standing Syrian Civil War which began as an uprising in 2011 has brought severe economic and social and environmental impacts in the country. One of the key environmental areas that require attention is the state of its limited water resources, particularly water quality which remains understudied due to lack of access to in situ data. This study addressed this research gap by utilizing remote sensing technology in the assessment of water quality (in terms of algal growth) of one of the most important waterbodies in the country – Lake Qattinah. Application of chlorophyll-a retrieval models revealed spatiotemporal patterns of algae characterized by relatively low algal concentrations in all seasons from 2013 to 2015, general increase and appearance of extremely high concentrations in certain areas of the lake beginning in 2016 , and decline from 2017 to 2020. These decreases and increases which imply degradation and improvement of water quality, respectively, were found to be driven by the changes in the magnitude of surrounding human activities influenced by the war.

The findings from this study can help in making better informed decisions on the management of Qattinah Lake. Moreover, as it provides quantitative and qualitative data on the algal dynamics in in an entire water body over a long period of time, it may serve as a framework for further research related both water quality and armed conflict. In practical terms, the methodological approach of this study can be adapted for the assessment of other remote and inaccessible inland lakes and reservoirs.



**Keywords: remote sensing, water quality, algae growth, chlorophyll-a, armed conflict**

# Table of Contents

# List of Figures

# List of Tables

# INTRODUCTION

Freshwater resources such as rivers, lakes and reservoirs provide a wide range of benefits and services vital to life. These include provision of water for consumption, energy production and natural hazard regulation among many others. However, these water bodies have been subjected to intense anthropogenic pressures like overextraction and pollution. Such pressures can threaten human and animal health, reduce the productivity and diversity of the ecosystems, and bring damage to agriculture, industries, aquaculture and other human activities relying on the water body. Lakes and reservoirs undergo a highly accelerated process of eutrophication driven by anthropogenic activities that discharge excessive nutrients to the water bodies, thereby causing degradation of water quality. Population growth, food production (agriculture, animal operations and aquaculture), and energy production and consumption are among the main driving forces of the phenomenon (Glibert et al., 2005).

One of the symptoms of degrading water quality is the proliferation of algae in the surface of the water bodies. Suspended algae or phytoplankton, photosynthesizing organisms whose growth and productivity depends on the supply of nutrients, are important source of organic matter that support the food chain in freshwater ecosystems. However, its excessive amount in freshwater bodies leads to water quality deterioration. On the global scale, there has been demonstrated strong correlations between phosphorus nutrient input and phytoplankton production in freshwaters, and between total nitrogen input and phytoplankton in estuaries and marine waters (Anderson et al., 2002). Other relevant factors that drive algal blooms are algal species presence/abundance, water exchange, weather conditions, and presence of grazers (zooplanktons that feed on phytoplankton). Deteriorated water quality due to algal blooms is characterized by foul odors and tastes, deoxygenation of bottom waters, toxicity, fish kills and alterations in food web (Anderson et al., 2002; Brooks et al., 2016).

Measurement of chlorophyll-a concentration is a widely used alternative in measuring algal biomass in water bodies. Conventional measurement of algal concentration in waters involve rigorous data collection wherein samples of water are taken and measured in the laboratory. While it provides accurate measurement, it is expensive, time-consuming, and labor intensive. It becomes more challenging for remote and inaccessible areas including those subjected to an armed conflict. In this case, remote sensing technology offers a wide spatial and temporal range of data that can be used to assess water quality in areas where in situ data collection is not feasible and/or safe.

This study presents the case of the freshwater lake in Syria – Qattinah Lake. The country, located in the Middle East has been struggling with a long-standing civil war which started as an uprising against the government in 2011. Years of intense fighting has claimed thousands of lives and has caused massive destruction of infrastructures and affected provision of basic services, forcing majority of the population to leave their homes and seek refuge either in other parts of Syria or in neighboring countries such as Lebanon and Turkey. Other than these direct impacts, war also brings about environmental damages – a form of damage that receives less attention but can potentially bring major harm on the economy, public health, and peace itself (Gaafar, n.d.). This study focuses on one environmental aspect which is the water quality of one of the major water resources in the country – Qattinah Lake. It aims to see the spatial and temporal patterns of water quality degradation in the lake with focus on estimating algal concentration before and during the war. In addition, it aims to relate these patterns with the development of war by looking at the impact of the armed conflict on the polluting human activities that surround the lake.

## Significance of the study

Determination of appropriate management strategies and policies to apply on lakes and reservoirs require data on water quality parameters ideally acquired over a wide range of time and encompassing the entire lake. For the case of Syria, collection of field measurements and access to historical data is challenging due to accessibility and safety issues brought about by the ongoing war. The water resources in the country is scarce and have been subject to the negative impacts of human activities. One of the main issues is quality degradation which has been a known phenomenon prior to the war. Situated in the most productive region of the country, Qattinah Lake has been one of the main sources of water for important activities in the country such as agriculture and industries. This lake has been known to be highly polluted (Fanack Water, n.d.). However, there have been no studies assessing its water quality since the war began. This is understandable due to the inaccessibility of the area, thus limiting the collection of data in the lake. Remote sensing technology can offer a wide range of multi-temporal data that can aid the lack of access to in situ data. The use of this technology can fill the knowledge gap and provide an understanding on how the war has influenced this water resource.

This study will utilize remote sensing technology as a tool to fill the knowledge gap on the more recent impacts of the conflict on the quality of a particular lake. Understanding the spatial and temporal patterns of algae will provide important insights towards proper management of the lake especially now that the country is undergoing some rehabilitation efforts. This study will solely be based on freely available satellite data and completely independent of in situ data. With this, the methods and findings that will be developed in this study can be applied to other lakes or reservoirs that are currently inaccessible or those that lack historical and present data. This study will also present a perspective on the indirect impact of war in a water quality in the form of its influences to the pollution sources around the lake.

## Research Aims and Research Questions

This study aims to assess the water quality of Qattinah Lake prior to and during the war by utilizing remote sensing technology to estimate algal concentrations. It also seeks to find the war-related anthropogenic driving forces that influence the water quality patterns. With these, the following research questions (RQ) will be addressed:

RQ1) What are the spatial and temporal patterns in the water quality of Qattinah Lake before and during the Syrian Civil War, particularly from 2010 – 2020?

RQ2) How do these changes in water quality (in terms of algal concentrations) relate to the conflict situation?

The following specific questions will contribute towards answering this RQ1:

-Which satellite data is most suitable to apply to the study area considering the lake's size, timeframe of analysis?

-What well-established chlorophyll-a retrieval algorithms can be applied to the study area?

The following specific question will lead to answering RQ2:

-What are the main sources of pollution in the lake which are linked to the proliferation of phytoplankton or the increase in chlorophyll-a concentrations?

## Outline of the thesis

Chapter 1 provides an overview of water quality degradation as an alarming issue among freshwater resources, focusing on the proliferation of algae and how it can be measured. This chapter also presents the challenges in measurement of algal biomass especially in inaccessible and dangerous areas like Syria and provides an overview of how remote sensing technology can be a powerful tool in assessing water quality in inland lakes and reservoirs. It also presents the significance of this study, the aims and the research questions of this study.

Chapter 2 provides sufficient information on the background of the study area and the war in the country and establishes the importance of the water resource and the Orontes basin to the country. It then presents the development of the Syrian Civil War and its implications on the said resources. The second part discusses related theoretical concepts that are the basic blocks of this study. It also gives an overview of the current knowledge with regards to the use of remote sensing in analyzing water quality, particularly algal biomass.

Chapter 3 presents the methods employed to gain answers to the research questions and to achieve the research aims. It presents the selected satellite data appropriate based on factors such as public accessibility, data availability, capability to analyze small to medium sized lakes, and some technical specifications such as spectral configuration and revisit days. It also presents the selected chlorophyll-a retrieval models that is used in the analysis. Above all, this chapter discusses the actual processes employed to assess the water quality in Qattinah Lake.

Chapter 4 presents the results of the analysis done in Chapter 3. It reveals the spatial and temporal variations of algae in the lake prior to and during the war. It is structured into three main parts such as spatial and temporal patterns of chlorophyll-a 1) prior to the war based on MERIS and Landsat 5 data 2) from 2013 to 2016 as derived from Landsat 8 data, and 3) from 2017 to 2020 as derived from Sentinel 2 data. It presents all the estimated chlorophyll-a concentrations and organizes them according to season to reveal variability.

Chapter 5 discusses the generated results from Chapter 4 and finds connection between the obtained patterns and the events related to the war. It looks at how the human activities around the lake have been influenced by the war and relates them to the proliferation of algae in the study area. It also discusses certain aspects of the study including the limitations of the data and the analysis in general, and their implications to the generated findings.

Chapter 6 summarizes the entire thesis study and draws conclusions based on the findings of the analysis and review of literature.

# REVIEW OF RELATED LITERATURE

## Background of the study area

### The Syrian Civil War

The Syrian Civil war is one of the biggest and most brutal conflict in the Arab world (Qaddour, n.d.). Mohammed et al. (2019) tagged it as one of the most complicated in the recent history due to several factors involved such as ethnical and religious diversity, the complexity of the political and social structure., and multilateral foreign and regional factors. There were several participants in the conflict namely the Syrian government, Syrian Kurds, Islamic rebels, the Islamic State terrorist group, and rebel groups backed by Western interests. It was also joined by other countries including Iraq, Saudi Arabia, Iran, Russia, Turkey, Qatar and the US.

The war began as a peaceful uprising in the city of Deraa located in the southern Syria, close to the border with Lebanon, as protesters demanded the government to end corruption and the abuses among security forces (Ford, 2019) and to free political prisoners, and call for a variety of reforms (BBC News, 2019; The Syria Institute, n.d.). The government responded with violence, thereby arresting, and shooting protesters which then triggered violent unrest that quickly spread over other areas in the country (DLIFLC, 2019; Ford, 2019; Kılıç, 2018; The Syria Institute, n.d.). Military defectors started organizing an armed group to defend and later to overthrow the Assad government (The Syria Institute, n.d.) and in 2012, the events turned into a full-blown civil war. While it was triggered by the government violence in Deraa uprising, other driving forces leading to the war were suggested by various researchers. (Gaafar, n.d.) stipulated that poor environmental conditions have been a primary driving force to the conflict. These conditions include mismanagement of natural resources and waste, inadequacy of government's response to mining pollution, and the severity of drought in 2006 to 2010 which incurred damages to the agricultural sector, increased unemployment, amplified food insecurity and lead to mass migration from the eastern parts of Syria to major urban centers such as Damascus, Aleppo and Deraa (Mohammed et al., 2020). He also added that the combined increase in population growth rate and water scarcity imposed a higher risk to political instability. Ford (2019) suggested that discontent to the government's response to the drought as well as the possible contagion effect of the Arab Spring revolts in nearby countries of Tunisia and Egypt could have also contributed. Other group of scholars claim that the economic and social governmental policies prior to the war are the main roots (Mohammed et al., 2020).

The Syrian Civil War involves fights in different regions of the country but this study focuses on the war mostly between government and the opposition forces in the western area where Orontes Basin – a key area where most resources are located (*e.g.,* water resource, agricultural areas, industrial areas). It has gone through several stages of power control since the beginning in 2011. In 2013 to 2015, the Syrian government supported by Iran and to a lesser extent by Russia, was losing the war of attrition against the armed opposition forces. In 2014, the government forces and the opposition groups each controlled around 40% while about half of the remaining 20% were combat zones, mainly located in Damascus suburbs, Aleppo City, Deraa district (Ford, 2019; Kılıç, 2018). By the end of Spring 2015, President Assad acknowledged publicly that his army has started to retreat. However, the situation reversed with the increased intervention of Russia which deployed aircraft and provided military support for the government. This stabilized the fighting followed by a supposed peace talk in 2016 which was then stalled by the Syrian government who believed that more areas could be secured in the battlefield with the Russian and Iranian help, than in peaceful discussions. Consequently, the opposition was weakened as the US whose priorities shifted from supporting the opposition and pressuring the Syrian government to negotiate towards fighting ISIS in the eastern Syria (Ford, 2019). In 2017, an agreement signed by Iran, Russia and

Turkey led to the implementation of de-escalation zones in the country. These areas included opposition-controlled areas in the provinces of Deraa and Quneitra, pockets around Damascus and Homs, the entire Idlib province and western parts of Aleppo province (Figure 1). Part of the agreement was the unhindered humanitarian access in such areas, restoration of basic services, cessation of hostilities between rebel groups and pro-government forces (Aljazeera, 2017; Internal Displacement Monitoring Centre, 2017). While the government agreed to abide by the agreement, it stated that it will continue fighting in areas where "terrorism" exists, parlance most armed rebel groups opposing the government (Aljazeera, 2017). The government attacked and recaptured three of four de-escalation zones, one after another between 2016 and 2018 (Ford, 2019). By 2018, the government regained control over most areas in the country and as of March 2020, only the area in the north western part of the country, Idlib, remained under the opposition control (Figure 2).

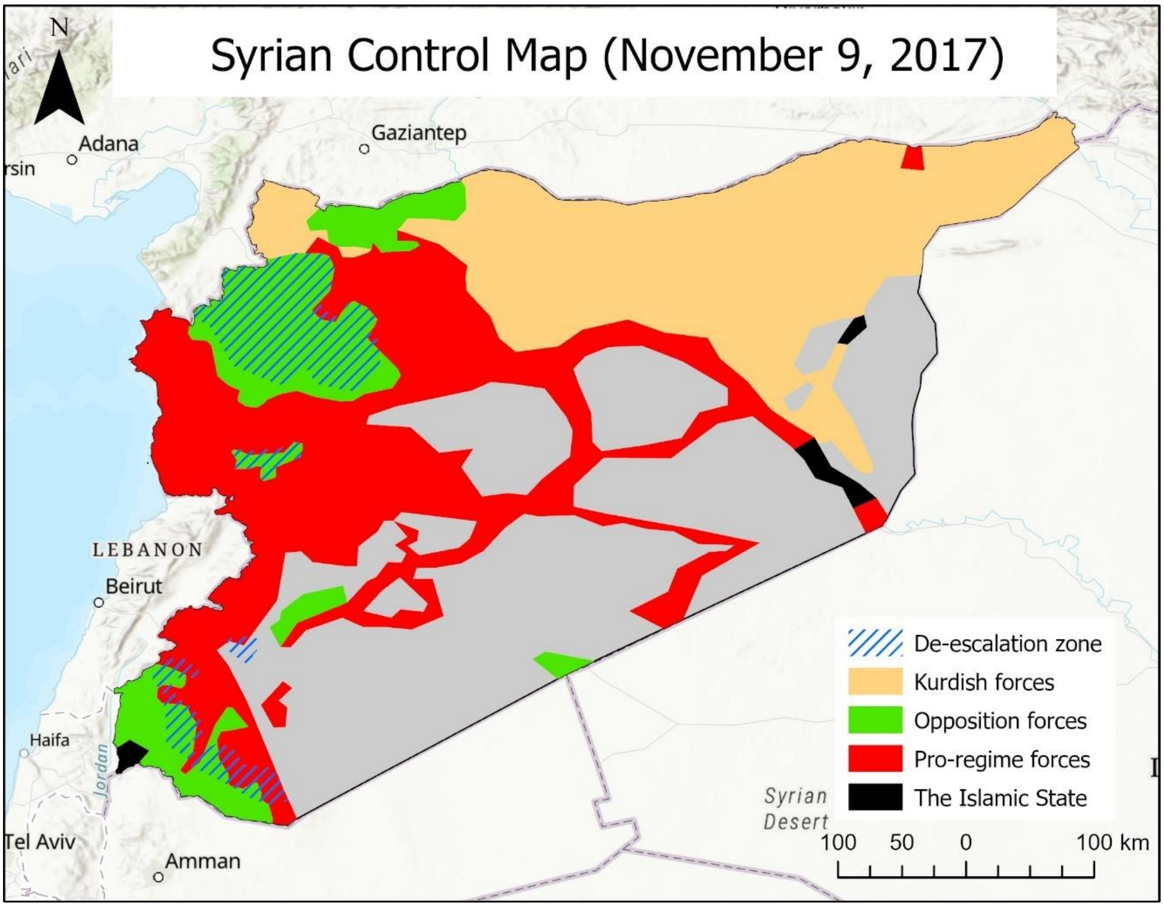


*Figure 1: Control Territories and four de-escalation zones established in 2017 (Adapted from (Internal Displacement Monitoring Centre, 2017)*

Control of Terrain in Syria: December 2020

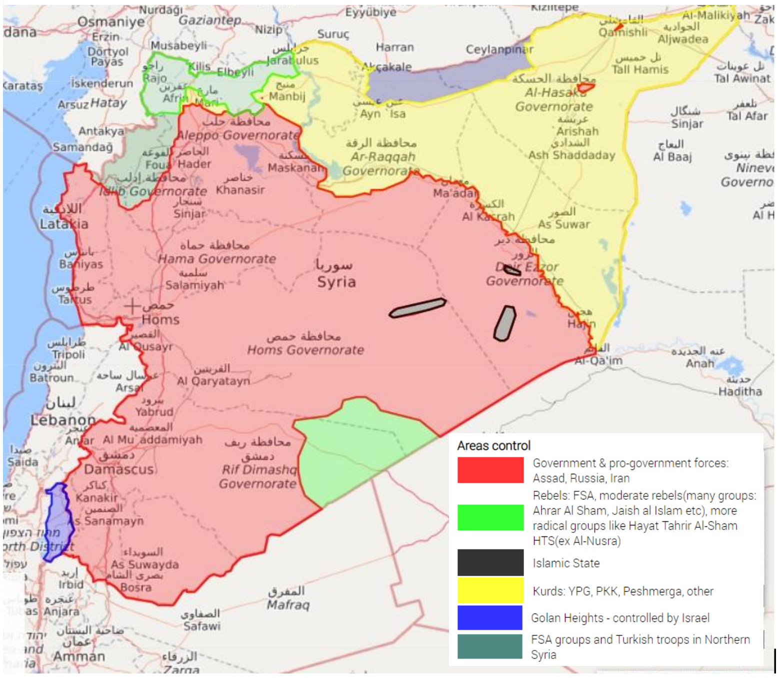


*Figure 2: Syrian control in December 2020 ( liveuamap.com, n.d)*

Although the war has not ended yet, rehabilitation and reconstruction efforts has been happening in several areas of the country. However, such efforts have remained highly politicized and unequal. According to Daher (2019), the government directs more effort in districts whose inhabitants historically favored the regime and not in the most damaged areas formerly under opposition control. The programs have been designed to expel the poorer, more antagonistic populations from key areas in many cities and to create real estate opportunities where the regime and its network of supportive business leaders can gain benefit from. The government made it difficult the displaced population to return to their homes. In 2018, a law empowering establishment of redevelopment zones was passed, empowering the government to confiscate residents' property without due process or adequate compensation. In Darayya and Qaboun, civilian residents who seek to return to their homes were restricted of access by the government, unlawfully demolishing private homes without notice, alternative housing or compensation

(Human Rights Watch, 2018). This pattern has happened in many areas in the country including some parts of Homs and Eastern Aleppo (Daher, 2019; The Syria Institute, n.d.).

The foreign support on reconstruction and rehabilitation varies among different countries. For instance, the European Union and the United States declined to fund reconstruction in government-held areas without a political transition. Several European countries including France and Switzerland have seek to support rehabilitation and stabilization efforts in areas reclaimed by the government. Most western donors have continued to provide humanitarian aid in areas controlled by opposition forces and Syrian Democratic Forces (Human Rights Watch, 2018).

These rehabilitation and reconstruction initiatives have a long way to go, given all the direct and indirect economic, social and environmental impacts brought about by the war. Ten years of continuous conflict has caused demise in the country's economy, killed thousands of lives, has left majority of its population displaced both internally and externally, and has brought about major damages to the surroundings. Specifically, the war led to the death of 384 000 to 593 000 people as of December 2020, caused the forced displacement of majority of its population – 6.5 million internally and another 2 million seeking refuge in neighboring countries mainly Lebanon and Turkey; and led to the decline of the country's economy incurring 428 billion USD worth of economic loss from 2011 to 2018 (Gaafar, n.d.; Mohammed et al., 2020) . Gaafar (n.d.) emphasized that in addition to the said direct impacts of the war, there are significant environmental aftermaths that gain less attention despite the major potential long-term negative impacts on public health, the economy and the peace itself. These impacts include damages to oil refineries leading to soil contamination, pollution and subsequent reliance to makeshift oil refineries causing higher pollution and the mismanagement of waste and water among many others. Walker (2021) emphasized the devastating aftermath of weaponization of water as reservoirs and wastewater treatment plants are targeted, diverted or hoarded by both the opposing parties to gain military advantage. This has contributed to the lack of access to safe water among over 90% of the population, having a direct link to public health and prevention of communicable diseases and has an impact to agriculture and food security (Walker, 2021; Zwijnenburg, 2019). Gaafar (n.d) and Zwijnenburg (2019) suggested that these environmental consequences to be the center of any post-conflict rehabilitation and reconstruction efforts.

Water resources, being a highly valuable resource especially in a water-scarce region including Syria requires substantial attention following the consequences of the conflict. As important as water quantity, water quality requires to be assessed so proper measures can be applied to prevent the irreversible impacts. In the next section, an overview of one of the important regions in Syria - the Orontes Basin - is presented to have a wide understanding of the water situation particularly in the western region of the country. The section will then focus on a specific water body within the basin, Lake Qattinah which will be the area of interest for this study. This section will be a baseline in understanding the changes brought about by the war.

## The Orontes Basin

Located in the western Mediterranean coast, the Asi-Orontes River Basin (Figure 3) is a transboundary basin with a total area of approximately 24 669 km2 shared by Syria (69%), Turkey (23%) and Lebanon (8%). The Asi-Orontes river, flows from Lebanon, passes through Syria and goes all the way to Turkey and released in the Mediterranean Sea. It is the only river in the region that flows in a northern direction (FAO, 2009; UN-ESCWA and BGR, 2013).

The climate condition of the basin is characterized by rainy winters with snow on the higher altitudes and rain elsewhere, and by hot and dry summers. The precipitation intensity is highest along the Mediterranean coast and it decreases going to the west (Figure 3). The hottest months range from June to September, also the time when the area barely receives precipitation. The highest amount of rainfall pours during the coldest months from November to February (Figure 4). As compared to the other parts of the country, the climate in the basin is most favorable, making it a region of key importance (UN-ESCWA and BGR, 2013).

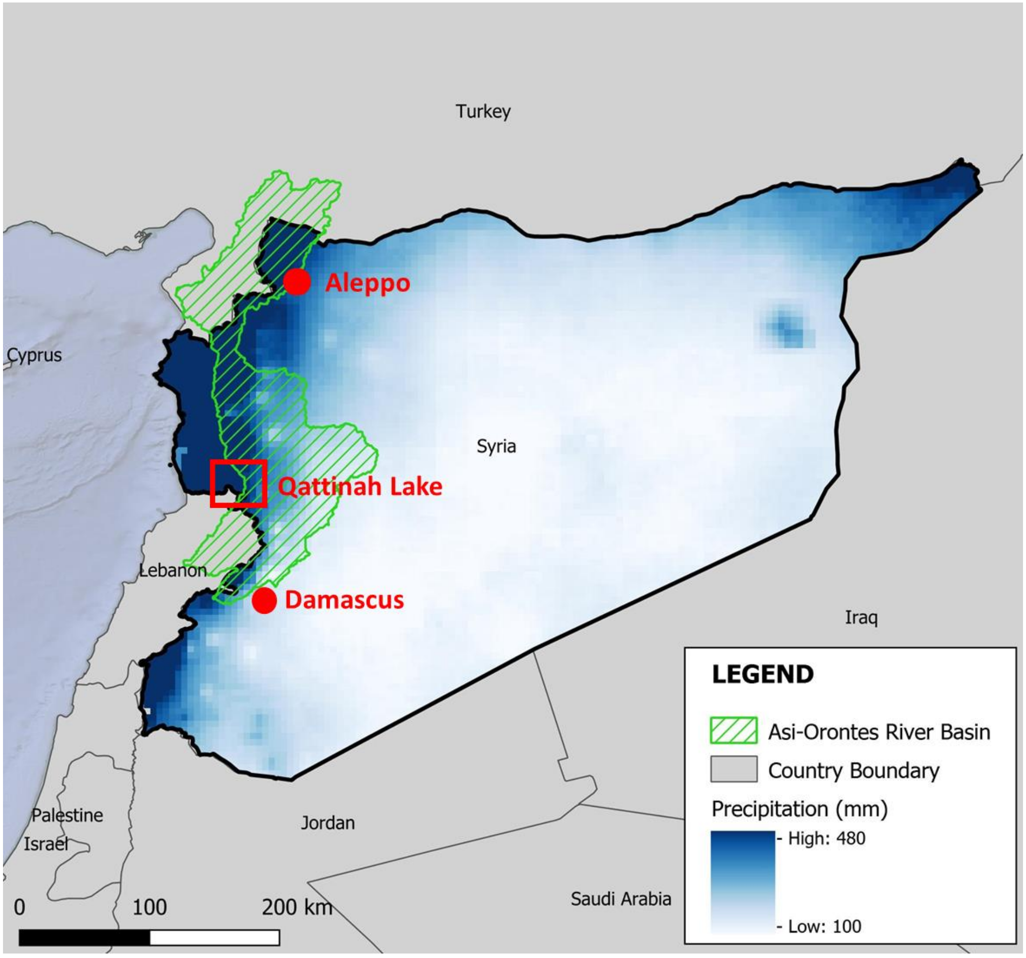


*Figure 3: Spatial pattern of precipitation in Syria (Own creation)*

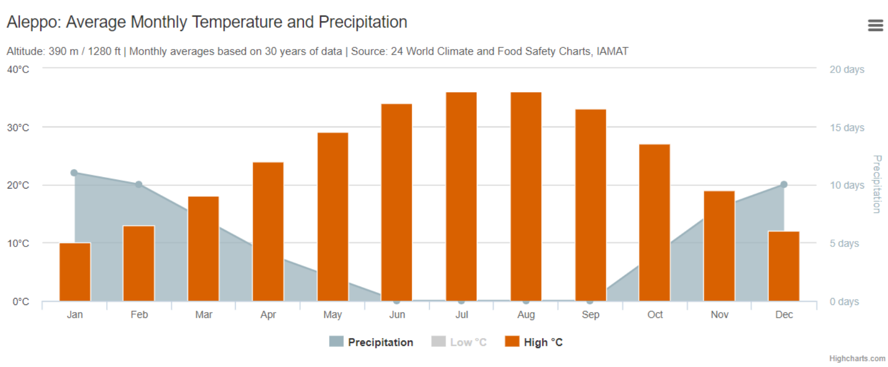

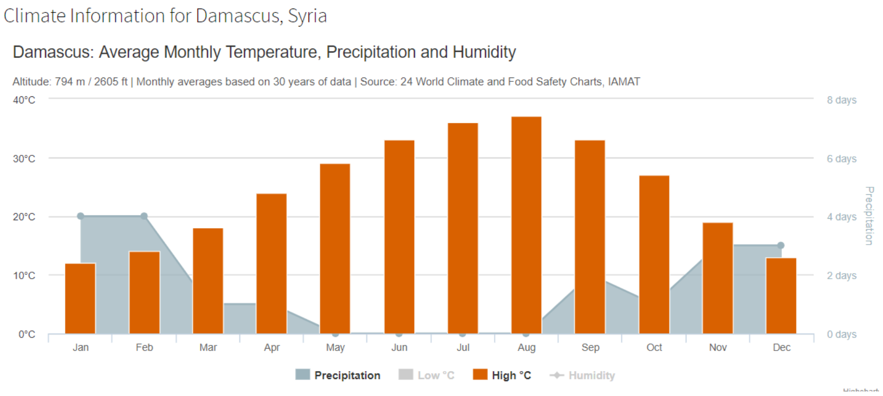


*Figure 4: Average monthly precipitation and temperature in parts of Orontes Basin a) Aleppo b) Damascus (IAMAT, n.d.)*

The Orontes Basin plays an important role in both agriculture and industry of the country. It covers a quarter of the agricultural production and one third of the industrial production. It houses several industrial activities (*e.g.,* oil refineries, sugar factory, fertilizer factory) being among the first industrialized regions in Syria. The basin also covers a total irrigated agricultural area of around 250 000 hectares in 2004 – 2008. Orontes River supplies water to two main agricultural areas in the country, in the region between Homs and Hama and in the Ghab, a former swampy valley reclaimed for irrigated agriculture (UN-ESCWA and BGR, 2013). Prior to the war, Orontes River Basin used to supply domestic water needs of Syrian cities Homs and Hama, delivering 16.52% of the cities' domestic water supply. It also tended to 40% of the industrial water needs, mainly from industries in Western Syria (Conker & Hussein, 2020).

The Orontes Basin has been subjected to serious issues of water pollution (Hollander, 2015; UN-ESCWA and BGR, 2013). According to UN-ESCWA and BGR (2013), the headwaters of the basin is clear but the middle and lower ranges of the river are heavily polluted from human activities while FAO (2009) and Haj Asaad & Jaubert (2014) specifically pointed out that the surface and groundwater are polluted by industrial and municipal wastes in areas near huge settlements In the period of 1995-2000, waterborne disease like typhoid and hepatitis were seen to increase tenfold, while diarrhea more than doubled in comparison to period of 1991 to 1995 (FAO, 2009). FAO (2009) suggested that this problem is exacerbated by scarcity of water resources, lack of infrastructure to treat wastewater, a general lake of awareness regarding pollution and failure to adopt regulations that protect the environment and public health.

### The Study Area – Qattinah Lake

Qattinah Lake is a shallow lake formed after the creation of a dam along Orontes River in 1938 (Hassan et al., 2010) which finished in 1976 (FAO, 2009). Orontes River originates from Lebanon, passing through Syria all the way to Turkey until it reaches the Mediterranean Sea. The dam, along with Rastan dam and Mhardeh dam, was created to increase the irrigation capacity in Syria. The said reservoirs have a total capacity of 741 million cubic meters and controls about 12 600 km2 of the basin upstream of Mhardeh (UN-ESCWA and BGR, 2013).

Located towards the southern portion of Orontes Basin and 15 km from the city of Homs, Qattinah Lake caters to some of the water needs in the agricultural region between Homs and Hama. It provides water to irrigate around 23 000 hectares of agricultural land while another 20 000 hectares in the said region is supplied by groundwater wells (UN-ESCWA and BGR, 2013). The lake has an average area of 57 km2 and a maximum depth of 10 meters in winter and 7 meters in summer. Orontes river flows through the lake in the southwestern portion and flows out in the northeastern part. The area in the west and northwestern part is mainly basaltic, with large blocks that are spread on the land primarily used as pasture (Hassan et al., 2010). The northern portion is also dominated by rainfed fruit bearing trees with some vegetables. The western side is a marshland that grows during the rainy months while the eastern side hosts a fertilizer factory and a relatively larger village. The southern part is dominated by irrigated agricultural lands mainly wheat and vegetables (Haj Asaad & Jaubert, 2014). The lake is also surrounded by several villages. The immediate vicinity of Lake Qattinah is shown in (Figure 5 and Figure 6).

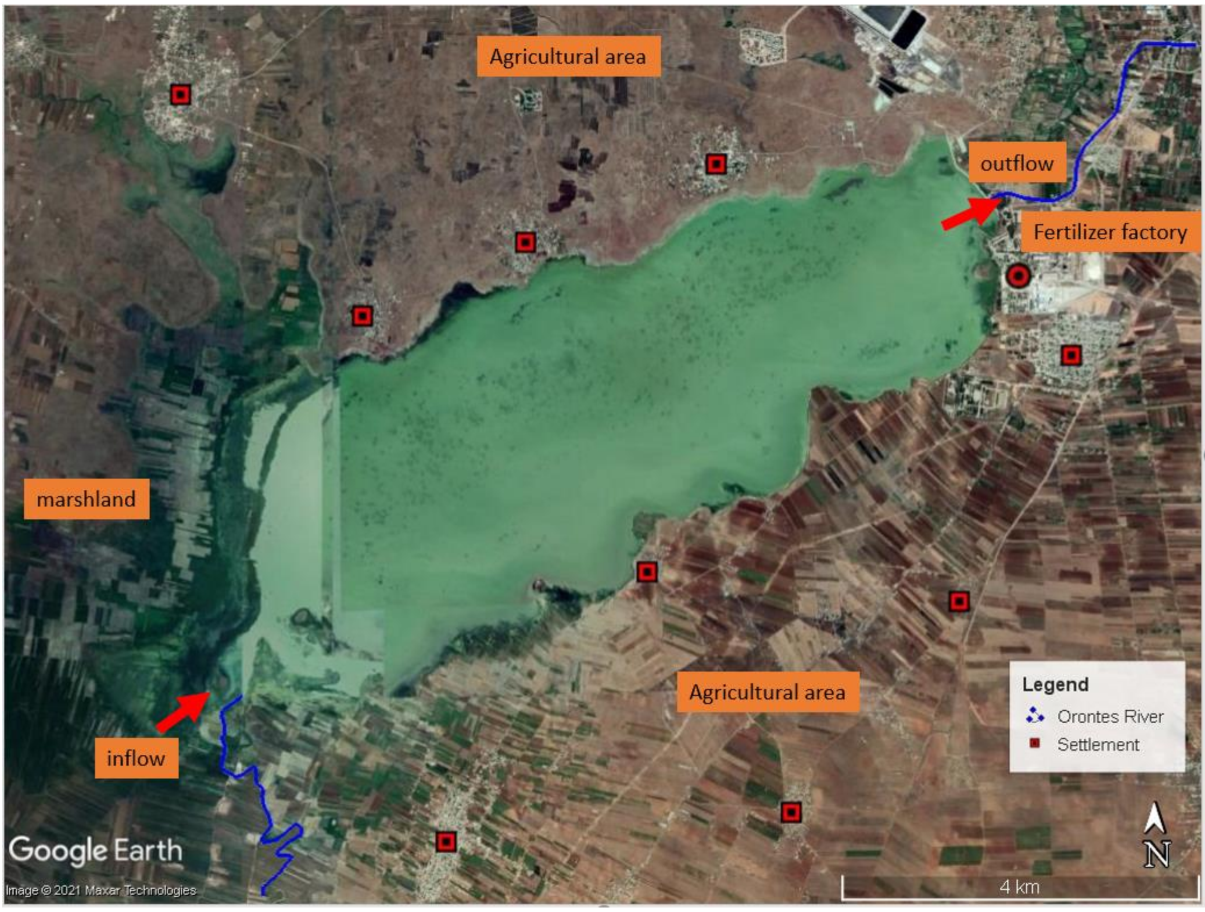


*Figure 5: Human activities surrounding Lake Qattinah (Own creation)*

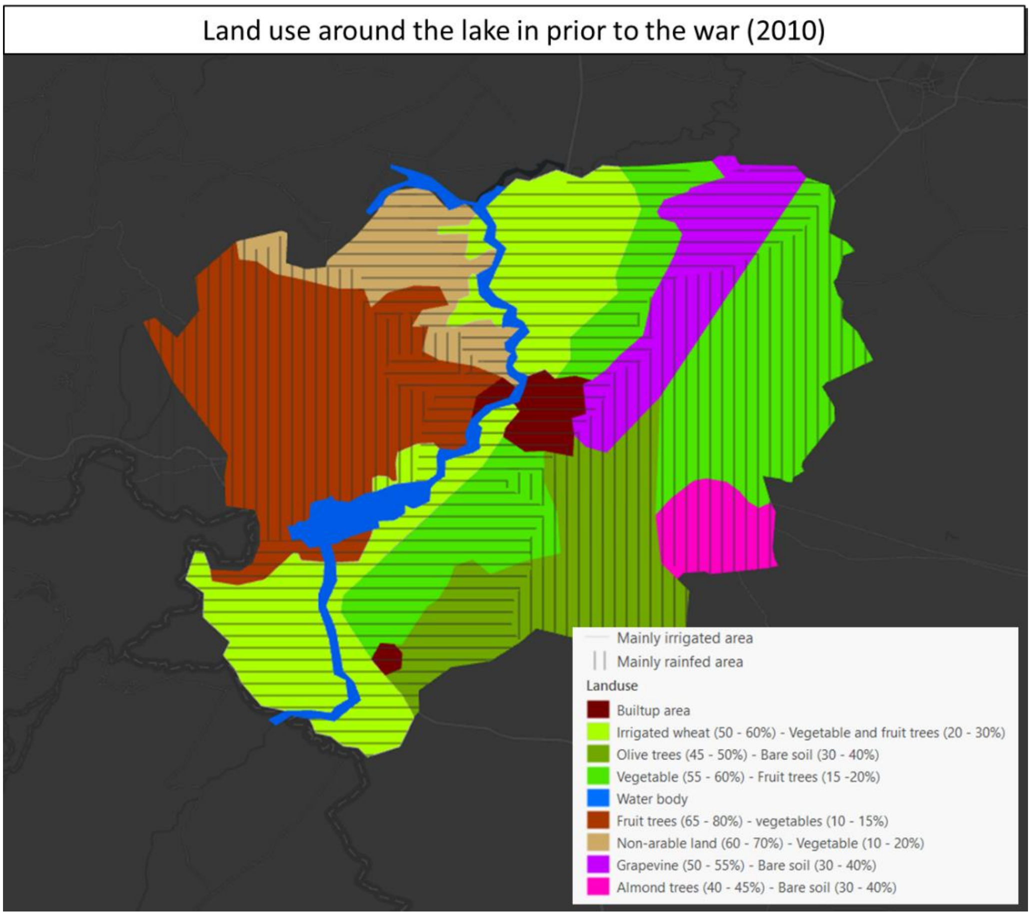


*Figure 6: Land use around Lake Qattinah in 2010 (Adapted from (Haj Asaad & Jaubert, 2014)*

The water quality of the lake had been poor even prior to the armed conflict, receiving excessive amounts of nutrients (primarily phosphorus and nitrogen) (Hassan et al., 2010; Manssour & Al-Mufti, 2010; UN-ESCWA and BGR, 2013). In a study conducted by Hassan et al., (2010), low macrophyte species richness was found in the lake and it was mainly restricted to a few tolerant species (i.e. M. spicatum, P. pectinatus and P. lucens ) which reflected the highly eutrophic conditions. This is based on the account that high nutrient loadings can lead to the shift from macrophyte-dominated clear waters to phytoplankton-rich turbid waters. Manssour & Al-Mufti (2010), who measured various water quality parameters in the lake also concluded that Lake Qattinah is a highly polluted water body with seasonal variations of total nitrogen, total phosphorus and oxygen parameters such as DO, COD and BOD which are all connected to the algal bloom that begins in April.

Several studies pointed to the phosphate factory in the eastern banks of the lake as one of the main polluters providing the highest nutrient input (Hassan et al., 2010; Manssour & Al-Mufti, 2010; Othman & Al-Masri, 2007). Hassan et al. (2010) also found out that Orontes river is the main source of nitrogen whereas the fertilizer factory is the main source of phosphorus. Manssour and Al-Mufti (2010) saw evidences of very clear algal blooms in the hot spots such as the location near the said factory as well as the agricultural and sewage drainages. They also found seasonal variations of total phosphorus peaking in September, mainly affected by the variations of discharges from the factory and the water level of the lake. Consequently, they found the highest value of total nitrogen in the algal season. According to Haj Asaad & Jaubert (2014) and Othman and Al-Masri (2007), there had been governmental control on the discharges of the industrial activities in the lake wherein routine monitoring and reporting of water quality was conducted ; however, it was not enough to mitigate the deterioration of the water quality.

In this study, the water quality of the lake will be assessed within different stages of the conflict. The specific area of study will be useful to understand how the dynamics of the war specifically affected pollution drivers around the lake. The next section of this study will discuss important concepts on water quality particularly in relation to phytoplankton. It will also tackle remote sensing as the tool that is useful for assessing an inaccessible area like Syria.

## Theoretical Concepts

To have a grasp on how remote sensing is used to estimate water quality in inland lakes, understanding of some basic concepts in necessary. The following theoretical concepts will be the basic building blocks in this study.

## Eutrophication

Eutrophication is the term used to describe the biological effects of an increase in the concentration of plant nutrients in aquatic environments - mainly phosphorus and nitrogen but sometimes include others such as silicon, potassium, calcium, iron and manganese (Harper, 1992). (Khan & Ansari, 2005) defined eutrophication as the sum of the effects of excessive growth in phytoplankton leading to imbalanced primary and secondary productivity and a faster rate of succession from existing to higher seral stage as caused by nutrient enrichment through runoffs that carry down overused fertilizers from agroecosystems and/or discharged human waste from settlements. Eutrophication is a very slow, natural processes which can be greatly accelerated by human activities increasing the rate of nutrient input in a water body (Frumin & Gildeeva, 2014; Khan & Ansari, 2005). The faster nutrient enrichment in water bodies due to anthropogenic activities was referred to by and Glibert et al. (2005) and Smith & Schindler (2009) as cultural eutrophication noting that it is one of the primary problems faced by most surface waters globally. Glibert et. al (2005) stated that population growth, food production (agriculture, animal operations and aquaculture), and energy production and consumption are among the main driving forces of the phenomenon.

Eutrophication has many undesirable side effects including but not limited to major economic costs and transnational implications (Smith & Schindler, 2009), habitat change and geographical and temporal expansion of some harmful algal bloom (HAB) species (Glibert et al., 2005), impact of animal and human health (Frumin & Gildeeva, 2014). Smith & Schindler (2009) enumerated some specific effects of eutrophication such as increase phytoplankton biomass and macrophyte vegetation, increased incidence of fish kills, reduction of species diversity, decreases in water transparency, foul taste and odor of water also causing drinking water treatment problems, and decreased perceived aesthetic value of the water body. Several studies have emphasized that the deterioration of water quality is due to eutrophication (Smith & Schindler, 2009).

As an effort towards a more convenient way to assess lakes, various classification schemes in relation to eutrophication, also referred to as the trophic state, have been developed. The term trophic state was originally proposed by Naumann (1919), based on lake production and was quantified through an estimation of algal biomass due to their impacts on a lake's biological structure. HE Naumann (1919) suggested a regional approach to trophic state because of interregional variation in lake production. In 1969, Vollenweider used nutrient concentration as a static parameter for lake classification (Nojavan A. et al., 2019). (R. E. Carlson, 1977) created an index to determine a lake's trophic state classifying lakes into oligotrophic, mesotrophic and eutrophic. Carlson's index is explained below:

*Table 1: Parameter value ranges of the water trophic classification system according to Carlson*

| Class | Total Phosphorus (ug/L) | Chlorophyll-a (ug/L) | Transparence (SDD) (m) |
|---|---|---|---|
| Oligotrophic | <12 | < 2.6 | >4 |
| Mesotrophic | 12- 24 | 2.6 – 7.2 | 2 - 4 |
| Eutrophic | >24 | >7.2 | <2 |

Trophic state index (TSI) is then calculated from each of the three parameters using the equations:

$$TSI\ (SD) = 60 - 14.41 * \ln(SD)$$

$$TSI\ (TP) = 14.42 * \ln(TP) + 4.15$$

$$TSI\ (CHLA) = 9.81 * \ln(CHLA) + 30.6$$

Where SD is secchi disk depth in meters, TP is total phosphorus concentration in ug/L, CHLA is chlorophyll-a concentration in ug/L and ln is the natural logarithm.

The Carlson trophic state index (CTSI) which integrates the three parameters is calculated by averaging the 3 TSIs.

$$CTSI = [TSI(SD) + TSI(Chla) + TSI(TP)]/3$$

The lake classification based on this index is presented in Table 2: TSI ranges of tropic state classification of lakes according to Carlson :

*Table 2: TSI ranges of tropic state classification of lakes according to Carlson*

| CTSI | Trophic State |
|---|---|
| CTSI < 40 | Oligotrophic |
| 40 <= CTSI <= 50 | Mesotrophic |
| CTSI > 50 | Eutrophic |

Another well-established classification scheme is that of OECD in 1981 wherein lakes are quantitatively classified as oligotrophic, mesotrophic, eutrophic and hypertrophic based on concentrations of N and P, chlorophyll a and Secchi disk (Table 3: Parameter value ranges of the water trophic classification system according to OECD) (Bougarne & Abbou, 2019; Cheng & Li, 2006)

*Table 3: Parameter value ranges of the water trophic classification system according to OECD*

| | Total Phosphorus $_m$ (µg/L) | Chl $a_m$ (µg/L) | Chl a $_{max}$ (µg/L) | SD $_m$ (m) | SD $_{min}$ (m) |
|---|---|---|---|---|---|
| Ultra-oligotrophic | $< 4$ | $< 1$ | $\leq 2.5$ | $> 12$ | $\geq 6.0$ |
| Oligotrophic | $< 10$ | $< 2.5$ | $\leq 8.0$ | $> 6$ | $\geq 3.0$ |
| Mesotrophic | 10-35 | 2.5-8 | 8-25 | 6-3 | 3-1.5 |
| Eutrophic | 35-100 | 8-25 | 25-75 | 3-1.5 | 1.5-0.7 |
| Hypertrophic | $> 100$ | $> 25$ | $\geq 75$ | $<1.5$ | $\leq 0.7$ |

In this study, trophic status of the lake from 2010 to 2020 will be assessed based solely on chlorophyll-a concentration following these two classification schemes.

### Phytoplankton and chlorophyll a

Chlorophyll is a green molecule in plant cells that carries out the bulk of energy fixation in the process of photosynthesis. In water studies, it is used as an estimator of algal biomass in lakes and streams. Chlorophyll is a family of related molecules namely chlorophyll a, b, c and d. Chlorophyll d is found only in marine red algae while chlorophylls b and c are common in freshwater. The relative concentrations within the cell of chlorophylls vary with the species of algae. Chlorophyll a is dominant in all the eukaryotic algae and the prokaryotic blue-green algae (cyanobacteria) (R. Carlson & Simpson, n.d.).

Chlorophyll provides a fairly accurate measure of algal weight and volume and it acts as an empirical link between nutrient concentration and a number of biological phenomena in lakes and reservoirs (R. E. Carlson, 1977; R. Carlson & Simpson, n.d.). According to (Dillon & Rigler, 2011), it has been used for many years as a key variable in defining levels of external loading of phosphorus for eutrophication. (R. E. Carlson, 1977) suggested that it should be given priority as a trophic state indicator because it is free from interference of non-algal particles such as bacteria or detritus.

### Optical remote sensing and the electromagnetic radiation spectrum

Remote sensing has many definitions but one of the current definitions that encompasses the concepts related to this study is as defined by (Campbell & Wynne, 2011) as the practice of deriving information about the Earth's land and water surfaces using images acquired from an overhead perspective, using electromagnetic ration in one or more regions of the electromagnetic spectrum, reflected of emitted from the earth's surface. (Navalgund et al., 2007) defined it as the technology of acquiring information about the earth's surface and atmosphere using sensors onboard airborne (aircraft, balloons) or space-borne (satellites, space shuttles) platforms. These sensors detect and record reflected or emitted energy, producing massive data of the earth. (Navalgund et al., 2007) added that remote sensing can be also classified into two namely optical and microwave. Optical remote sensing uses sensors that detect solar radiation in the visible, near, middle and thermal-infrared wavelength, reflected or scattered or emitted from the earth, which then forms images resembling photographs taken from space.

### Optical water constituents and Case II waters

In the remote sensing field, water quality is generally measured through optically active water constituents like suspended particulate matters (SPM), colored dissolved organic matter (CDOM) and chlorophyll-a which can all be captured by the optical sensors. Chlorophyll-a, the green pigment present in photosynthetic plants and organisms including algae or phytoplankton, is used as an indicator of phytoplankton biomass in inland waters. Analyzing chlorophyll-a via remote sensing employs methods or algorithms which differ between two water body types – Case I and Case II. The definition that is commonly used today refers to Case I waters as those whose inherent optical properties (IOPs) are primarily determined by phytoplankton and related CDOM and detritus degradation products. These typically includes most open ocean waters. On the other hand, Case II waters refer to those that do not fall under the first type. These waters have optical properties that are significantly influenced by other constituents such as CDOM, mineral particles, or microbubbles whose concentrations do not covary with that of phytoplankton. (Matsushita et al., 2012; Mobley et al., 2004). This differentiation has been relevant in modelling purposes, with many bio-optical models developed to predict inherent optical properties such as absorption, scattering and backscattering coefficients (Mobley et al., 2004) which are used in different water studies.

### Reflectance spectra / spectral signature

Features on earth reflect, absorb, or transmit energy and the amount of this energy varies for every wavelength. The plot of all the variations of this energy as a function of wavelength is called the spectral signature. This signature is unique for every feature, allowing researchers to use this information to identify various earth features (NASA, n.d.-b; Navalgund et al., 2007). In water quality analysis in Case II waters, algorithms for chlorophyll-a estimation are based on reflectance spectra of waters with algae and/or other water constituents. Figure 7 shows the spectral signature of some selected land features while Figure 8 shows that of clear waters against algae-laden waters with the latter characterized by a reflectance peak in the green region of the spectrum, a second peak in the near-infrared (NIR) region and a maximum absorption (minimum reflectance) in the red region. This serves as the basis of most established chlorophyll-a retrieval algorithms or models.

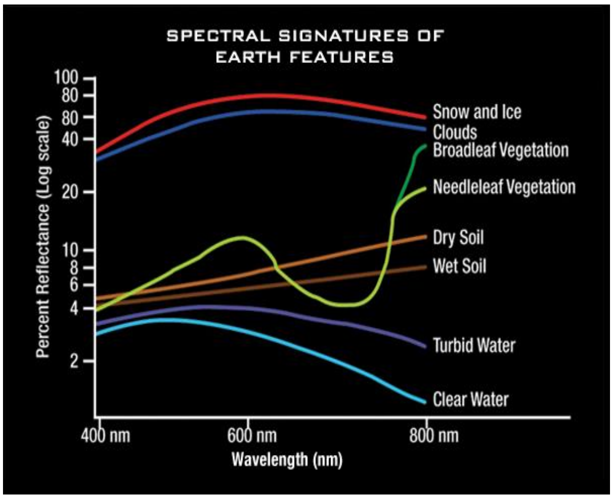


*Figure 7: Spectral signature of various land covers (NASA, n.d.-b)*

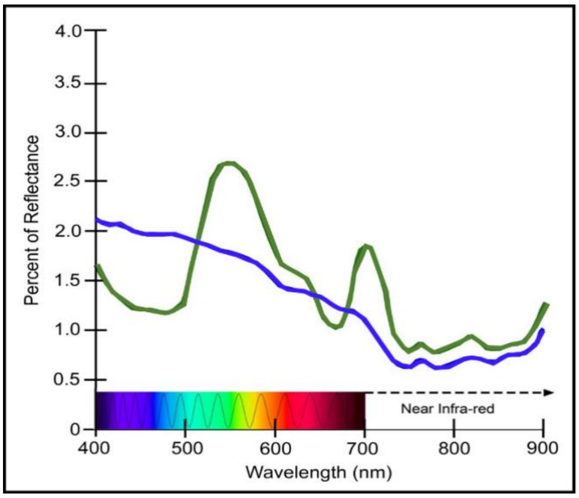


*Figure 8: Spectral signature - clear vs algae-rich waters*

## Application of remote sensing in water quality assessment

### Overview

In situ methods of data collection and analysis has been the conventional way of measurement for many environmental applications. The process of estimating chlorophyll-a from field data basically includes extraction of planktonic cells and measurement of chlorophyll-a pigment in the laboratory (Aminot & Rey, 2002). While this method provides specific and accurate measurement of chlorophyll-a from water samples, it also poses certain challenges. As an example, most conventional data are still related to point locations or to transects, which are commonly interpolated to obtain results. In situ methods in this case becomes more satisfactory when numerous points are observed or measured, to achieve an acceptable level of accuracy. This method involves high costs, time and labor, especially for monitoring programs involving wide temporal and spatial scale. In situ measurements are also challenging for areas that are hardly accessible (Barrett & Curtis, 1999).

Remote sensing is a growing technology that has been seen to address some challenges of in situ methods (Barrett & Curtis, 1999; Navalgund et al., 2007). It provides a vast amount of information in specific to large geographic areas with wide temporal coverage. Trends in satellite imageries have shown improving spatial resolution and more frequent image capture, thus making remote sensing increasingly useful for temporal and spatial assessment of water bodies (Allan et al., 2011; Hadjimitsis et al., 2010).

Remote sensing has been widely applied in assessing water quality of inland lakes and reservoirs in many regions of the world. (Dörnhöfer & Oppelt, 2016) reviewed research trends of the application of remote sensing in water quality assessment and saw an increasing pattern brought about by the improved spatial resolution of several satellite sensors which allowed analysis of small to medium sized lakes which used to be challenging due to poor resolution of water quality specific sensors such as MERIS and MODIS. Allan et al. (2011) used Landsat 7 to estimate chlorophyll-a concentrations in various lakes in New Zealand and saw levels of variations that are comparable to traditional ground-based monitoring. (Peppa et al., 2020) used Sentinel-2 data and revealed spatial variations of algae in Pamvotis Lake, a eutrophic lake in Greece. (Andrzej Urbanski et al., 2016) created a tool to support regional lake quality assessment of 2800 lakes in Poland using Landsat 8. Several other remote sensing studies have been conducted throughout the years (*e.g.,* Ansper & Alikas, 2018; Bramich et al., 2021; Cazzaniga et al., 2019; Deutsch et al., 2018; Mishra & Mishra, 2012; Ouma et al., 2020).

In Syria, most of the remote sensing studies found are related to impacts of the war on other aspects (land use and land cover changes (Mohamed et al., 2020), mapping of destruction in urban area (Lubin & Saleem, 2019; Marx, 2016) and water quantity (Avisse et al., 2017). It appears that there are currently no published studies analyzing the impacts of the war on the water quality of inland lakes in Syria. This presents a huge opportunity to utilize the vast information that satellite data can provide to fill this current research gap.

### Remote sensing of algal concentration in Case II inland waters

Remote sensing of algal concentration in water bodies typically involves mapping of chlorophyll-a using water-leaving reflectances stored in satellite data. This approach generally involves utilization of models developed based on the combination of reflectances measured at different wavelengths in such a way that the model has maximum sensitivity to the changes in the concentration of chlorophyll-a and minimum sensitivity to the changes in concentrations of other constituents present in the water (A Gitelson et al., 2009).

Historically, remote sensing has been more popular in estimating chlorophyll-a concentrations in Case I waters with models are generally based the visible spectrum specifically on the absorption peak (minimum reflectance) in the blue region near 440 nm and the reflectance peak in the green region around 550 nm (A Gitelson et al., 2009). These models are generally not suitable for Case II waters which are dominated by at least three optically active constituents (i.e chlorophyll-a, TSM, CDOM) making it generally more complex (Matthews, 2011; Mobley et al., 2004). The use of reflectances in the visible region of the spectrum alone is found to less appropriate in turbid productive waters and many studies have suggested the use of the red and NIR regions in developing models for these complex waters (Ansper & Alikas, 2018; Gurlin et al., 2011; Moses et al., 2009; Yacobi et al., 2011).

**Remote sensing algorithms for chlorophyll-a estimation in Case II waters**

The reflectance pattern of chlorophyll-a is the key in understanding the algorithms used to estimate its concentrations in inland lakes or Case II waters. (A Gitelson et al., 2009) summarized three main features of chlorophyll-a to which many models are based. First, chlorophyll-a has strong absorption in the red region specifically around 670 nm, forming a trough in the reflectance spectrum. However, this feature is not driven by chlorophyll-a alone but has contributions from total suspended solids, making the reflectance near 670 nm alone not a reliable estimator of chlorophyll -a concentration. Second, chlorophyll-a has a peak near 685 nm called the solar-induced chlorophyll -a fluorescence. The peak near this wavelength increases with increased chlorophyll-a concentration. However, this is found to be only reliable for estimation of low chlorophyll-a concentrations – not more than 10 – 15 mg/m3 as higher concentrations lead to reduced available light, limits fluorescence efficiencies and affects the measurement. The third feature of chlorophyll-a reflectance is a peak in the NIR region near 700 nm. Its magnitude and position depend on chlorophyll-a concentration but is also influenced by other constituents.

Most of established chlorophyll-a models are based on this feature as it allows fairly accurate estimation in water bodies with wide ranges of chlorophyll-a concentrations. Some examples are the two-band NIR-red ratio (2BDA) which takes the ratio of the NIR reflectance peak near 700nm to the red maximum absorption near 670nm (Gurlin et al., 2011; Matthews, 2011) chapter 18; the three-band NIR-red ratio (3BDA) with involves a third reflectance near 750nm in addition to the those used in two-band NIR-red ratio (Dall'Olmo et al., 2003); the Normalized Difference Chlorophyll-a Index (NDCI) which involves reflectance near 709 nm and 665 nm (Mishra & Mishra, 2012).

In this study, 2BDA and 3BDA were selected as such are well-established models which have been successfully applied in several studies of inland lakes with wide ranges of algal concentrations and under various climatic and environmental conditions and using MERIS, Landsat 8 OLI, and Sentinel 2 (i.e. Bramich et al., 2021; Deutsch et al., 2018; Gilerson et al., 2010; Gurlin et al., 2011; Johansen et al., 2018; Masocha et al., 2018; Moses et al., 2009; Sòria-Perpinyà et al., 2021; Watanabe et al., 2015; Yacobi et al., 2011) which are the satellite data used in this study.

## Conclusions

The findings from the review of related studies has contributed towards the achievement of the research aims of this study. The first section has provided relevant background of the study area and the ongoing war in Syria. It has helped in identifying the surrounding human activities that historically caused degradation of the lake's water quality. It also provided some insights on the known past and current conditions of the lake helping the author to select methods that are appropriate (i.e. selection of chlorophyll-a models suitable for Case II and highly polluted water body). Looking at the key events of the conflict situation became useful in selecting suitable data for the analysis, interpreting the results and finding linkages between the war and the lake's water quality.

The second section has integrated relevant theoretical concepts and explored how remote sensing is utilized in assessing water quality. Its major contribution in the study is the proper selection of methods to determine algal concentrations in the specific lake.

# MATERIALS AND METHODS

## Selecting the satellite data suited for the study period

This study investigates periods before and during the Syrian Civil War and covers years 2010 to 2020 excluding 2012 due to lack of satellite data. No single satellite dataset covers the entire period so data from multiple satellite sensors were used. Suitable satellite data were identified, mainly based on availability and accessibility, prioritizing those with good spectral and spatial resolution necessary for chlorophyll-a assessment of a medium-sized lake. The timeframe is therefore divided into three based on the availability of each of the satellite data used (Table 4: War periods and corresponding satellite data used).

*Table 4: War periods and corresponding satellite data used*

| Time Period – War | Satellite Sensors and Data Availability | Properties |
|---|---|---|
| Pre- war (2010 – 2011) | MERIS (May 2002 -April 2012)<br><br>Landsat 5 (March 1984 – May 2012) | MERIS: high spectral resolution, low spatial resolution<br><br>Landsat 5: high spatial resolution, spectral configuration inferior than that of MERIS |
| War(2012 to 2016) | Landsat 8 (April 2013 to present) | Landsat 8; high spatial resolution; spectral configuration inferior than that of MERIS |
| War (2017 to 2020) | Sentinel 2 (2017 to present) | Sentinel 2; high spatial resolution; spectral configuration inferior than MERIS but spectral bands are positioned close to chlorophyll-a estimation important wavelengths; |

### Medium Resolution Imaging Spectrometer (MERIS).

MERIS sensor is attached to the Envisat-1 satellite owned by the European Space Agency (ESA). MERIS data consists of 15 bands across spectral range 390nm to 1040nm. It has a global coverage and acquires data every 3 days making it suitable for monitoring purposes in any region in the world (LAADS, n.d.). The primary goal of MERIS mission is the measurement of sea color in oceans and in coastal areas, which can be basis in measuring chlorophyl pigment concentration, suspended sediment concentration and atmospheric aerosol loads over water (ESA, 2006). MERIS has also been utilized in several water quality studies in lakes (Gilerson et al., 2010; Gower et al., 2008; Gurlin et al., 2011). The central bands are positioned in wavelengths that are identified important in chlorophyll-a analysis. The MERIS bands against important chlorophyll-a wavelengths is presented in the Figure 9. Table Table 5: Spectral bands of MERIS data shows the specifications of each of the MERIS bands.

*Table 5: Spectral bands of MERIS data*

| Band Number | Central wavelength (nm) | Bandwidth (nm) |
|---|---|---|
| 1 | 412.5 | 10 |
| 2 | 442.5 | 10 |
| 3 | 490 | 10 |
| 4 | 510 | 10 |
| 5 | 560 | 10 |
| 6 | 620 | 10 |
| 7 | 665 | 10 |
| 8 | 681.25 | 7.5 |
| 9 | 708.75 | 10 |
| 10 | 753.75 | 7.5 |
| 11 | 760.625 | 3.75 |
| 12 | 778.75 | 15 |
| 13 | 865 | 20 |
| 14 | 865 | 10 |
| 15 | 900 | 10 |

Source: (ESA, 2006)

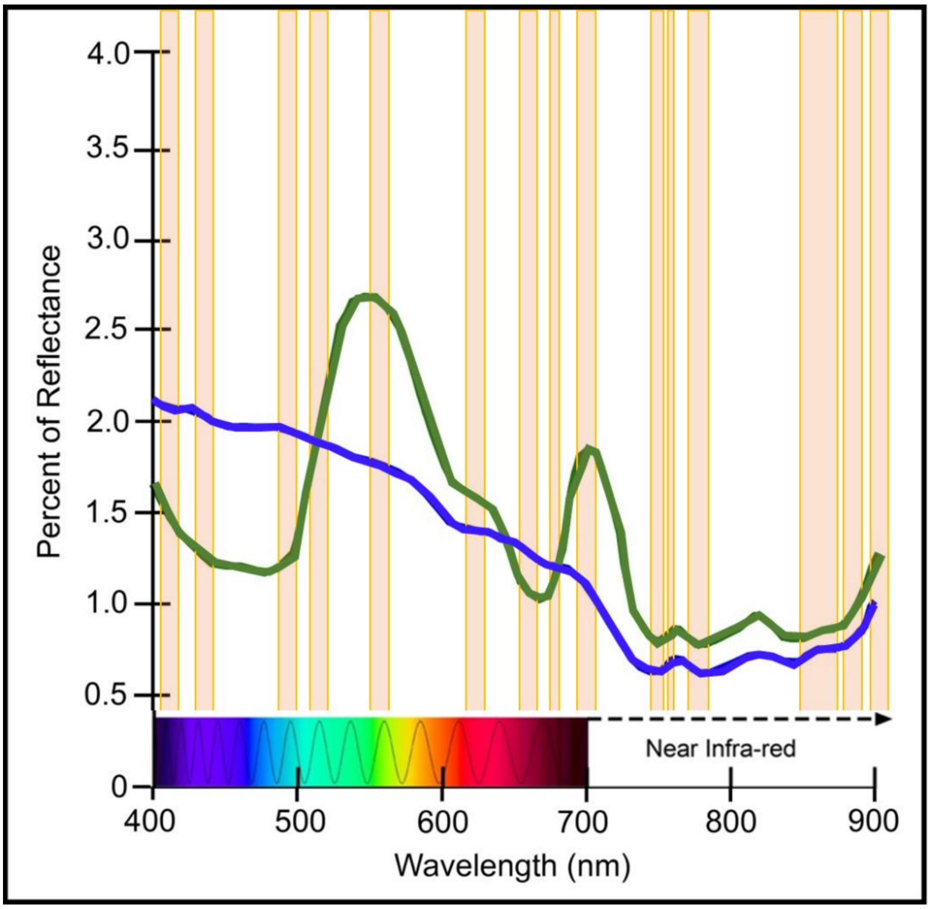


*Figure 9: MERIS 2 bands against reflectance pattern of chlorophyll-a ; Adapted from (ESA, 2006; Han, 1997; SEOS, n.d.)*

One drawback of using MERIS is its low spatial resolution – 300m. Given that the study area is a medium-sized lake with an area of around 60 square kilometers, the coarse images from MERIS limits the analysis of the area. To aid this, Landsat 5 which has a 30-meter spatial resolution (10 times higher than that of MERIS) but inferior spectral resolution, was used to conduct visual inspection of the area to look for obvious spatial and temporal patterns.

MERIS Level 2 data was downloaded from ESA website and processed using SNAP and ArcGISPro. Due to long download time for each satellite data (5-8 hours per satellite image), only one day image for selected months were analyzed. Clear images with no cloud cover were selected and downloaded ( Table 6).

*Table 6: MERIS data assessed prior to the war (2010)*

| Date | Filename |
|---|---|
| June 12, 2010 | EN1_MDSI_MER_FRS_2P_20100612T074412_20100612T081238_043304_0164_20180124T063555_0100 |
| July 14, 2010 | EN1_MDSI_MER_FRS_2P_20100714T074749_20100714T075605_043762_0121_20180126T080104_0100 |
| August 15, 2010 | EN1_MDSI_MER_FRS_2P_20100815T074203_20100815T074724_044220_0078_20180128T122031_0100 |
| September 16, 2010 | EN1_MDSI_MER_FRS_2P_20100916T073535_20100916T074136_044678_0035_20180202T161938_0100 |
| October 17, 2010 | EN1_MDSI_MER_FRS_2P_20101017T075931_20101017T081007_045122_0479_20171225T131119_0100 |

### Landsat 5 Thematic Mapper (TM)

Landsat 5 Thematic Mapper was attached to the Landsat 5 satellite, developed by NASA and launched on March 1984. Landsat 5 became operational for 29 years until I decommissioned on June 2013. The satellite captured data of global coverage every 16 days. Landsat 5 TM data consists of 7 bands across spectral range 450nm to 2350 nm (USGS, n.d.). Its specifications are shown in Table 7.

Table 7: Band specifications of Landsat 5

| Band number | Band name | Wavelength (µm) | Resolution (m) |
|---|---|---|---|
| 1 | Visible Blue | 0.45 - 0.52 | 30 |
| 2 | Visible Green | 0.52 - 0.60 | 30 |
| 3 | Visible Red | 0.63 - 0.69 | 30 |
| 4 | NIR | 0.76 - 0.90 | 30 |
| 5 | SWIR 1 | 1.55 - 1.75 | 30 |
| 6 | Thermal | 10.40 - 12.50 | 120 |
| 7 | SWIR 2 | 2.08 - 2.35 | 30 |

Source: (USGS, n.d.)

**Landsat 8 Operational Land Imager (OLI).**

The second to fifth year of the war (2013 to 2016) was assessed using Landsat 8 OLI. For this time period, Landsat 8 OLI and Landsat 7 ETM+ are both available. The former was selected over the latter which has had a sensor deficiency since 2003 producing images with black line gaps. Landsat 8 was developed under the collaboration of NASA and USGS. It was launched on February 11, 2013 to acquire data on landmass. The satellite carries two sensors – the Operational Land Imager (OLI) sensor and the Thermal Infrared Sensor (TIRS). It collects data at spatial resolution of 30m in the visible, NIR and SWIR; 100 m in the thermal region (Table 8) (NASA, n.d.-a; USGS, 2013). The positions of its bands (until 900nm) against clear and algae-laden waters spectral pattern is presented in Figure 10. Its spectral bands do not all coincide with the important wavelengths in chlorophyll-a estimation. Despite this, many studies have employed this data (Deutsch et al., 2018; Masocha et al., 2018; Watanabe et al., 2015), concluding that it can be used for the said purpose.

*Table 8: Spectral bands of Landsat 8 (NASA, n.d.-a)*

| Band number | Band name | Wavelength (μm) | Resolution (m) |
|---|---|---|---|
| 1 | Coastal | 0.43 - 0.45 | 30 |
| 2 | Blue | 0.45 - 0.51 | 30 |
| 3 | Green | 0.53 - 0.59 | 30 |
| 4 | Red | 0.63 - 0.67 | 30 |
| 5 | NIR | 0.85 - 0.88 | 30 |
| 6 | SWIR 1 | 1.57 - 1.65 | 30 |
| 7 | SWIR 2 | 2.11 - 2.29 | 30 |
| 8 | Pan | 0.50 - 0.68 | 15 |
| 9 | Cirrus | 1.36 - 1.38 | 30 |
| 10 | TIRS 1 | 10.60 - 11.19 | 100 |
| 11 | TIRS 2 | 11.50 - 12.51 | 100 |

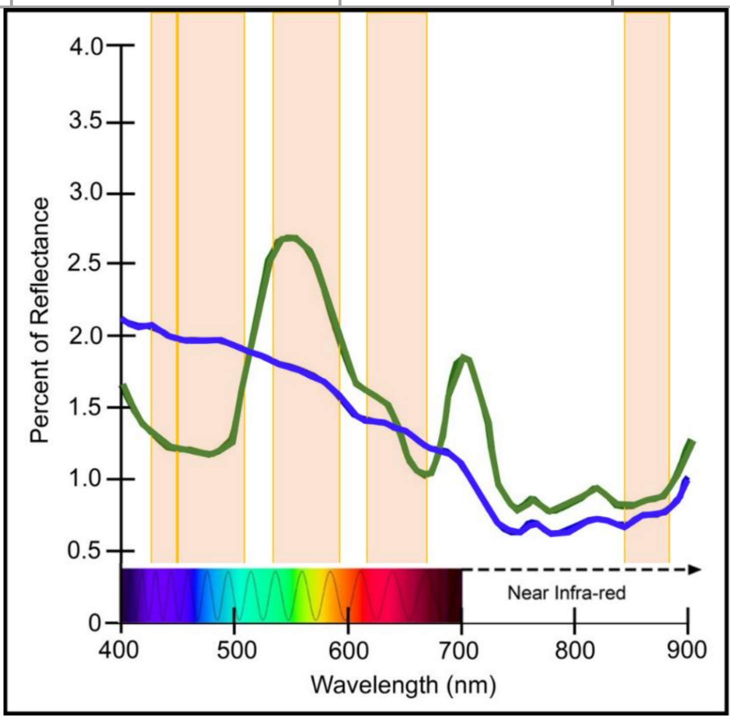


*Figure 10: Landsat 8 OLI bands against chl-a reflectance spectra; Adapted from (Han, 1997; NASA, n.d.-a; SEOS, n.d.)*

For the more recent period of the war (2017 – 2020), Sentinel 2 and Landsat 8 data are both available but the former was selected for the analysis for its spectral positioning to which most chlorophyll-a indices selected in this study are more applicable. This data is available from 2016 onwards, but the processed level 2 data to be used in the analysis is only available in the Data Cube platform from 2017.

### Sentinel 2

The Copernicus Sentinel 2 was launched by the European Space Agency on June 23, 2015 with the main aim to monitor variability in land conditions. The mission consists of two satellites (Sentinel 2A and Sentinel 2B) flying in the same orbit but phased at 180 degrees, and together provides data every 5 days. Each of the satellites are equipped with a sensor called Multi-Spectral Instrument (MSI) which has 13 bands with spatial resolution ranging from 10 to 60 m and a spectral coverage in the visible, near infrared region (NIR), and short wave infrared region (SWIR).

Sentinel 2A and Sentinel 2B were launched separately with latter on March 7, 2017. In this study, only Sentinel 2A data was used as it is the only available Sentinel 2 data in Data cube Water Quality Script during the time of analysis. Independent from its twin satellite, it captures data every 10 days (EOS, 2017; ESA, n.d.-a). The spectral ranges and spatial resolution of Sentinel 2A bands are presented in Table 9. The positions of its bands (until 900nm) against clear and algae-laden waters spectral pattern is presented in Figure 11. It is seen that there are bands positioned in important peaks and troughs of the chlorophyll-rich waters.

*Table 9: Spectral bands of Sentinel 2A; (EOS, 2017)*

| Band number | Band name | Central wavelength (nm) | Bandwidth (nm) | Resolution (m) |
|---|---|---|---|---|
| 1 | Coastal aerosol | 443.9 | 20 | 60 |
| 2 | Blue | 496.6 | 65 | 10 |
| 3 | Green | 560 | 35 | 10 |
| 4 | Red | 664.5 | 30 | 10 |
| 5 | Vegetation Red Edge | 703.9 | 15 | 20 |
| 6 | Vegetation Red Edge | 740.2 | 15 | 20 |
| 7 | Vegetation Red Edge | 782.5 | 20 | 20 |
| 8 | NIR | 835.1 | 115 | 10 |
| 8b | Narrow NIR | 864.8 | 20 | 20 |
| 9 | Water vapour | 945 | 20 | 60 |
| 10 | SWIR – Cirrus | 1373.5 | 30 | 60 |
| 11 | SWIR | 1613.7 | 90 | 20 |
| 12 | SWIR | 2202.4 | 180 | 20 |

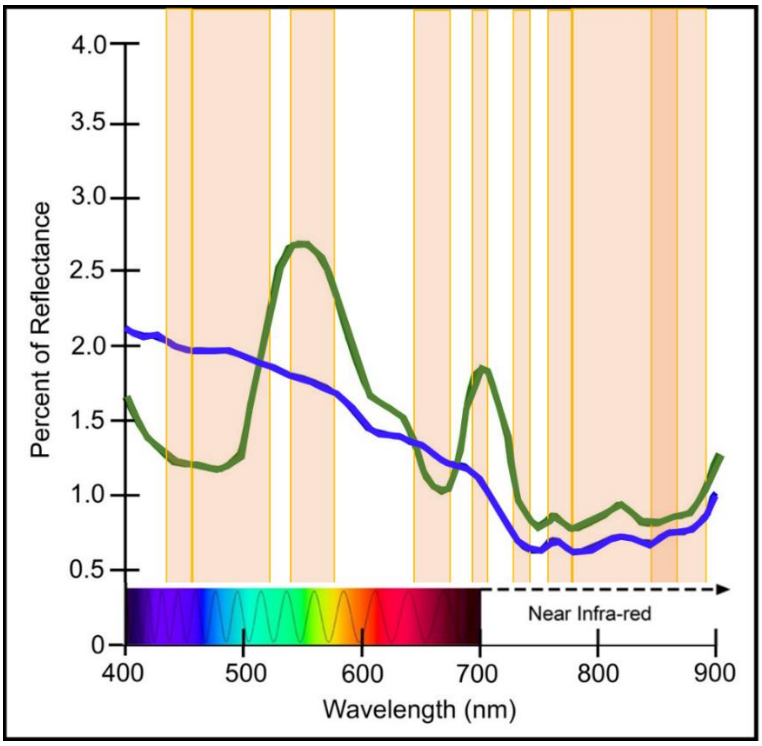


*Figure 11: Sentinel 2 bands against chlorophyll-a reflectance spectra; Adapted from (EOS, 2017; Han, 1997; SEOS, n.d.)*

## Analysis Software and platforms

In manipulating the datasets, the following software and platform were used:

### Sentinel's Application Program (SNAP).

SNAP is an open source common architecture for ESA Toolboxes ideal for the exploitation of Earth Observation data. SNAP is a free and open toolbox for processing data products from numerous satellite missions including Copernicus Sentinel-1, Sentinel-2 and Sentinel-3. It also allows processing of large amounts of satellite data owned by other organizations (e.g. Landsat, MODIS and RapidEye) (ESA, n.d.-b; Sharma, 2021).

SNAP was used in the preprocessing and visual analysis of MERIS data.

### ArcGis Pro

ArcGis Pro is a powerful single desktop GIS application that supports data visualization; advanced analysis; and authoritative data maintenance in 2D, 3D, and 4D (ESRI, n.d.). Although chlorophyll-a assessment can also be done in SNAP, it was preferred to use ArcGis Pro for convenience purposes. Data cleaning and mapping was also employed using this software.

*Google Earth Engine.* Earth Engine is a platform for scientific analysis and visualization of geospatial datasets. It is used for several purposes such as academic, non-profit, business and government uses. The platform hosts satellite imagery and stores it in a data archive made available to the public. This archive includes historical earth images going back more than forty years. The data are made available for global-scale data mining. Google Earth Engine also provides tools to enable the analysis of large datasets (Google, n.d.).

### Google Earth Engine

Google Earth Engine is a convenient tool in analyzing satellite data as it removes the need to download and preprocess data, and allows on-the-fly analysis. These data and processes are generally huge, time consuming, and has high computing requirements. Visual analysis of Landsat 5 and Landsat 8 images was done in this platform (Google, n.d.).

### iMMAP MENA Analysis Ready Data Cube (ARDC) - UN SDG Indicator 6.3.2

iMMAP MENA ARDC is a platform that allows big data queries and rapid time-series analysis of large satellite data archives including Sentinel 2, Landsat 5, Landsat 7 and Landsat 8. It was developed by iMMAP - an international not-for-profit organization providing information management services to humanitarian and development organizations. This research study was conducted in partnership with iMMAP which granted access to this analysis platform. iMMAP MENA ARDC allows on-the-fly analysis, thus eliminating processes such as data download and complex data preparation as well as the need for analysis tools and software and hardware resources (iMMAP, n.d.). Part of the platform is the UN SDG Indicator 6.3.2, a Python script developed for monitoring water quality. In this study, the script was slightly modified by adding the chlorophyll-a indices and equations selected from literature. Landsat 8 and Sentinel 2 were analyzed using this platform.

## Selection of indices for Chlorophyll-a Estimation

Chlorophyll-a index is an indicator of chlorophyll-a and not the concentration itself. Indices or algorithms are developed based on the chlorophyll-a reflectance pattern across the spectral wavelengths. When applied to satellite data, it takes as inputs reflectance values from corresponding satellite bands. To retrieve chlorophyll-a concentration estimates, values calculated from these indices is calibrated and validated with chlorophyll-a measurements taken in the field. Field data is represented by point locations of collected water samples which are analyzed in the laboratory. Statistical analysis is applied to the field data and the satellite-derived indices to establish a relationship or a model (in the form of an equation) which is then applied to the entirety of the lake throughout a given period.

In this study, three indices for chlorophyll-a retrieval were selected based on the following factors 1) well-established algorithms that has been successfully implemented in several studies on Case II waters with a wide range of chlorophyll-a concentration 2) utilizes the red-NIR region and not only the visual spectral region 3) applicability to the publicly available satellite sensors with respect to their spectral band positioning.

As there is no available and accessible in situ data of chlorophyll-a in Lake Qattinah, development of a model specific to the study area was not possible. To aid this, chlorophyll-a retrieval equations calibrated and validated in previous studies were used as alternative. In selecting such equations, additional factors listed below were considered:

1) utilization in a turbid productive lake with wide ranges of chlorophyll-a concentration. It was ensured that the algorithm and the equations were applied to water bodies similar to Lake Qattinah in terms of trophic status. As the study area is known to be eutrophic, studies covering eutrophic inland lakes, were selected. It was also ensured usage on a wide range of chlorophyll-a providing flexibility of the algorithms and the relationship to in situ data.

2) the scale to which they were used, calibrated and validated against a wide geographic coverage and seasonal variability on the study. Only those used in multiple lakes in different regions of the world, with varying climatic and environmental conditions, yet successful were selected. In cases when the model applied on a particular satellite data is not calibrated or validated in wide geographic range, studies on inland lakes of similar pollution status, climatic conditions were selected.

Two algorithms were used in this study and each is described in the next subsections.

### Two band NIR-red algorithm (2BDA)

This algorithm is based on two chlorophyll-a reflectance properties. First is the reflectance peak in the NIR region near 700nm and second is the strong absorption in the red region around 670nm (Matthews, 2011). Compared to traditional blue-green ratio, it is less sensitive to absorption by CDOM and scattering by mineral particles, thus making it suitable for turbid productive waters like lakes, which are dominated by such water components (A Gitelson et al., 2009; Matthews, 2011). Chlorophyll-a concentration is highly correlated with the magnitude of reflectance around 670nm. However, the latter is not only driven by chlorophyll-a but is also influenced by the concentration of other water constituents such as total suspended solids. In the NIR region, the absorption by all particles and dissolved constituents is null (A Gitelson et al., 2009). The NIR-red ratio combines the two properties by taking the ratio of the reflectance near 700nm to the reflectance near 670nm. The height and the position of the peak is highly correlated with chlorophyll concentration, with the peak shifting towards greater wavelengths and the magnitude increasing with increasing chlorophyll concentration (Matthews, 2011) for lakes with chlorophyll-a range greater than 3-5mg/m3 (Moses et al., 2009). Moses et al. (2009) added that in this chlorophyll-a concentration range, the minimum in reflectance resulting from the phytoplankton absorption peak around 675nm also becomes more pronounced as chlorophyll-a increases.

The two band NIR-red ratio is not limited to wavelengths at 700nm and 670nm. Some studies employed some slight modifications of this index. Gitelson (1993) and Gitelson et al. (1993) used the ratio of the reflectance in 705 nm and 670 nm. Gons (1999) used the ratio of reflectances at 704 and 672, the absorption coefficients of water at these wavelengths and backscattering coefficient at 776nm in estimating chlorophyll concentration with a range from 3 to 185mg/m3. Other studies found strong correlation of chlorophyll concentration and the ratio with red wavelength near 675 and NIR region ranging from 700nm to 725nm (Dall'Olmo & Gitelson, 2005; Oki & Yasuoka, 2002; Zimba & Gitelson, 2006).

In using the two band NIR-red algorithm, it is important to note the assumptions in its development. 2BDA assumes that some optical parameters such as the phytoplankton absorption coefficient and chlorophyll-a fluorescence quantum to remain constant. In reality, these parameters widely vary depending on the physiological state and structure of the phytoplankton community (Gitelson et al., 2009); hence, such assumption poses a level of uncertainty that must be taken into consideration. Nevertheless, this algorithm has provided good results in well-mixed, high biomass waters, has been widely used in chlorophyll-a concentration estimation (Matthews, 2011) and tested on several water environments (Gholizadeh et al., 2016). This algorithm has been successfully applied and validated in different satellite data including but not limited to MERIS

(Gilerson et al., 2010; Gurlin et al., 2011; Yacobi et al., 2011), Sentinel2 (Bramich et al., 2021; Johansen et al., 2018; Sòria-Perpinyà et al., 2021) and Landsat 8 (Deutsch et al., 2018; Masocha et al., 2018; Watanabe et al., 2015).

Generally, the model is expressed as follows:

$$2BDA = R(\lambda 1)/R(\lambda 2)$$

where $R(\lambda 1)$ and $R(\lambda 2)$ refer to the reflectance peak in the NIR region near 700nm and the minimum reflectance in the red region near 670nm, respectively.

When applied to MERIS, Sentinel 2 and Landsat 8 bands, the equations are as follows:

$$2BDA_{MERIS} = R_{708.75nm}/R_{665nm} = R_{B9}/R_{B7}$$

$$2BDA_{L8} = R_{850\text{-}880nm}/R_{630\text{-}670nm} = R_{B5}/R_{B4}$$

$$2BDA_{S2} = R_{703.9nm}/R_{664.5nm} = R_{B5}/R_{B4}$$

**Three band NIR-red algorithm (3BDA)**

The advanced version of the red-NIR algorithm is the three band NIR-red algorithm proposed by (Dall'Olmo & Gitelson, 2005). By including three bands, this index enables better separation of the absorption by chlorophyll-a from the absorption and scattering contributed by other water constituents.

Three band algorithm uses three optimal wavelengths selected in a way that contributions due to absorption by constituents other than chlorophyll-a and backscattering by particles are kept to negligible minimum, and the model output is maximally sensitive to chlorophyll-a concentration (A Gitelson et al., 2009).

The general formula is as follows:

$$3BDA = \qquad R(\lambda_3)\left[\frac{1}{R(\lambda_1)} - \frac{1}{R(\lambda_2)}\right]$$

where R(λ1) is the reflectance in the wavelength (red region near 670nm) where chlorophyll-a absorption is maximal but may be affected by absorption by other pigments and scattering by all particulates; R(λ2) is the reflectance in the wavelength where there is minimal absorption by chlorophyll-a and the absorption by other constituents is about the same as in λ1 (NIR near 710 nm). Thus, R(λ1) accounts for the absorption by chlorophyll-a and other constituents, R(λ2) accounts for absorption by other constituents other than chlorophyll-a (nonalgal particles and CDOM), and the difference accounts for the absorption by chlorophyll-a only. R(λ3) is the reflectance in the wavelength beyond λ1 in the NIR region which is minimally affected by absorption by all particles and dissolved constituents such as chlorophyll-a, CDOM and non-algal particles and represents the scattering by particles (near 750nm). 3BDA is therefore an algorithm that enables negligibility of contributions due to absorption by water constituents other than chlorophyll-a and backscattering by particles. This model is maximally sensitive to chlorophyll-a concentration (A Gitelson et al., 2009; Matthews, 2011; Moses et al., 2009).



In various studies, the three wavelengths (λ1, λ2 and λ3) slightly vary. (Dall'Olmo & Gitelson, 2005) identified that the optimal wavelengths for chlorophyll-a concentration ranging from 2 to 180mg/m3 are as follows: 1 = 670nm, 2 = 710nm and 3 = 740nm. According to Gitelson, Schalles and Lhadik (2007), optimal wavelengths can be wider: 1 = 660 – 670nm, 2 = 700 to 720nm, 3 = 730=760nm (All in Chapter 18). These studies provided accurate chlorophyll-a concentration estimates. (Dall'Olmo & Gitelson, 2005) reported that 3BDA success in predicting accurate estimate of chlorophyll-a in turbid productive water bodies with a wide range of optical complexity. (Moses et al., 2009) validated the algorithm using MERIS data in the Azov Sea, and reported that the algorithm retrieved chlorophyll-a concentration successfully for a range of 18.37 to 47.86mg/m3.

When using the three band algorithm, it is important to note the main assumptions 1)that backscattering coefficient is considered spectrally uniform across wavelengths (lambda 1 to 3) and that it can be sufficiently estimated from the wavelengths in the NIR.; 2) the absorption by suspended solids and CDOM beyond 730nm is approximately equal to that at the red region (665-675nm) and the difference between them is negligible 3) the total chlorophyll-a, CDOM and TSS absorption beyond 730nm is nearly zero (Dall'Olmo & Gitelson, 2005; Mishra & Mishra, 2012). 3BDA has been successfully applied and validated using various satellite data including but not limited to MERIS (Gilerson et al., 2010; Gurlin et al., 2011; Moses et al., 2009) and Sentinel 2 (Ansper & Alikas, 2018; Buma & Lee, 2020; Grendaitė et al., 2018; Johansen et al., 2018).

When applied to MERIS data, the formula is:

$$3BDA_{MERIS} = [(R_{B7})^{-1} - (R_{B9})^{-1}] \times (R_{B10})$$

For Sentinel 2,

$$3BDA_{S2} = [(R_{B4})^{-1} - (R_{B5})^{-1}] \times (R_{B6})$$



## Chlorophyll-a retrieval equations from literature

In developing empirical algorithms for chlorophyll-a retrieval, the steps include 1) calculating the chlorophyll-a index from satellite data band reflectance (*i.e.*, 2BDA equation is calculated from corresponding MERIS or Sentinel 2 input bands; the data is preferably concurrent with the collection dates of field data) 2) field or in situ data is gathered then divided into two sets – one is a training or calibration set and the other is a validation set 3)regression is applied to get the relationship between the calculated index from 1 and training data set in order to formulate a chlorophyll-a retrieval equation. Corresponding $R^2$ is noted, and generally, 0.50 and higher values of $R^2$ is considered highly correlated in literature. 4) the formulated retrieval equation for chlorophyll-a estimation is then again compared with the second set of field data for validation. High $R^2$ values indicate that the model accurately estimates chlorophyll-a.

In order for a model to be robust, it is important that the in situ data gathered is huge enough to represent different parts of the water body. It is also necessary that seasonal variability is considered in field data gathering to ensure stronger representation of the lake's status in various conditions. In this study, no in situ data is available and accessible so development of an empirical model specific to Lake Qattinah is not possible. As an alternative, chlorophyll-a retrieval models from literature selected based on factors given in the previous section, were directly applied to the study area. Four different 2BDA equations and  four different 3BDA equations were selected. 3BDA index was not used in Landsat images due to lack of necessary band. The equations are presented in Table 10.

*Table 10: List of chlorophyll-a retrieval equations retrived from previous studies*

| Index | Equation | Equation: chla = | Source | Direct application of equations | | |
|---|---|---|---|---|---|---|
| | | | | MERIS | Landsat 8 | Sentinel 2 |

| | | | | | | |
|---|---|---|---|---|---|---|
| 2BDA | chl_2bda_eqn1 | $25.28x^2+ 14.85x - 15.18$ | (Gurlin et al., 2011) | Yes | Yes | Yes |
| 2BDA | chl_2bda_eqn2 | $41.127x-23.484$ | (Yacobi et al., 2011) | Yes | Yes | Yes |
| 2BDA | chl_2bda_eqn3 | $61.324x - 37.94$ | (Moses et al., 2009) | Yes | Yes | Yes |
| 2BDA | chl_2bda_eqn4 | $(35.75x-19.30)^{1.124}$ | (Gilerson et al., 2010) | Yes | Yes | Yes |
| 3BDA | chl_3bda_eqn1 | $315.5x^2 + 215.95x + 25.66$ | (Gurlin et al., 2011) | Yes | No | Yes |
| 3BDA | chl_3bda_eqn2 | $80.167X + 17.105$ | (Yacobi et al., 2011) | Yes | No | Yes |
| 3BDA | chl_3bda_eqn3 | $232.329X + 23.174$ | (Moses et al., 2009) | Yes | No | Yes |
| 3BDA | chl_3bda_eqn4 | $(35.75X - 19.30)^{1.124}$ | (Gilerson et al., 2010) | Yes | No | Yes |

Where x is the corresponding index value; e is a mathematical constant equal to approximately equal to 2.7182818.

**Chl_2bda_eqn1 and chl_3bda_eqn1.** These models developed by (Gurlin et al., 2011) were calibrated and validated using spectral bands of MERIS and field data collected in Fremont Lakes in Nebraska USA. Field data were collected from 89 stions in summer and autumn of 2008 and at 63 stations in spring and summer 2009. Fremont Lakes consist of 20 sandpit lakes whose chlorophyll-a concentrations range from 2.3 to 200.8 mg/m3 in the study years. These lakes have a highly variable bio-physical and bio-optical conditions which are typical for many inland and coastal waters, making these lakes ideal for algorithm development for remote estimation of chlorophyll-a concentrations in turbid productive waters. The models were calibrated using dataset collected in summer and fall 2008, resulting to R2 of 0.95 for both 2BDA and 3BDA indices. The validation of the model was done using the 2009 field data and MERIS reflectance resulted to 3BDA model with an MAE of 2.5mg/m3 for chl range of 0 to 100mg/m3 and MAE of 1.9mg/m3 for chlorophyll-a range of 0-25mg/m3. 2BDA estimated chl with an MAE of 2.3mg/m3 for chlorophyll-a range of 0-100mg/m3 and 1.2mg/m3 for chl range of 0-25mg/m3.

This model was also tested by Yacobi et al (2011) who studied the performances of two and 3 band models in Lake Kinneret, Lebanon. Chl a was accurately estimated using a model that is only silightly different from the models.

**Chl_2bda_eqn2 and chl_3bda_eqn2.** These models were calibrated and validated using in situ acquired from four campaigns on Lake Kinneret, Israel in May and June 2009. This in situ data covers a total of 56 samples. Lake Kinneret is a meso-eutrophic, Case 2 water body. This model was compared to a model calibrated using in situ data from Fremont Lakes in Nebraska (as in equation 1), and the results were highly similar.  In other words, the model for chlorophyll retrieval, calibrated using field data from Fremont lakes was applied to Lake Kinneret. It produced almost similar chlorophyll-a estimates from the model calibrated using local in situ data collected from lake Kinneret. These findings suggested that the MERIS models 2BDA and 3BDA can be applied universally in other regions.

**Chl_2bda_eqn3 and chl_3bda_eqn3. These models were calibrated and validated** using MERIS satellite reflectances and in situ data collected in Tanganrog Bay and Azov Sea in April, July, September and Oct 2008 and March 2009. 2008 data collected from 18 stations were used to calibrate the relationship between chlorophyll-a concentrations and the values from the indices. Data collected in 2009 were used to validate the chlorophyll-a retrieval models. The calibration of the model resulted to an R2 of 0.95 and 0.97 for both 3BDA and 2BDA respectively. The RMSE is 5.02mg/m3 and 3.65mg/m3 for 3BDA and 2BDA respectively.

The 2 BDA and 3BDA chlorophyll-a retrieval models were compared to the model derived from in situ data collected in 2008 from several lakes in Nebraska (as in Chl_2bda_eqn1 and chl_3bda_eqn1). It was found out that there is only a slight difference in the 2 models.

**Chl_2bda_eqn4 and chl_3bda_eqn4.** These advanced models were developed by Gilerson et al (2010) who combined simulated datasets of reflectance spectra and inherent optical properties, with in situ data from Fremont Lakes. The simulated data includes about 2000 reflectance spectra simulated using Hydrolight for a wide range of typical conditions of inland and coastal waters. MERIS data was the satellite bands used in the study. It considered differences in values of absorption by various water constituents such as algae, non-algal particles, CDOM and absorption by water. The advanced algorithms were validated using the 2009 in situ data of Fremont Lakes. 3BDA an 2BDA advanced accurately estimated chlorophyll-a in chlorophyll-a ranges of 0-25mg/m3 and 0-100mg/m3. There was a very close relationship between the field data with both 2BDA and 3BDA models, with $R^2$ above 0.95 for both.

Most of these equations was calibrated in Fremont Lakes and tested on other regions of the world. Results of the comparison showed chlorophyll-a estimates close to in situ data collected from each of the study areas. While most of the equations were developed using MERIS bands, they were also applied to Sentinel 2 bands for a reason that the latter also have bands positioned in necessary wavelengths (near 700 and 670). These sentinel bands, however, have broader band widths than

MERIS, which could possibly cause some differences in values. As for Landsat 8, other chlorophyll-a equations had to be included for because it lacks bands near 700nm, a typical challenge in estimating chlorophyll-a from the satellite data L8.

## Assessment of algal concentration of the lake prior to the war

### Visual inspection and spectral inspection of the lake

The first step in analyzing the water quality of the lake prior to the war was looking at the temporal and spatial patterns of algae. A simple visual analysis was employed on Landsat 5 data using Google Earth Engine. Landsat 5 TM imageries were loaded in Google Earth Engine for each of the months of 2010 and 2011. The image taken during the clearest date was selected per month. Some months, mostly in winter and spring, were not represented due to thick cloud coverage obstructive view of the lake. Each of the available images were visually analyzed by applying false color composite (FCC) provides information on algal growth in a lake. FCC uses the NIR, green and blue spectral bands to channels RGB respectively. In this band combination, vegetation and algae appear red because of high reflectance in the NIR spectrum. FCC shows lighter color in areas not covered by floating/emergent vegetation. This method was employed to make use of the high spatial resolution of Landsat 5 allowing the capture of spatial variations of algae in the lake, especially those areas highly impacted by point source pollution sources.



While Landsat 5 data can provide clearer spatial variations, MERIS data is limited to its coarse images. However, its spectral configuration is superior than that of Landsat 5 in terms of algae or chlorophyll-a assessment. It was used to compliment the visual results of Landsat 5, providing information on other areas of the lake where algae are not obvious.

The processes employed are as follows:

**Data preparation.** MERIS data is not included in the Data Cube platform nor in Google Earth Engine, so manual data processing was employed. The data was processed using SNAP and ArcgisPro, instead of an on-the-fly analysis. Downloading a single satellite data took 6 to 8 hours. For this reason, only one day data were analyzed for selected months (Table ). While this cannot capture the changes throughout time of algal growth, this is only a supporting process to quantify chlorophyll concentration in the lake prior to the war, which in the first place is already known to be highly eutrophic. The chlorophyll estimates were computed using this data to gain insights on the potential range of chlorophyll values in the lake, calculated from the models.

The processes employed are elaborated below:

**Data preparation.** The first part of the analysis was to prepare the data. The subset of the MERIS bands were first generated to cover only the study area and the bands necessary for the analysis - "rho_w". The purpose of this is to reduce the data size and increase the speed of processing. The next step was reprojecting the subset into "Geographic Lat Long WGS 84" so it can be overlayed and analyzed along with other data (satellite basemap, Lake Qattinah shapefile) in the ArcgisPro.

**Spectral Visualization.** Following the data preparation was a simple visualization and spectral pattern inspection, both possible in SNAP software. False color composite was also applied to MERIS bands 13, 5, 1 to easily see the bounds of the lake and the areas around it; however,

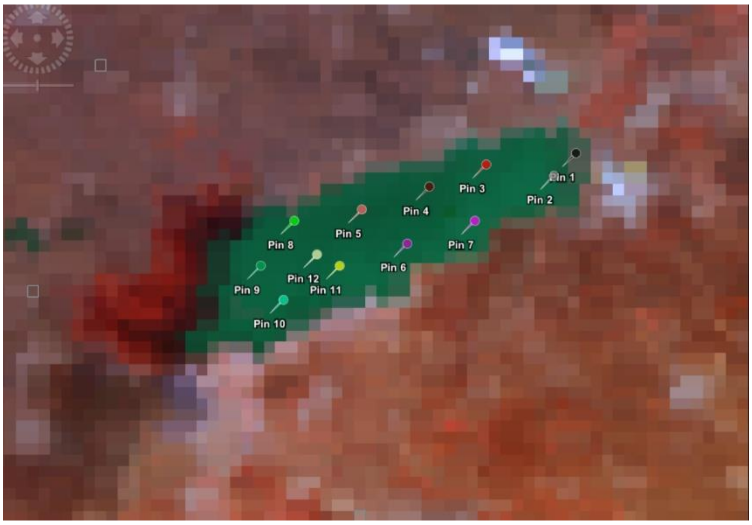


*Figure 12: Distribution of sample points in the lake; own creation*

unlike Landsat 5 and Landsat 8, it was not useful in looking at the spatial distribution of algae due to its coarse spatial resolution. MERIS data being specifically used for water quality studies provides important information that Landsat 5, Landsat 8 and Sentinel 2 does not fully capture due to spectral band positioning differences. To take advantage of such information at least for the years prior to the war, the spectral signature of some selected sample points in the lake were inspected, taking into consideration the typical reflectance pattern of chlorophyll-a rich waters. The **12** sample points (Figure 12) were randomly located in different areas of the lake, to be able to capture the status of the lake not seen in the visual inspection done using Landsat 5.

The spectral signature of each of the selected images are presented in graphs.

### Estimation of chlorophyll-a concentration using 2BDA and 3BDA models applied on MERIS

Only 2 images (one for August and one for September) were analyzed. These months were prioritized as algae generally proliferates during the hottest and driest months, which is also supported by the results from Landsat 5 inspection. Other images for months of June, July, and October were also initially processed but later removed from the analysis due to several erroneous pixels in the images resulting from atmospheric correction.

Although the analysis can be done in SNAP, QGIS was chosen convenience purposes. Raster Calculator was used to calculate the indices. In total, 6 results were generated from 3 indices for Aug and September 2010 Table 11. From each of the indices, 4 different equations for chlorophyll-a concentration estimation were used. In total, 20 outputs are generated from the MERIS data: 2 indices for August, 2 indices for September, 8 chlorophyll-a concentration estimates for August, and another 8 for September. To finalize the chlorophyll-a estimates, the average of the 4 equations for each of the two indices were calculated.

The general process flow is elaborated in Figure 13 :

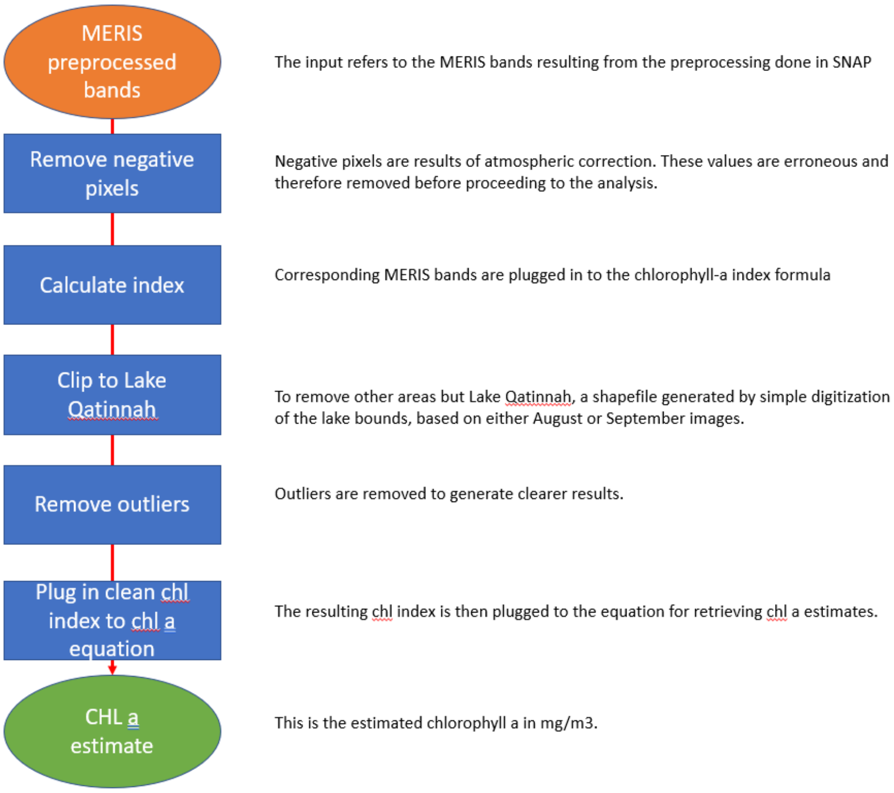


*Figure 13: Process flow for estimating chlorophyll-a concentrations from MERIS; own creation*

*Table 11: Generated data from MERIS analysis (indices and chlorophyll-a estimates)*

| August 2010 | | September 2010 | |
|---|---|---|---|
| Index 1: 2BDA | Chl a est from Equation 1 | Index 1: 2BDA | Chl a est from Equation 1 |
| | Chl a est from Equation 2 | | Chl a est from Equation 2 |
| | Chl a est from Equation 3 | | Chl a est from Equation 3 |
| Index 2: 3BDA | Chl a est from Equation 1 | Index 2: 3BDA | Chl a est from Equation 1 |
| | Chl a est from Equation 2 | | Chl a est from Equation 2 |
| | Chl a est from Equation 3 | | Chl a est from Equation 3 |
| | Chl a est from Equation 4 | | Chl a est from Equation 4 |

To summarize the results into a single chlorophyll-a estimate for each of the indeces, the average of the estimates from the four equations were taken. The results from equations using 2BDA were close to one another. Similarly, the estimates from the 3BDA-based equations were also not highly variable. However, an inter-index comparison showed huge difference in chlorophyll-a concentrations with 3BDA models acquiring higher values than 2BDA models. For this reason, the averages were taken separately based on the index used.

## Assessment of algal concentration of the lake during the war

Landsat 8 and Sentinel 2 were analyzed using DataCube. which allows processing of huge data without the need to download them. Rather, the analysis is done online and only the desired results are exported to the computer. With the help of this program, a more encompassing analysis became possible. The platform allows several user inputs such as the satellite sensor (Landsat 5 to 8 and Sentinel 2), date range and study area bounds. The satellite data in the Data Cube are already atmospherically corrected; hence, representing only water reflectances and excluding the atmospheric contribution.

For this part of the study, seasonal analysis was conducted for years 2013 to 2020; DataCube was run for each of the seasons for all the years, generating different chlorophyll indices and chlorophyll estimates from all the above mentioned algorithms and equations.

Figure 14 provides an overview of the processes undertaken when running the code for a specific period.

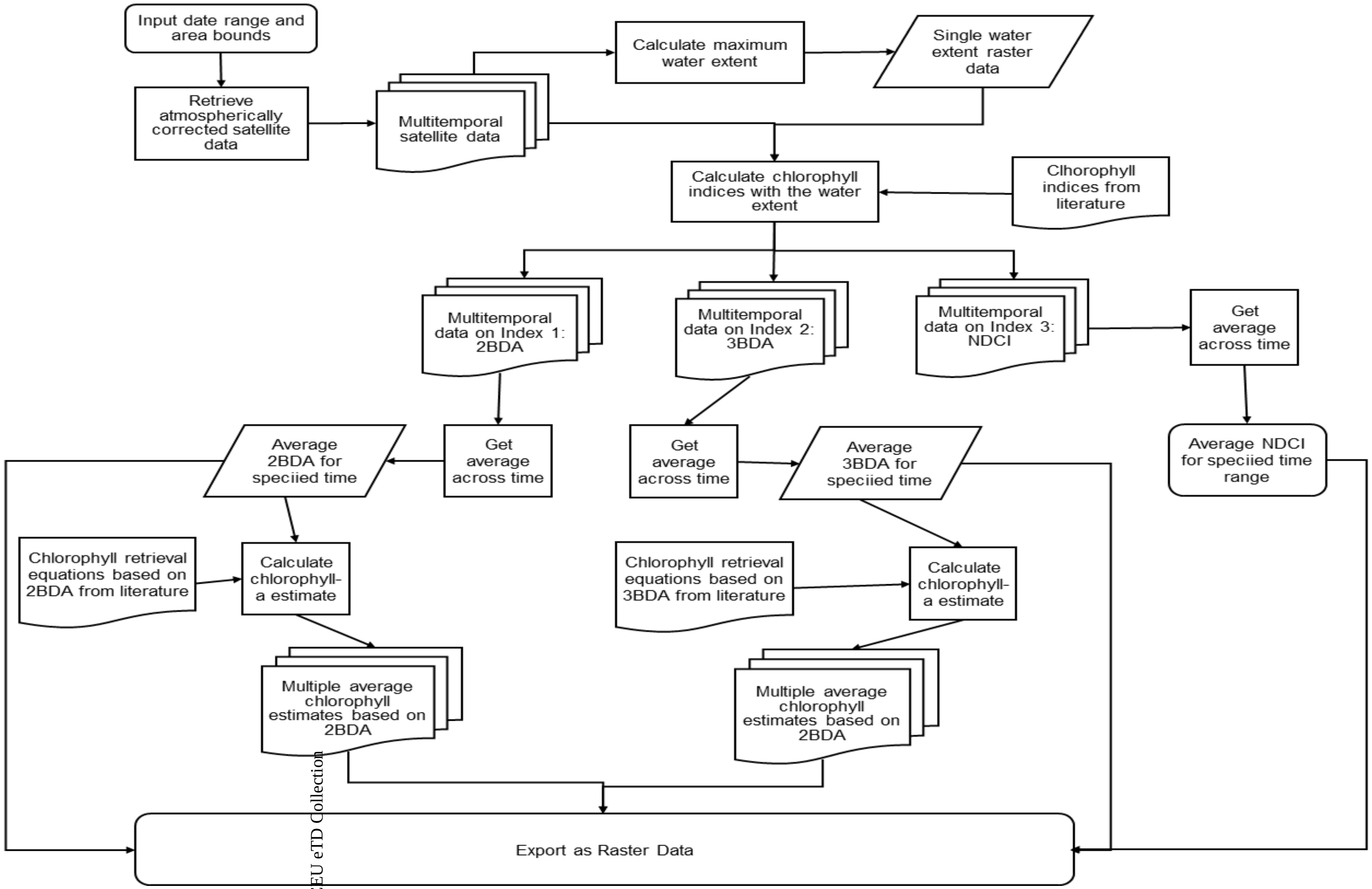



*Figure 14: Workflow for the multitemporal assessment of chlorophyll-a concentrations from Landsat 8 and Sentinel 2; own creation*

For instance, to get the water quality status of the lake for summer 2018 from Sentinel 2, the following inputs are fed to the script:

Date = 2018 – 06 – 01 to 2018 – 08 – 31

Satellite = S2

latitude = (34.600, 34.671)

longitude = (36.500, 36.620)

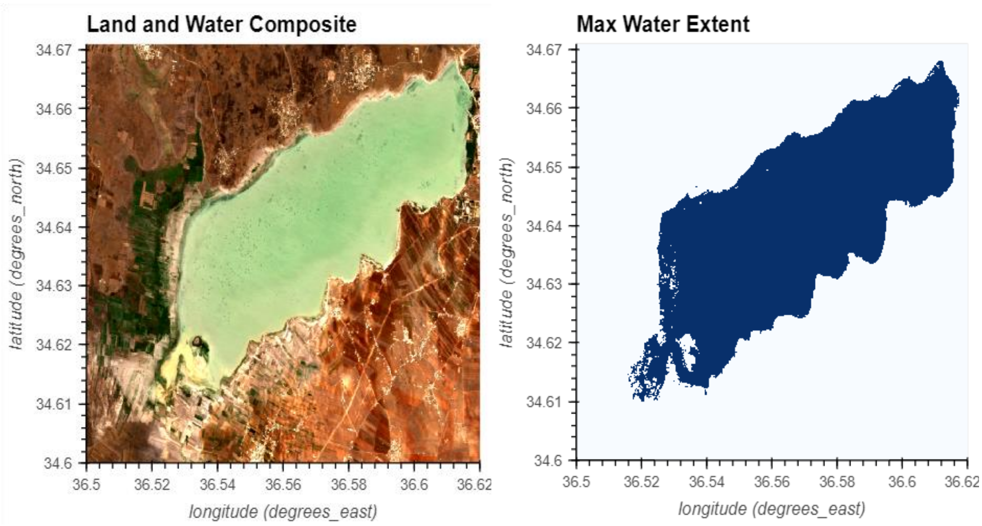


*Figure 15: Sample image composite and water extent generated from DataCube*

When the code is run, it returns all the Sentinel 2A satellite images within the date range of the specified study area, with cloud cover already masked, if any. It then generates the maximum water extent from the multiple satellite images. Next, it calculates the chlorophyll indices as the chlorophyll-a estimates derived from the indices masked using the generated water extent. Then, it gets the average values of each of pixels from June 6, 2018 to August 31, 2018, producing 12 different raster data for summer of 2018, 2 of which are the indices, 4 chlorophyll estimates from 3BDA index and another 4 from 2BDA, 1 natural color composite image, and 1 water extent file (Figure 15 and Figure 16) . This dataset is for one season of a year. Ideally, for 8 years (2013 – 2020), the total number of generated files from Datacube is 384. However, due to cloud cover mainly during winter and spring, some seasons were not represented.


*Figure 16: Generated raster outputs from running DataCube*

All the mentioned generated data are downloaded and further manipulated in ArcgisPro as such processes are currently outside the current scope of Datacube.

Similar to MERIS data in the previous section, the chlorophyll-a estimates from the equations using 2BDA index are closely related and same is true for 3BDA equation estimates. However, comparing across different indices, 3BDA chlorophyll-a values are generally higher than those from 2BDA-based equations and getting their overall mean was not seen to be the best option. To present the values of chlorophyll from different equations, they are averaged per index using Raster Calculator as described by the formula below:

$$\text{Avg chla}_{2BDA} = (\text{chl2bda\_eqn1} + \text{chl2bda\_eqn2} + \text{chl2bda\_eqn3} + \text{chl2bda\_eqn4})/4$$

$$\text{Avg chla}_{3BDA} = (\text{chl3bda\_eqn1} + \text{chl3bda\_eqn2} + \text{chl3bda\_eqn3} + \text{chl3bda\_eqn4})/4$$

Consequently, the resulting raster averages were cropped out using the water boundary. This boundary was based on the water extent generated from Datacube (*e.g.,* Figure 15) modified by cropping out areas that are obviously flooded. Shallow areas can include reflectance contributions of the bottom surface of the lake, leading to erroneous water leaving reflectance values. To simplify this process, summer and autumn water levels (which are generally lowest in any given year) were used as the basis for delineating the water boundary.

The processes from Datacube to ArcgisPro is repeated for the other seasons from 2013 to 2020.

**Comparison of the performances of Landsat 8 and Sentinel-2.**

The data used in the second and third time period came from two different satellites – Landsat 8 and Sentinel 2, respectively – which have differences in some configurations  including band width and positioning. With this, it is expected that the results from the two data sources are different. To understand up to what extent this might affect the results of the study, chlorophyll-a estimates were compared for a period that is both captured by the satellites -2017 onwards. For simplification and convenience purposes, only autumn season from 2017 to 2020 were compared, considering that algae is generally highest and most variable across the lake at this time of the year.

# RESULTS

## Chlorophyll-a concentrations and patterns before the war

### Spatial and temporal patterns from Landsat 5.

The results of the visual inspection using Landsat 5 as shown in Figure 17, provides initial insights on the spatial and temporal pattern of algae proliferation in the lake. No clear images were taken for the months of January, May and September but the results remain representative of different seasons of the year. The lake appears blue and clear from  February to April when there is significantly abundant rainfall and low temperature in the area. As the months get drier and hotter starting June, floating or emergent vegetation and/or algae began to show especially on the eastern portion of the lake. It became more apparent in October, then decreased in November until it can be barely seen in December, with the increased rainfall and decreased temperature.

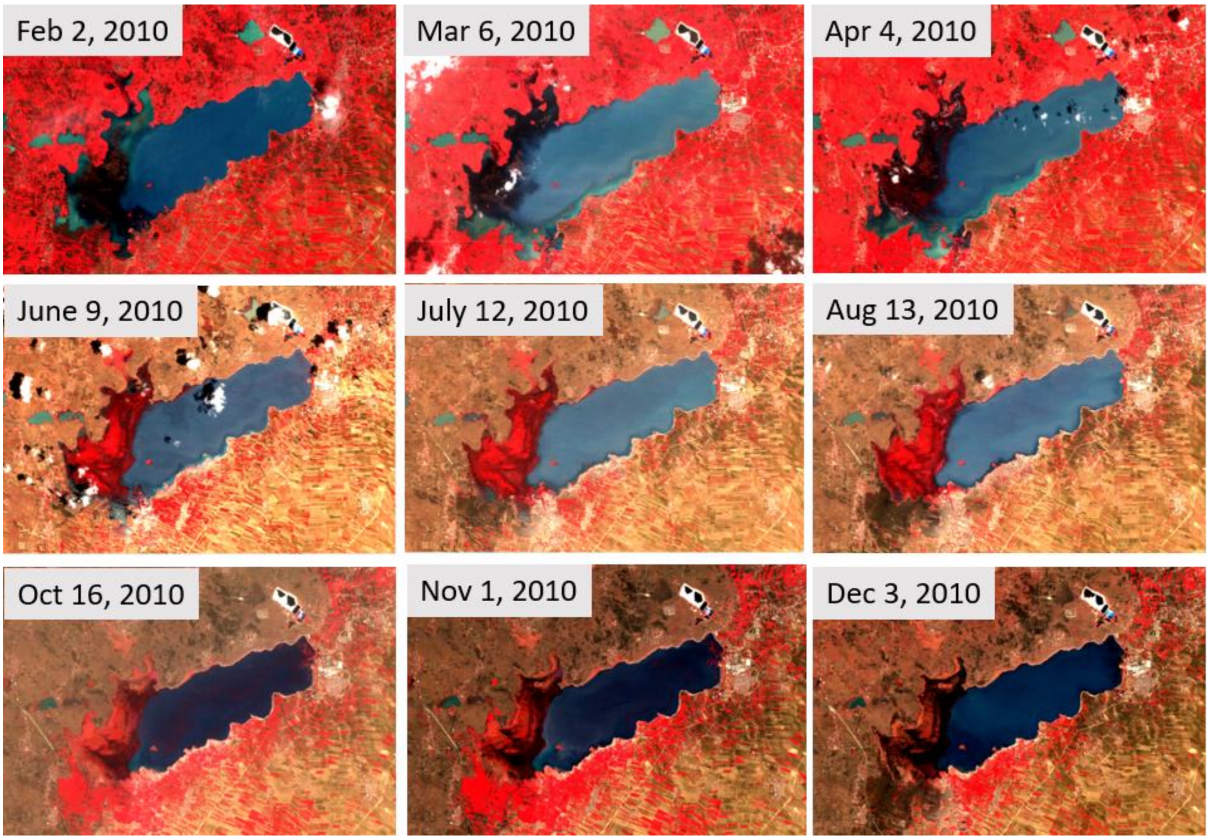


*Figure 17: Landsat 5 FCC emphasizing prominent spatial feature of algae in 2010*

The same pattern is seen in 2011 when clear images were acquired for 6 months (Figure 18). Bluish water is seen in the first quarter of the year (January and April), and floating vegetation and/or algae become prominent on the eastern side from July to October. There are no clear images for the months of November and December, but it is expected that the eastern side of the lake would clear up as in 2010.

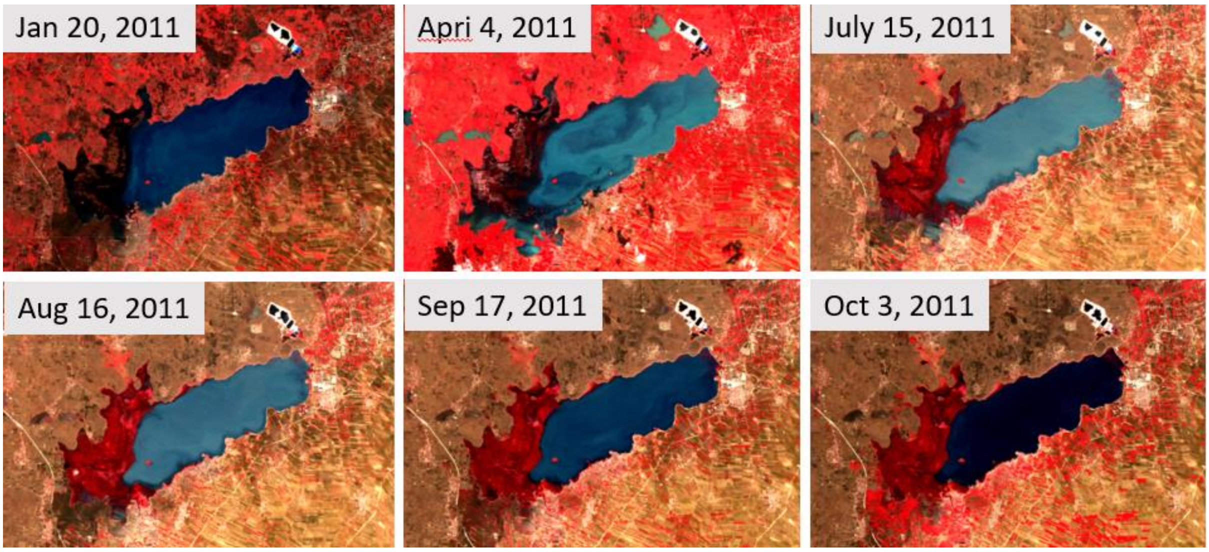


*Figure 18: Landsat 5 FCC emphasizing prominent spatial feature of algae in 2011*

### Spectral patterns and chlorophyll-a concentration estimates from MERIS

Simple visual inspection via FCC is not well-appropriate to MERIS data due to its lower spatial resolution limiting its capability to capture spatial differences. As seen in figure below, it is more difficult to deduce whether the spatial pattern seen from Landsat 5 is consistent with that of MERIS as the image is coarse. Nevertheless, MERIS provides data with more pronounced spectral information. Figure 19 shows the reflectance pattern at different days of 15 random sample points located in different areas of the lake. The spectral signature of each of these points exhibit similar patterns are similar to that of algae-rich waters as represented by chlorophyll-a. For the months of June and July, there are some sample points with negative reflectance. This is due to some error from the atmospheric correction to generate only water leaving reflectance. This data is not included in the analysis.

The spectral signature approach applied on MERIS data provides findings not seen in the simple FCC visual inspection done with Landsat 5. Results suggest that algae are present not only on the eastern side but also on all tested areas of the lake.

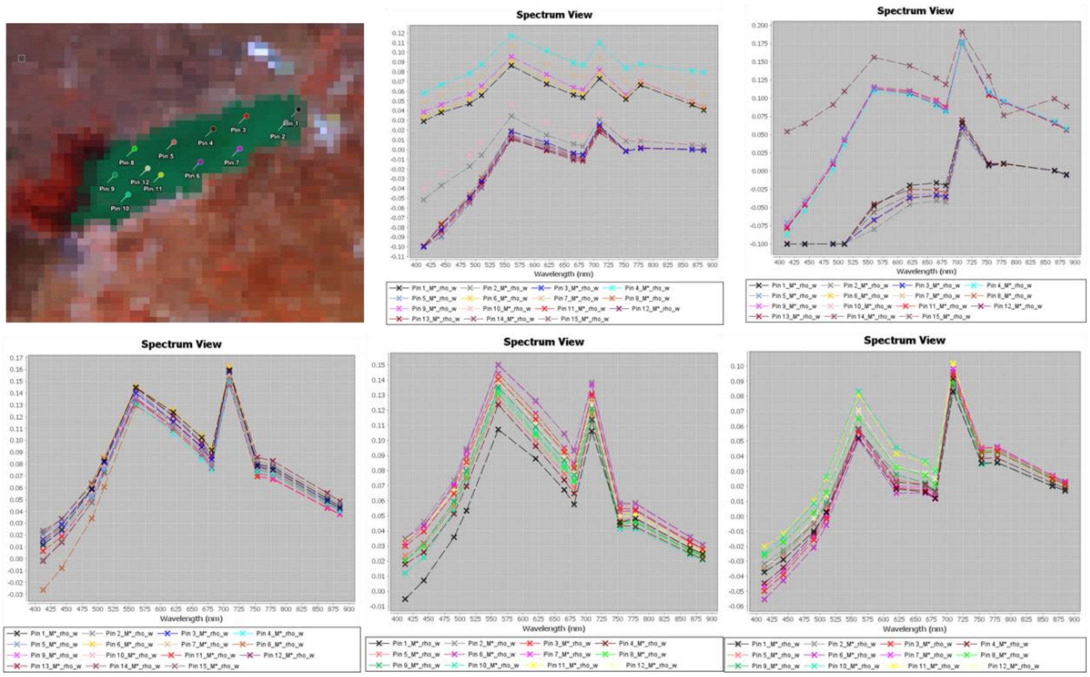


*Figure 19: Reflectance pattern of MERIS data in different areas of the lake; ; own creation*

While the results generated further provides evidence that the lake was already polluted before the war, it lacks information on the spatial and temporal trend generated from MERIS data, that would support the findings from Landsat. Moreover, it also lacks information as to the estimates of chlorophyll-a concentration in the lake. For this process, only August and September were analyzed due to the negative reflectance in other months that removed most pixels of the images. The results of the chlorophyll-a index retrieval in August is shown in Figure 20. High index values entail high chlorophyll-a concentration. The pattern obtained from the three different indices is similar, with high values on the northern as well as the eastern and western edges of the lake, and relatively low values on the southern portion. It is important to note that the lowest (darkest blue) and highest (yellow) valued pixels on the edges of the lake are probably affected by the land adjacency error and/or bottom surface noise and therefore must be out of consideration.

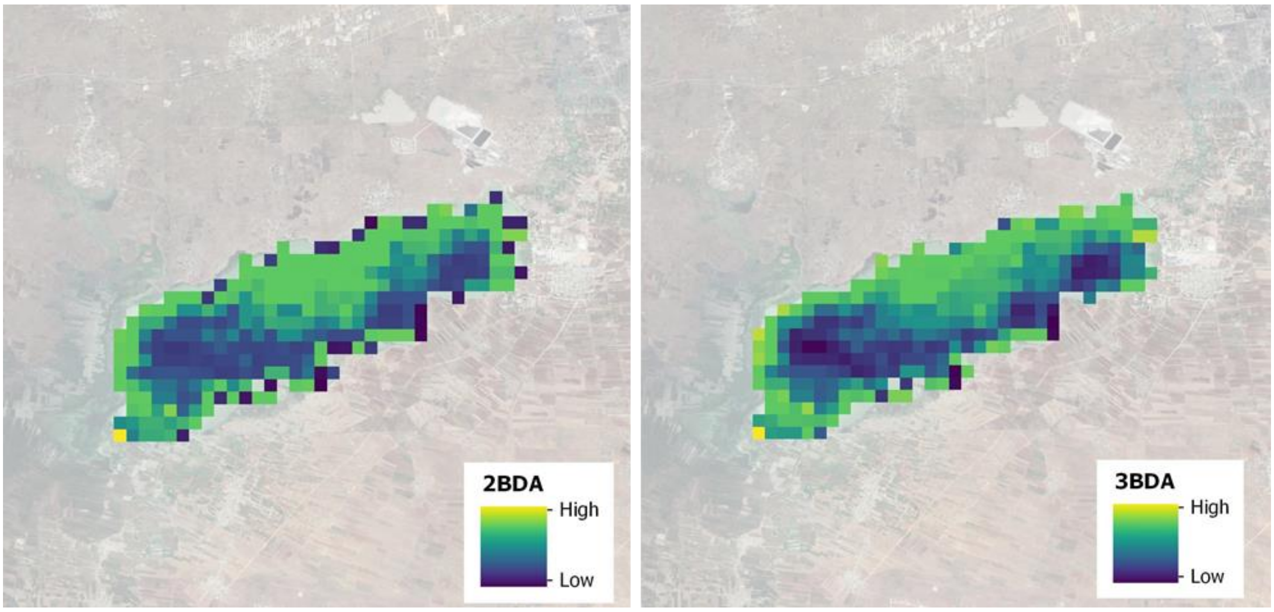


*Figure 20: Sample of generated 2BDA and 3BDA indices (August 15, 2010)*

Figure 21 and Figure 22 show the chlorophyll-a estimates of Lake Qattinah in August 15 and September 16, 2010 derived from 2BDA and 3BDA models. Both models resulted to high chlorophyll-a concentrations in the lake with the earlier date having higher values. The estimated average chlorophyll-a concentration (mg/m3) from 2BDA retrieval equations ranges from 41.3 to 216.4 mg/m3 with a mean of 69 mg/m3 for August 15 and a range of 36.1 to 129.9 mg/m3 with a mean of 51.6 mg/m3 for September 17. 3BDA model had higher estimates than the 2BDA model. The estimated values range from 72.2 mg.m3 to 124.8 mg/m3, with a mean of 98.3 mg/m3 on August 15 and 44 – 98.3 mg/m3 with m mean of 57.9 mg/m3 in September 16 (Figure 21). Following both Carlson index and the OECD criteria for classification of lakes, Lake Qattinah is a eutrophic water body. On the other hand, 2BDA appears to be more sensitive to land adjacency error and/or bottom surface noise as reflected by the extremely high values of pixels in the edges of the lake. Despite the differences in the estimates, both models exhibit almost similar spatial and temporal patterns. The northern part of the lake has higher chlorophyll-a concentration than the south. Both models resulted to higher concentration in August 15 than September 16.

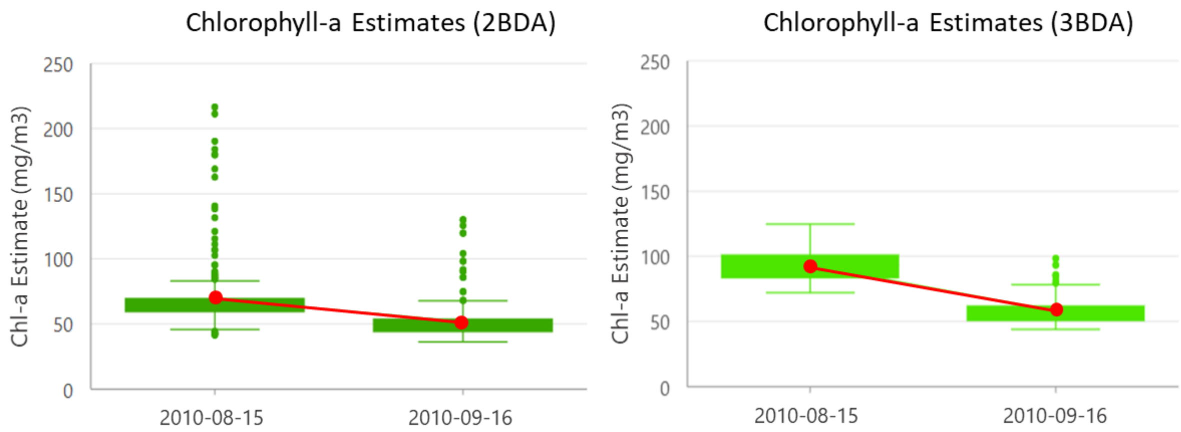


*Figure 21: Boxplots presenting statistical values (mean, percentiles, outliers and extremes) of chl-a concentrations in 2010*

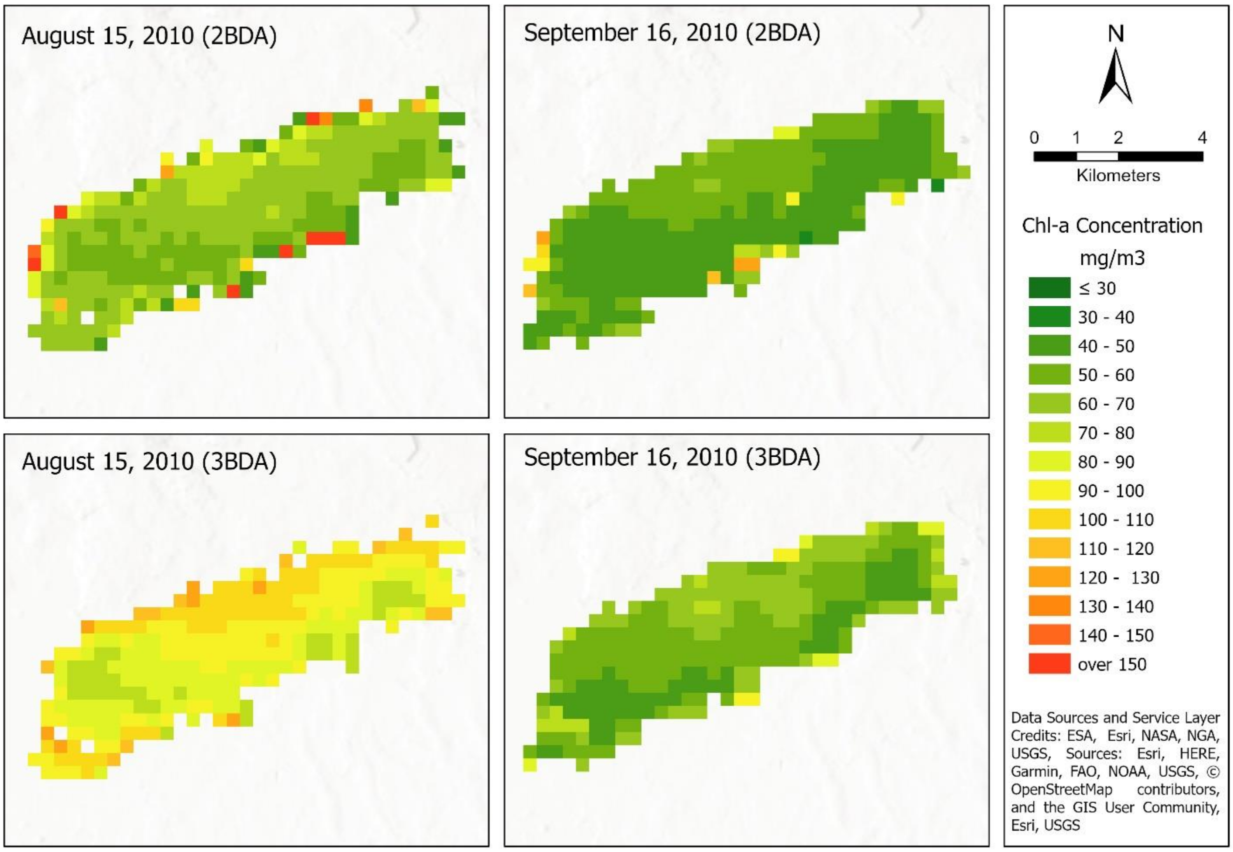


*Figure 22: Map of chlorophyll-a concentration estimates derived from 2BDA and 3BDA*

## The spatial and temporal pattern of chlorophyll-a concentration during the war (2013 – 2016)

This section presents the results from analyzing chlorophyll-a concentration of the lake using Landsat 8 data from 2013 to 2016. The war began in 2012 but the data presented in this section covers years 2013 to 2016 due to lack of available satellite data in the said.

Figure 23, Figure 24 and Figure 26 show the trends of chlorophyll-a concentration for each season from 2013 to 2016, some of which are not represented due to lack of clear satellite data caused by cloud cover. In the available data, it can be observed that outliers mostly lie above the highest quartile. In cases of winter and spring, these data points represent the areas in the edges of the lake whose reflectance have contributions from the adjacent land (with corresponding error called land adjacency error) and shallow areas with reflectance contribution from the bottom surface of the lake (also known as the bottom surface noise). Winter (which only had clear data on 2016) estimates range from 12.3 to 27.2 mg/m3 with a mean of 14.7 mg/m3. In spring, a decreasing trend with mean values of 13.6 mg/m3, 12.8 mg/m3 and 11.7 mg/m3 is seen from 2014 to 2016. In summer, an increasing trend is observed from 2013 to 2016 with mean values of 14.5 , 15.4, 16 and 19.7 mg/m3 whereas in autumn, an opposite trend is observed from 2013 to 2016 with mean values of 65.8, 65.9, 57.5 and 26.1 mg/m3. Unlike spring and winter, the outliers in summer and autumn represent not only the edges and shallow areas of the lake but also those with extremely high chlorophyll-a concentration mostly in the central and eastern parts. Looking at the overall trend from 2013 to 2016 (Figure 24), it appears that in 2013 and 2014, the lake had lower chlorophyll-a concentrations than in 2015 and 2016. In all years, the peak values are in summer and autumn. In 2015 and 2016 which have complete seasonal data, the most polluted season is autumn whereas spring is the least polluted. Overall, the highest level of pollution happened in 2016 particularly autumn and summer.

Figure 25 presents the spatial distribution of chlorophyll-a concentrations in the lake. It appears that from 2013 to 2014, there is barely any prominent changes in the chlorophyll-a concentration of the lake across different seasons. It then becomes more polluted in summer and autumn of 2015 and 2016, with extremely higher chlorophyll-a concentrations observed in the eastern side and some patches in the central areas of the lake. These areas look more pronounced in summer and autumn of 2016. Moreover, it can also be observed that the northern half of the lake have higher concentrations than the southern part in autumn 2016.

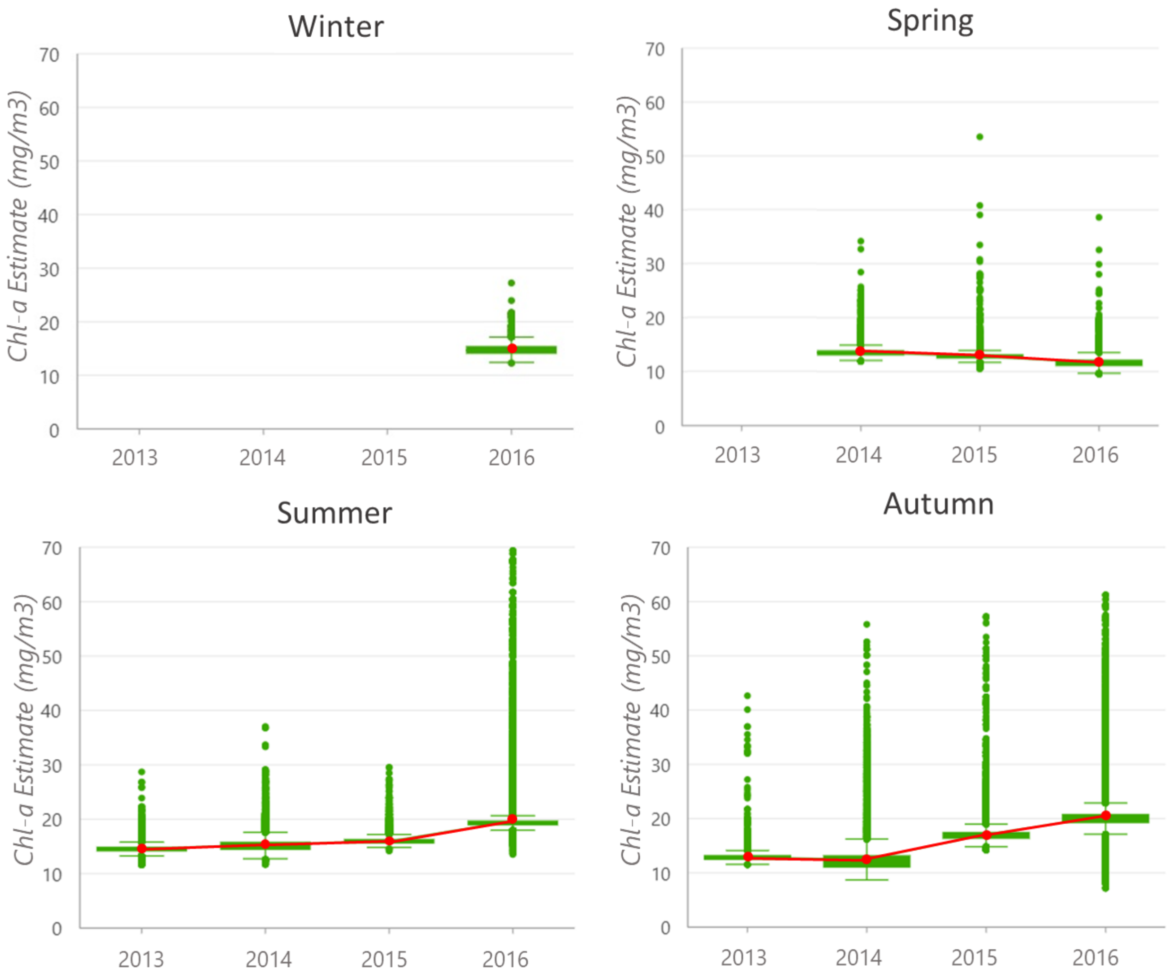


*Figure 23: Temporal trend and chlorophyll-a distribution per season from 2013 to 2016*

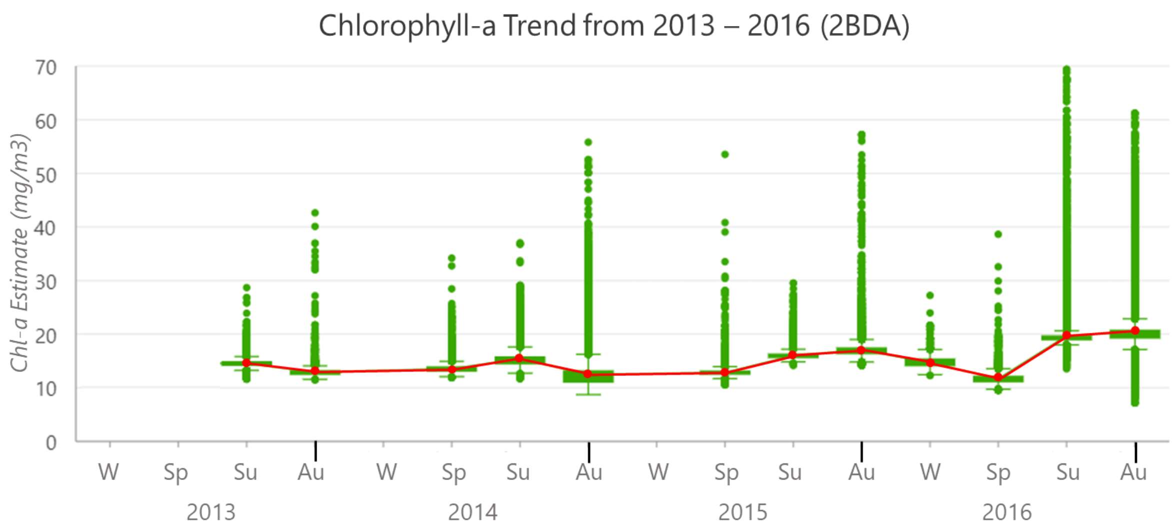


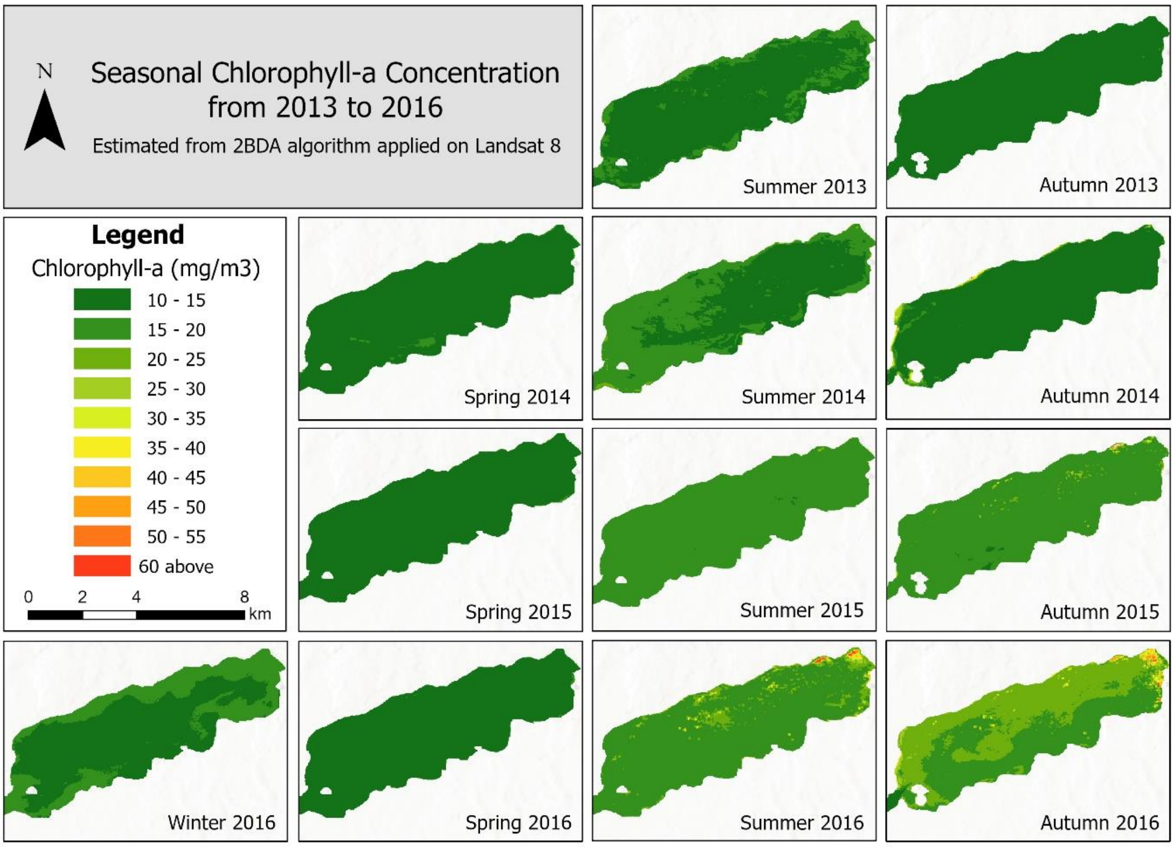


*Figure 25: Map showing spatial variability of chlorophyll-a per season from 2013 to 2016*

*Figure 24: Temporal trend (continuous) and chlorophyll-a distribution from 2013 to 2016*

## The spatial and temporal patterns of chlorophyll-a concentration during the war (2017 to 2020)

This section presents the chlorophyll-a estimates of the lake from 2017 to 2020, using 2BDA and 3BDA models.

Figure 26 shows the temporal trends and distribution of chlorophyll-a concentration values for each season from 2017 to 2020 as generated from 2BDA model. Some seasons are not represented due to lack of clear satellite data caused by cloud cover. Similar to Landsat, the outliers represent areas affected by the land adjacency effect and the bottom surface noise, as well as some areas with extremely high and low chlorophyll-a values. In winter, mean chlorophyll-a concentration is higher and more variable in 2017 than in 2020 (68 mg/m3 to 27.6 mg/m3. In autumn, the mean value decreased from 61 mg/m3 in 2018 to 27.5 mg/m3 in 2019; in summer, a decreasing trend is observed from 2017 to 2019 (mean values of 60 mg/m3, 45 mg/m3, 33 mg/m3) followed by a slight increase in 2020 when mean is 36.5 mg/m3. In Autumn, there is barely any change in the mean chlorophyll-a from 65.8 mg/m3 in 2017 to 65.9 mg/m3 in 2018. It then decreases to 57.5 mg/m3 in 2019 and to 26.1 mg/m3 in 2020. Generally, it can be observed that there is a decreasing trend in chlorophyll-a for almost all seasons from 2017 to 2020, suggesting improvement in water quality of the lake.

The overall trend is presented in Figure 27. It appears that the mean of chlorophyll-a concentration of the lake has decreased from winter 2017 to autumn 2020, with some seasonal fluctuations characterized by peaks during autumns of 2017 to 2019. The season with the lowest concentration could not be concluded due to incomplete data. It is also noteworthy that autumn have the widest range of values across the lake.

Figure 28 presents the spatial distribution of chlorophyll-a concentration in the lake. Based on the seasons with available clear data, the entire lake have high concentrations of chlorophyll-a in all seasons from 2017 and 2018. In most seasons for these years, higher concentration runs in the central to northern portion of the lake, then decreases outwards. It is also observed that the central area has patches with higher values as clearly seen in summer 2018 to winter 2020. The most prominent changes are on the eastern side of the lake with extremely high algae beginning to be visible in summer and autumn then decreasing in magnitude from 2017 to 2020 suggesting improvement of water quality.

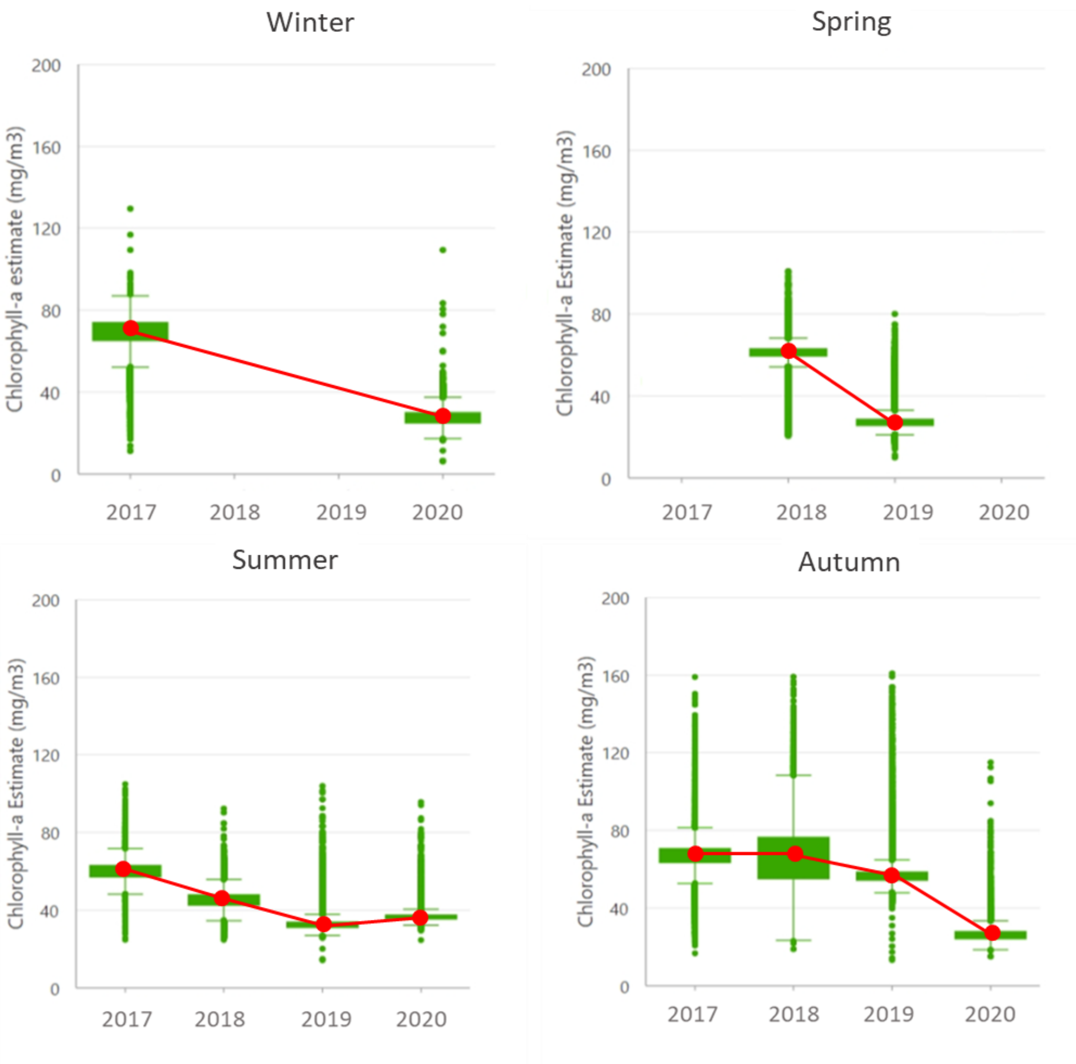


*Figure 26: Temporal trend and chlorophyll-a distribution per season from 2017 to 2020 as derived from 2BDA model*

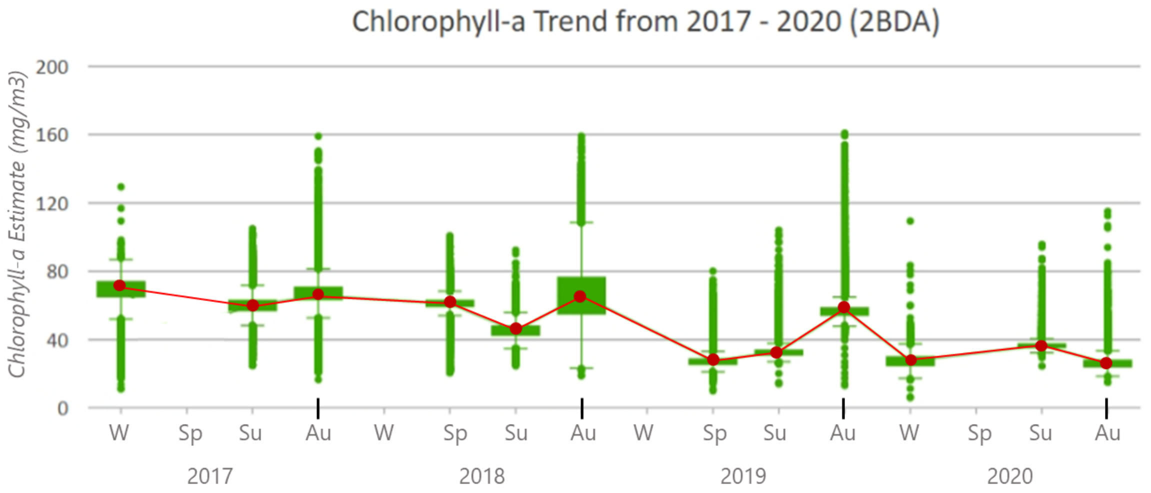


*Figure 27: Temporal trend (continuous) and chlorophyll-a distribution from 2017 to 2020 as derived from 2BDA model*

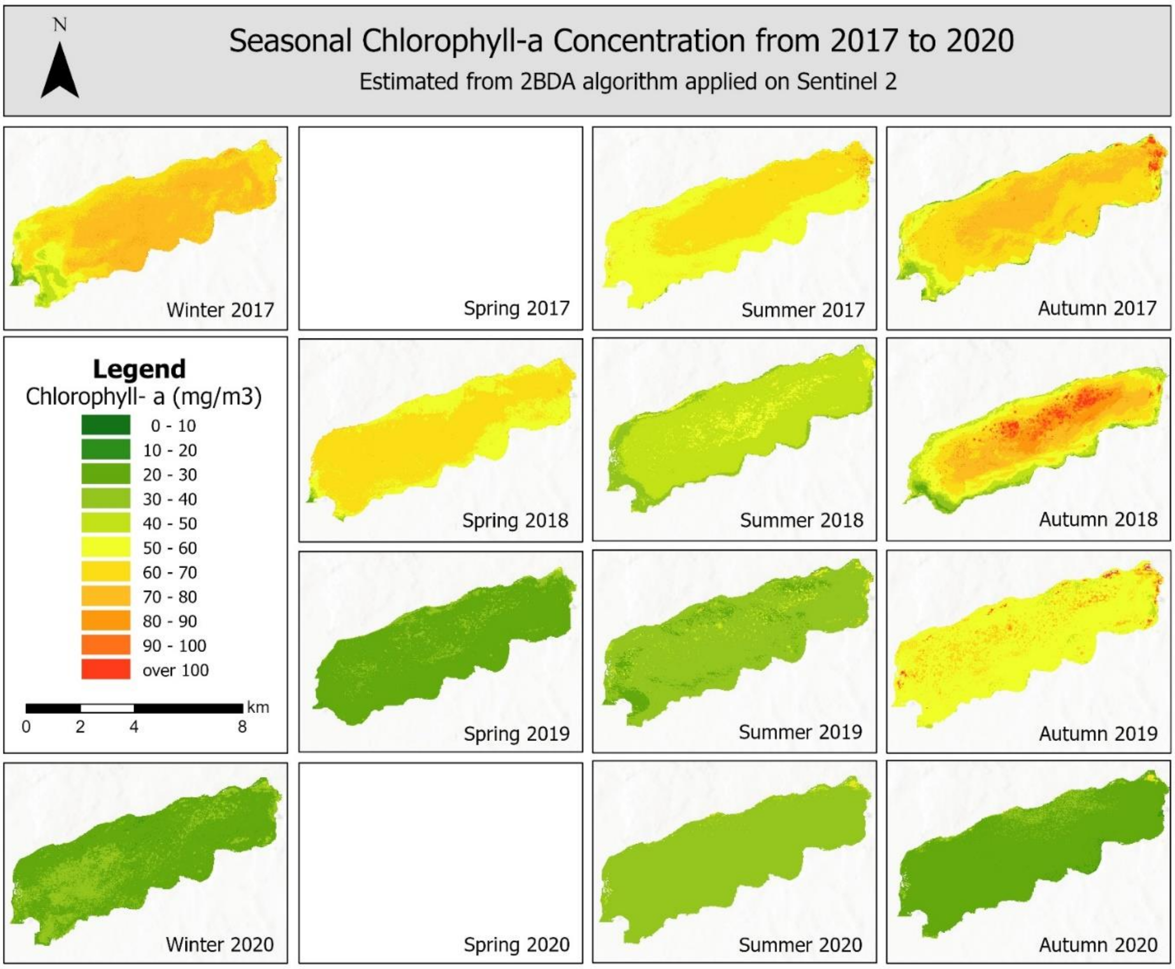


*Figure 28: Map showing spatial variability of chlorophyll-a per season from 2017 to 2020*

Figure 29 and Figure 30 show the temporal pattern of chlorophyll-a estimates using 3BDA model while Figure 31 shows the spatial patterns in the lake. In comparison to the first model – 2BDA, the estimates of 3BDA are higher, but the temporal and spatial patterns are similar.

In winter, mean chlorophyll-a concentration is higher in 2017 than in 2020 (96.3 mg/m3 to 30.3 mg/m3). Additionally, 2017 has a wider range of values than 2020. In spring, the mean value decreased from 99.3 mg/m3 in 2018 to 31.1 mg/m3 in 2019. In summer, a decreasing trend is observed from 2017 to 2019 (mean values of 124.7 mg/m3, 87.9 mg/m3, 44.3 mg/m3) followed by a slight increase in 2020 to 50.6 mg/m3. In Autumn, the mean chlorophyll concentration increased from 95.2 mg/m3 in 2017 to 127.7 mg/m3 in 2018, then decreased to 85 mg/m3 in 2019 and to 27.1 mg/m3 in 2020. Generally, it can be observed that there is a downward trend in chlorophyll-a for almost all seasons from 2017 to 2020.


*Figure 29: Temporal trend and chlorophyll-a distribution per season from 2017 to 2020 as derived from 3BDA model*

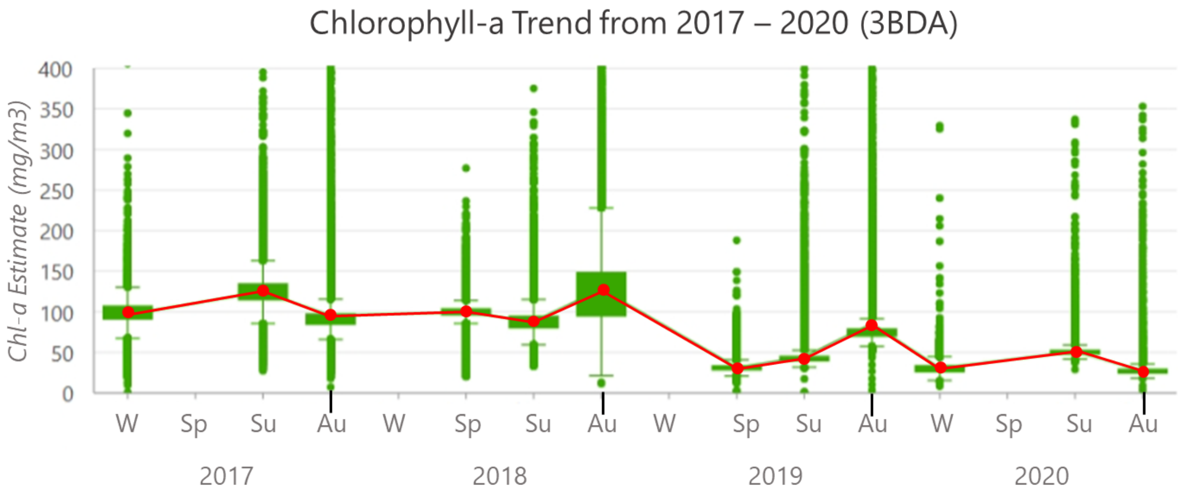


*Figure 30: Temporal trend (continuous) and chlorophyll-a distribution from 2017 to 2020 as derived from 3BDA model*

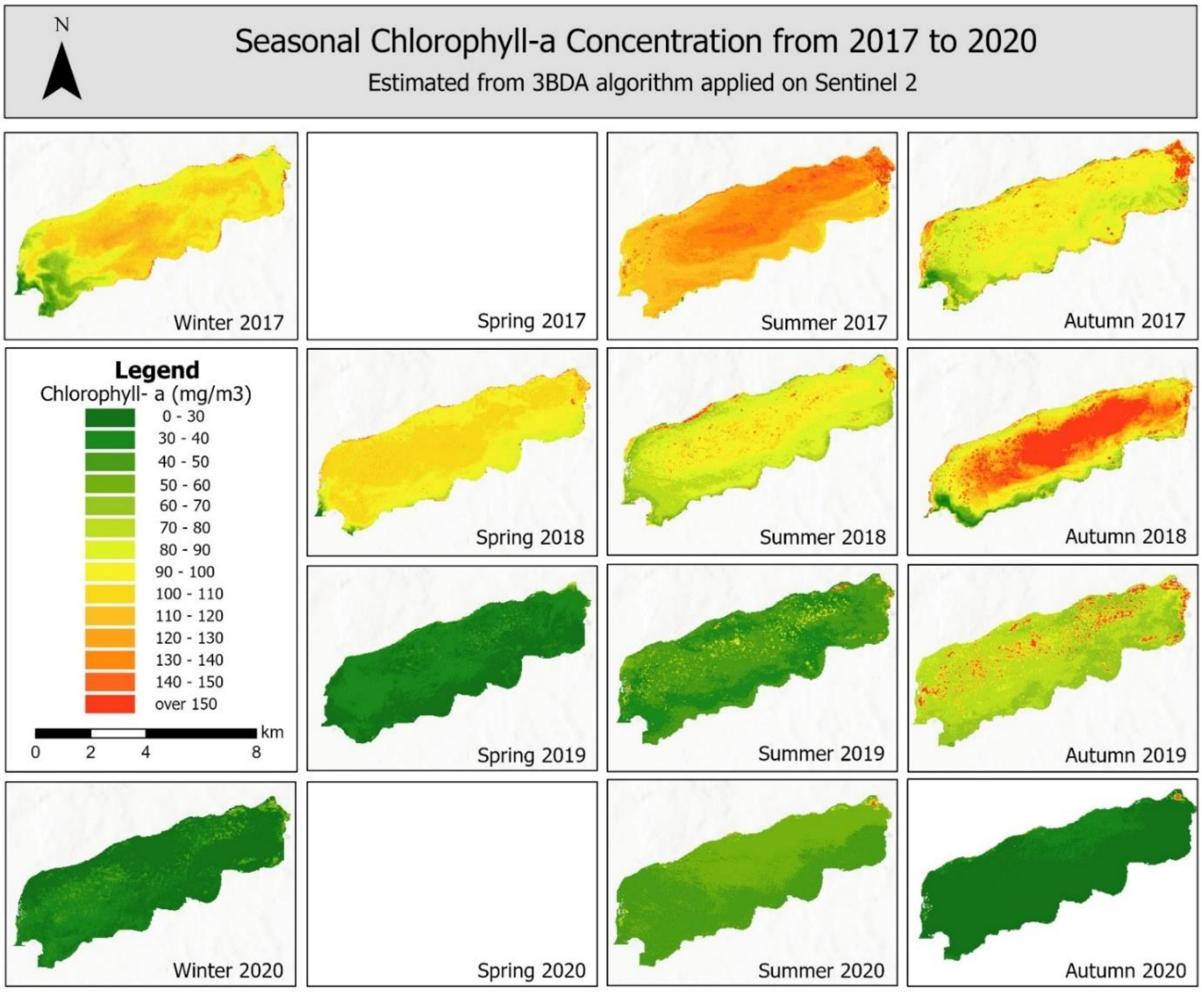


*Figure 31: Map showing spatial variability of chlorophyll-a per season from 2017 to 2020*

## Comparison of Landsat 8 and Sentinel 2 Results

Landsat 8 is challenging to use in chlorophyll-a estimation because it lacks a band in the wavelength near 700nm wherein the NIR reflectance peak is located. Sentinel 2, on the other hand, has a band near the peak in the wavelength 703.9 nm, making it relatively ideal in using 2BDA and 3BDA models. With the lack of available Sentinel 2 data in 2013 to 2016, Landsat 8 is used in the analysis of the said period. To establish whether Landsat 8 can provide some insights on the status of the lake, it was first compared with Sentinel 2 results using a common period (2017 to 2020) when both satellite data are available.

Figure 32 and Figure 33 compare the retrieved chlorophyll from Landsat 8 (left) and Sentinel 2 (right) from years autumn 2017 (top) to 2020 (down) using a common model – 2BDA. Landsat 8 produced lower values than Sentinel 2, which is expected as chlorophyll-a reflectance declines beyond the NIR peak that Landsat 8 is not able to capture. Despite this, the results show that while it produces lower values, it is still able to capture the spatial pattern of the algae and it determines which areas have relatively higher algae. It mostly shows patterns similar to that of Sentinel 2. For instance, the high pollution in the eastern banks, the high concentration patches scattered in the central area of the lake, the relatively higher values in the central part (SW to NE direction) decreasing outwards. It also provided a similar temporal pattern to Sentinel 2 wherein the water quality improves from 2018 to 2020 during autumn. With these findings, it is therefore shown that Landsat 8 can provide insights on the water quality for years 2013 to 2016 – years that Sentinel 2 data is unavailable. The results run for such period will be governed by the important note that Landsat 8 possibly underestimates the chlorophyll values as compared to MERIS and Sentinel 2, and therefore, the actual values can possibly be higher than those computed. The best insight that can be obtained from this data are the spatial and temporal patterns.

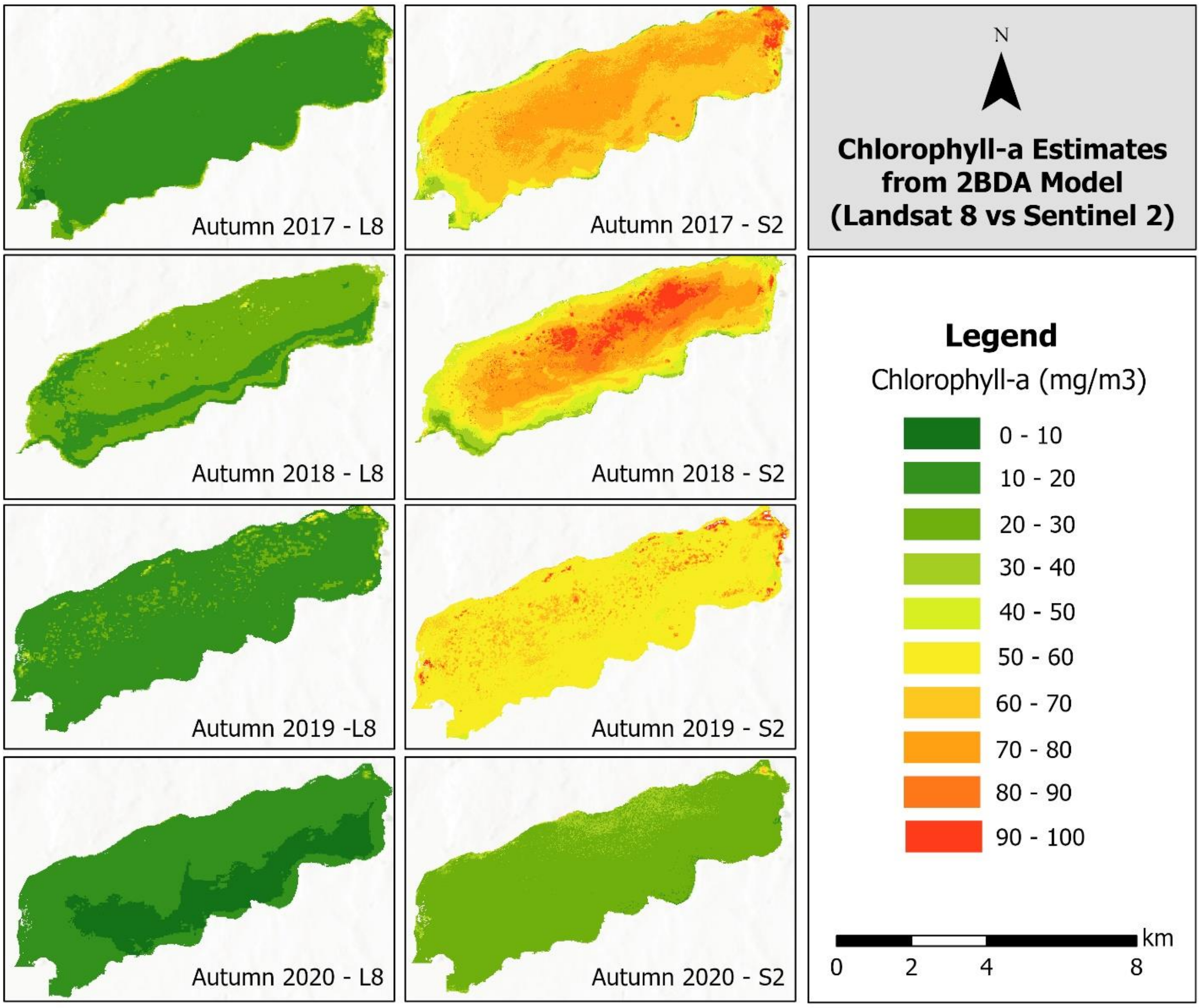


*Figure 32: Landsat 8 vs Sentinel 2 Results ( Autumn 2017 - 2020)*

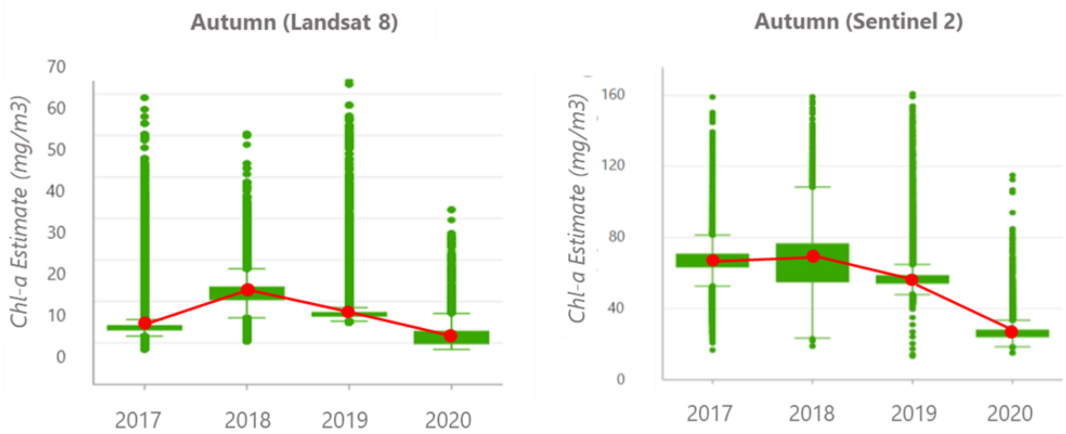


*Figure 33: Landsat 8 vs Sentinel 2 results (Autumn 2017 - 2020)*

# DISCUSSION

## Spatial and temporal patterns in relation to the Syrian Civil War

### The state of Lake Qattinah and the surrounding pollution sources prior to the war (2010 – 2011)

The results of chlorophyll-a assessment from two different satellite data set the baseline of water quality of Qattinah Lake. Visual inspection of Landsat 5 images revealed the seasonal variability of algae and emphasized relatively higher pollution in the eastern side of the lake, near the fertilizer factory. The prominence of this pattern in summer and autumn aligns with the general condition of algal proliferation in higher temperatures (Manssour & Al-Mufti, 2010). Spectral patterns of MERIS in the sampling points and the high chlorophyll-a estimates from both chlorophyll-a retrieval modes revealed pollution in other areas indicating contributions of surrounding human activities such as agriculture and human settlement on top of the discharges from the factory.

The results of the pre-war analysis agree with the findings from several previous studies indicating that the lake was highly polluted prior to the war (Hassan et al., 2010; Manssour & Al-Mufti, 2010; UN-ESCWA and BGR, 2013). The spatial and temporal patterns revealed by this study align with the findings from (Manssour & Al-Mufti, 2010) who measured several water quality parameters in Qattinah Lake and found 1) high eutrophication level all over the lake mainly owing to the discharges of a fertilizer factory, agriculture and sewage drainages, and 2) seasonal variation of nutrients particularly total phosphorus which was highest in April – the starting period of algal bloom in the lake.

The estimated chlorophyll-a concentrations from two different models both represented a highly polluted lake but had high discrepancies. 3BDA estimates were significantly higher than those of

2BDA. This suggests that while the lake is highly polluted, the magnitude remains uncertain. Estimates from one model might be more accurate than the other, or both models may highly deviate from actual concentrations. On the positive side, the models showed consistent spatial pattern characterized by relatively higher estimates in the northern part of the lake as compared to the south. The possible reasons for this are either1) higher pollution discharges in the northern areas or 2) the bathymetry of the lake, possibly more shallow in the northern area which can be affected by the bottom surface noise. However, the relationship of bathymetry and chlorophyll-a is outside the scope of this study.

These results leads to the main takeaway that although the actual estimates from any of the models should not be taken as absolute, the spatial pattern generated can provide relevant information on assessing the lake.

### The state of Lake Qattinah and the surrounding pollution sources during the Syrian Civil War (2013 – 2020)

The spatial and temporal patterns of chlorophyll-a in 2013 to 2020 suggest that the war had an impact on the pollution level of the lake. The most prominent spatial patterns seen to be changing throughout different stages of the war are 1) the hotspots in the eastern part of the lake 2) the several small patches with high concentrations in the central and northern part of the lake from the southwest to northeast direction 3) the relatively higher concentrations in the same areas as in 2, decreasing outwards. Hotspot 1 is mainly driven by the fertilizer factory and the settlements located in the eastern banks of the lake. Hotspot 2 could be macrophyte species that can co-exist with high levels of phytoplankton. This hypothesis is based on the study conducted Lake Qattinah by (Hassan et al., 2010) who found low macrophyte species richness mainly restricted to a few species that can tolerate its highly eutrophic conditions. The third spatial pattern could be related to possibly higher pollution in the northern areas or may be caused by interventions from the bottom surface of the lake (as mentioned in the previous section).

The relatively low and barely increasing algal concentrations in all parts of lake Qattinah and the absence of high concentration areas in the identified hotspots in all seasons from 2013 to 2015 imply the decline in pollutants (with respect to the baseline). This is potentially caused by lower magnitudes of surrounding human activities such as the fertilizer factory, agricultural areas and human settlements as the country was torn in battles over power and control. The rapid increase from 2015 to 2016, the presence of high concentration in the hotspots, and the decline from 2017 to 2020 might be related the regained control by the government over most areas in the country which to some extent brought back higher intensity of human activities but also possibly improved management efforts towards the lake.

To have a better grasp on these water quality variations in the lake, the main pollution sources such as agricultural areas, human settlements and the fertilizer factory are investigated within the context of the ongoing war.

**Agricultural areas and human settlements.** Agricultural production suffered a significant loss during the war (Enab Baladi, 2019; FAO, 2017). Figure 34 shows the decline in crop production in the surrounding areas of the lake from 2010 to 2013. It can be observed that the highest production drop occurred in areas that are mainly irrigated while mainly rainfed areas in the north of the lake were barely affected. According to (Jaafar et al., 2015), irrigated agricultural production decreased between 15 and 30% in the Syrian part of Orontes River Basin, with hotspots in Idleb, Homs, Hama, Daraa and Aleppo. (Haj Asaad & Jaubert, 2014) stated that water infrastructures were purposely targeted by both government and the opposition forces to gain advantage through opponent's reduced access to resources including agriculture and water. Some were destroyed during bombing, military passage or were looted.

Population displacement was also one of the direct influences of the war. According to FAO (2017), the conflict also caused drop of population which drove the decline in production. Destruction of agricultural land with orchards or crops, shortages and/or increase in prices of agricultural inputs including seeds, fertilizers, fuel for irrigation pumps and electricity were prevalent during the war. These forced many rural farmers and herding families to migrate and seek other sources of income (FAO, 2017). Figure shows the decline in population around the vicinity of the lake. Some areas particularly agricultural areas upstream of the lake as well as some surrounding areas in the southern banks were wiped out of almost all the population. Some were displaced on the account of bombing and intense fighting, while others were forced to leave as selected districts were established as military zones to prevent the return of the population. One of the two main military zones is located in Qattinah district, south of the lake (Figure 35) while the other is in Al-Qusayr situated farther south near the borders with Lebanon (Haj Asaad & Jaubert, 2014).

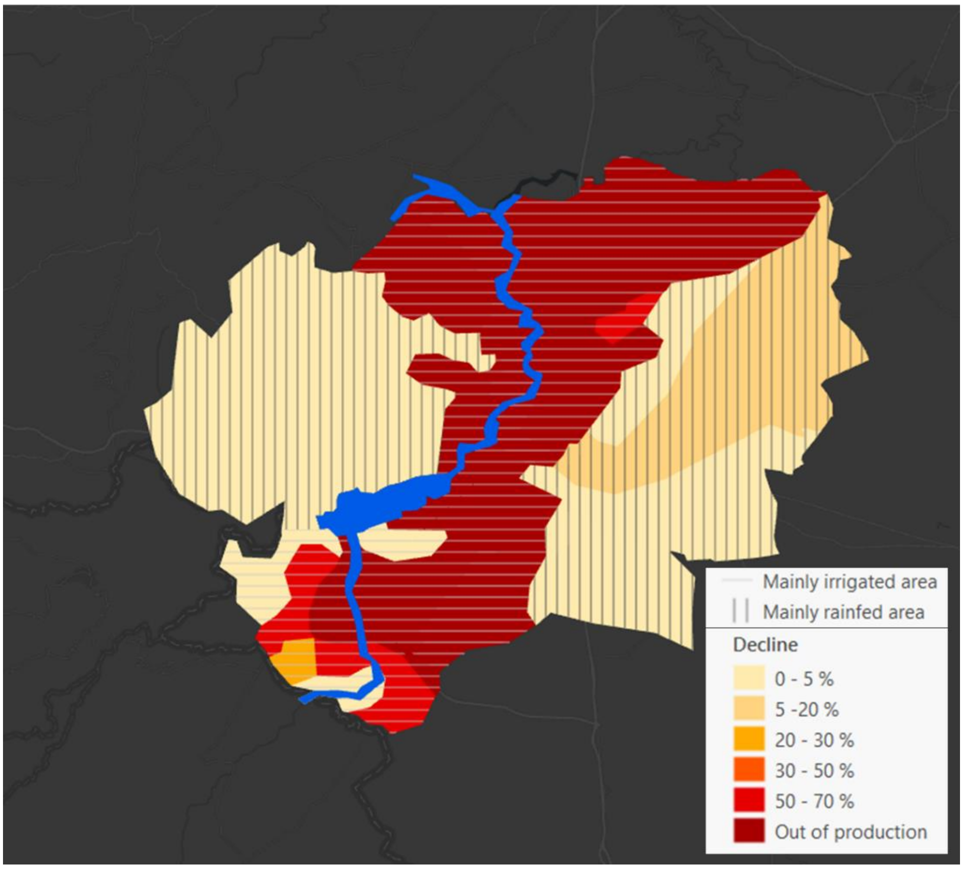


*Figure 34: Agricultural production decline around the lake from 2010 to 2013*

Adapted from: (Haj Asaad & Jaubert, 2014)

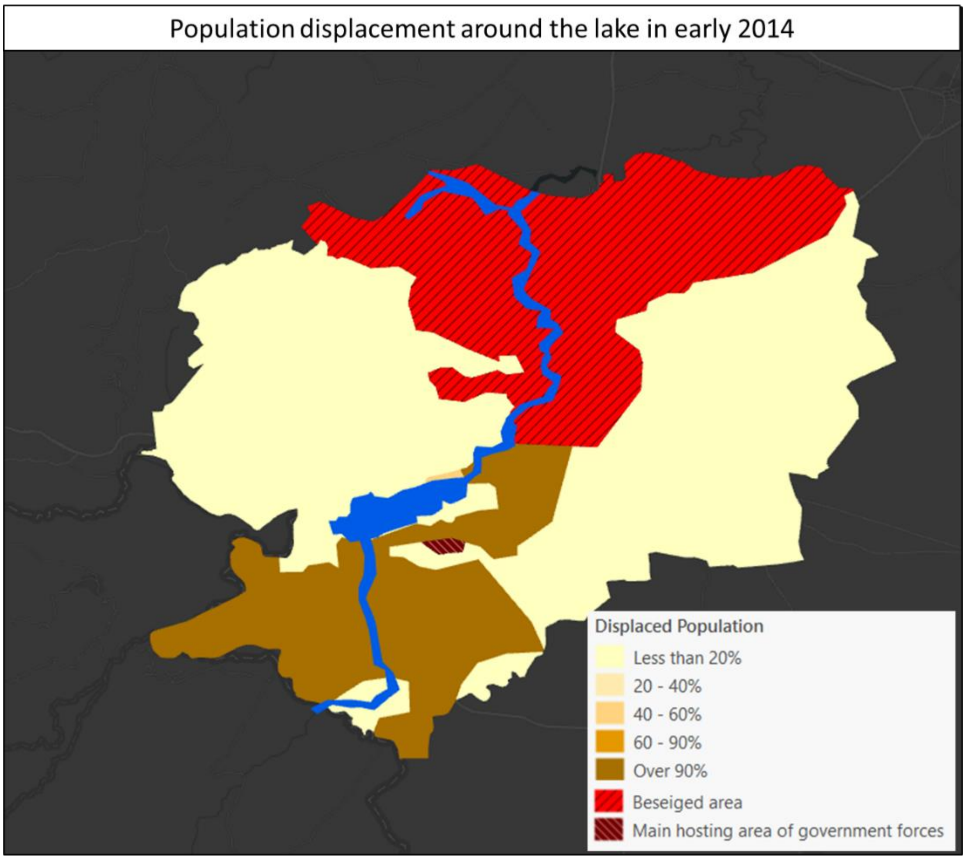


*Figure 35: Percentage of displaced population in areas around the lake; Adapted from: (Haj Asaad & Jaubert, 2014)*

The findings from the abovementioned previous studies clearly show how the war affected the surrounding human activities that have been identified as the major sources of pollution in the lake. The decline in agricultural production upstream as well as in the areas next to the southern banks of the lake, coupled by the displacement of a high percentage of population could indicate less magnitude of human activities and therefore potentially less discharges of pollutants to the lake coming from these sources. This supports the relatively low mean chlorophyll-a concentration in all seasons from 2013 to 2015.

Following the same arguments, it is possible that when the Assad government forces strengthened and positioned itself on the winning side after 2015, the activities surrounding the lake increased again. However, a simple inspection of vegetation around the lake in selected years revealed higher cultivated areas (green) on years before the war (2009 and 2010), a decline between 2010 and 2014, followed by barely any changes until 2018. This suggests that the ups and lows of chlorophyll-a concentration in the lake might not be mainly driven by agriculture as reflected by the minimal changes in agricultural lands yet prominent changes in water quality after 2011. Moreover, the relative increase in cultivated areas in 2020 does not seem to align with the improvement of water quality in 2020 (Figure 36).

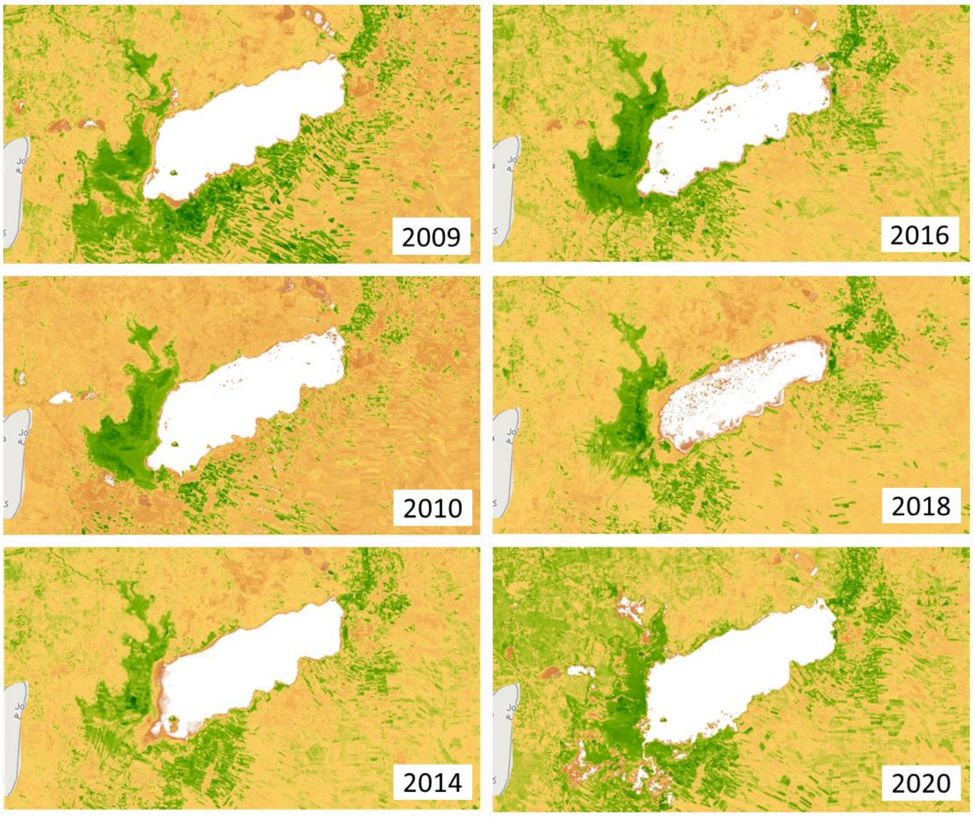


*Figure 36: Changes in agricultural areas before and during the war*

These findings suggest that while the agricultural areas have their fair share of nutrients being discharged to the lake, the most prominent increases and decreases in the algal concentration seen during the war might not be mainly driven by this activity.

With regards to the human settlements in the vicinity, no information was found on the return of displaced population but considering that military zones were established to prevent the return of population (Haj Asaad & Jaubert, 2014), it is possible that many villages remained as it was. Following these assessments, it is hypothesized that the fertilizer factory is potentially the main driver of the algal growth in lake Qattinah.

**Fertilizer factory.** According to (Enab Baladi, 2019), the General Fertilizers Company is the largest chemical industrial complex in Syria and located on the banks of Lake Qattinah. It used to cater to the agricultural sector needs of different types of fertilizers such as fertilizers of Urea, Ammonium Nitrate and Phosphate. Such fertilizers used to be delivered to farmers at a subsidized price via Agricultural Bank. Prior to the war, GFC used to have around 3000 employees but in 2011, employment decreased in half.

GFC has three factories for fertilizer production. First is the Ammonia Urea Plant which stopped production in 2015 due to gas cuts resulting from the conflict and the lack of required production inputs including phosphate and electricity. In mid-2017, it resumed its operations at a production rate of 900 tons per day. In addition, it also contributed to the monthly production of 25000 tons of urea fertilizer, along with other products. Second is the ammonium nitrate fertilizer plant can produce 400 tons daily. This plant does not regularly run but is only operational when on demand for production due to the decline in workforce and expertise brought about by the conflict. Third is the phosphate fertilizer plant which resumed work in December 2019 and started production reaching 400 tons per day of phosphate fertilizer.



These accounts on the factory operations align with the findings of this study. The decline in algal concentration in the eastern part of the lake after 2011 (in this case 2013) highly relates to the state of operations of GFC. The decrease in the workforce which began after 2011 influenced its production, and thus the pollutants it discharges to the lake. This supports the disappearance of the extremely high algal biomass in the eastern part in summer and autumn of 2013 to 2015 when such are predominant. The return of high algal concentration in the same area in summer and autumn 2016 does not fully align with the suspension of the first plant's operation in 2015. However, it is possible that it was driven by the second fertilizer plant which during the war remained operational upon demand. The return of operations of the first fertilizer factory in mid-2017 partially aligns with the high concentrations in the lake especially in the hotspots, however, the resumption of activities in the third plant in 2019 seems to negate the improvement in water quality especially in 2020. It is hypothesized that that application of certain management strategies on the lake might have played a role in this improvement. The lack of more recent data specific to the fertilizer company and the rehabilitation efforts related to the lake makes it difficult to prove such assumption.

## Important considerations on data and the analysis

This section discusses the limitations of the data, the conducted analysis, and interpretation of results. It also provides information on how such limiting factors were accounted for.

**Incomplete data.** One of the challenges in using satellite imagery is cloud cover interfering with measurements and making the affected areas not feasible for water quality assessment. Prior to the assessment, these clouds were masked resulting to some images having incomplete coverage of the lake. When cloud cover is removed in a single image, the eliminated lake area is patched with image pixels of the same area taken from other days within the specified data range. This process makes it possible to have a clear image of the lake that is representative of an entire season. However, in seasons when cloud cover is intense for almost all days, no clear composite image is generated. For this reason, there are missing data particularly during winter and spring of some years. As a result, the study becomes limited to having a more holistic look at the seasonal patterns of algal growth in the lake.

**Variability of algae over short periods of time.** Algal growth is highly variable even in a short amount of time. With this, one day satellite images is typically not enough to capture the variability of the water quality indicator. Because of the issues on long download time of MERIS data, only one day images were analyzed to estimate chlorophyll-a concentration prior to the war. These images may not well represent the varying conditions of the lake over a long period of time. Complementing MERIS data with one image per month of Landsat 5 accounted for the monthly changes of algae in the lake, to some extent. However, the analysis could have been stronger if mean of several Landsat 5 images per month were used instead of picking a single day. This is resolved in the assessment of the lake during the war when seasonal data were obtained from several cloud-free day images.

**Multiple satellite data.** This study covers 11 years. Ideally, the inconsistencies of estimated values of chlorophyll-a would have been lessened if a single satellite data was all throughout the analysis. To be able to look at each of the years and the corresponding changes in water quality, a combination of multiple satellite data was used, keeping into consideration the differences in specifications such as spatial resolution, spectral resolution, and revisit days among others. MERIS which has superior spectral resolution most suitable for chlorophyll-a retrieval but low spatial resolution was combined with Landsat 5 whose spectral resolution is inferior but spatial resolution capable of visualizing variability across the lake, were used to establish a baseline prior to the war. This shows how the two different data sources were used together to address each of the data's limitations and to have stronger results.

The application of multiple models in different satellite data with varying specifications added an additional level of uncertainty to the results. It is a major constraint that there is no in situ data to validate the estimates from the models. To make up for this, the estimated chlorophyll-a concentrations a particular satellite data was treated independent from that obtained from the others. No comparison of algal biomass was done among period cuts, except for the case when two satellite data were both available for a certain timeframe – the case of 2017 to 2020.

The lack of satellite data in 2012 did not hinder the assessment of the lake during the war. 2013 to 2016 were well represented by the results of Landsat 8 and the same goes for 2017 to 2020. While there are multiple satellite data used in this study, not all are expected to produce results which are most probably closer to the absolute values. Most of the retrieval models applied in this study were developed and validated on MERIS data. Such models relied on wavelengths near 709 nm (peak in the NIR), 665nm (maximum absorption in the red region), and/or 753 nm. Sentinel 2 have bands located near these three spectral locations: 703.9 nm, 665 nm, and 7__ nm. Moreover, previous studies have used the same chlorophyll-a indices on Sentinel-2 and successfully retrieved chlorophyll-a concentrations close to in situ data. On the other hand, Landsat 8 lacks a band near the 709 nm peak, as well as the 753 nm wavelength. Instead of 709 nm, the band in 830 nm quite far beyond the NIR peak was used in the 2BDA model. This led to chlorophyll-a estimates that are lower than those calculated from Sentinel 2 using a common model. In spite of this spectral limitation, the applicability of the model to generate results that can still provide important insights on the lake was proven by comparing computed values from Landsat 8 and Sentinel 2 using a common model (2BDA) within a common timeframe in which both data are available (2017 – 2020, represented by the season with the most variable algal biomass - autumn). This showed the lower estimates from Landsat 8 but it also revealed the data's capability to capture similar spatial and temporal patterns as that of Sentinel 2, thus supporting the data and the model's compatibility regardless of spectral limitations. In this context, the chlorophyll-a estimates from 2013 – 2016 were hypothesized to be possibly an underestimation. In other words, if Sentinel-2 or MERIS happened to be available in the said period and were used instead of Landsat 8, the chlorophyll-a estimates would most likely be higher but would also reveal similar (or more pronounced) spatial and spectral patterns.

**Lack of in situ data.** While this study promotes remote sensing, the empirical approach is not entirely independent from in situ data. It calibrates and validates a model from data collected on the site. This poses a major setback due to unavailability and/ or inaccessibility of the data, but at the same time an opportunity to look at ways to make the most out of the freely available and rich satellite data to study water quality in remote and inaccessible areas where filed data collection is not possible. Selected algorithms and equations calibrated and validated in huge geographical scale, varied seasons, and areas with similar climatic conditions as the study area were assumed to be universal and tested on the lake. While many studies have tried doing this and found the non-universality of many models, and the need for calibrating data to a specific location and time, this study still used such models with less focus on the absolute chlorophyll-a concentrations but more attention given to spatial and temporal patterns. This approach provided important takeaways in understanding the state of the lake amidst the war. The comparison of results from multiple chlorophyll-a indices and retrieval equations established the reliability of the trends and patterns which were consistent among indices. The comparison between 2 different satellite data where a common model was applied provided consistent spatiotemporal patterns in the lake and established the reliability of utilizing different satellite data in various war stages.

While looking at all the concentration calculated from different indices applied on different satellite data all revealed chlorophyll-a concentration ranging from as low as 10 mg/m3 to as high as 400mg/m3, these values reflect chlorophyll-a concentration of a eutrophic lake. In other words, all indices and models applied on various satellite data provided chlorophyll-a concentrations of a highly polluted lake, but at varying levels. The best way to find out whether the chlorophyll-a estimates in this study represent the actual algal concentration in the lake is to collect in situ data when possible. Nevertheless, this study proves significant in revealing variations of algal concentration in different parts of the lake across different seasons and years.

**Small scale assessment specifically looking at pollution sources.** The interpretations of the results are limited on the study area and its immediate vicinity and do not extend on other parts of Syria. The water quality was evaluated solely based on the impact of the immediate surroundings and thereby not considering other factors that might have effects on the water quality as well. It also does not include assessment of climatic changes throughout the conflicted years. Moreover, the smaller geographic coverage of this study has made it difficult to find information specific to the area (i.e. movement of population, rehabilitation and management strategies in the lake, more recent state of the fertilizer company).

# CONCLUSIONS

This study mainly aimed to analyze water quality of lake Qattinah by looking at the spatial and temporal patterns of algae before and during the war (2010 to 2020). It utilized multiple chlorophyll-a retrieval models applied on various satellite data to make up for the lack of in situ data. In addition, this study attempted to find possible causes of the changes in water quality by finding relevant information from published and grey literature with focus on the influences of the war on the human activities surrounding the lake.

This study concluded that the lake had been highly polluted prior to the war and it is supported by the findings from previous studies. It also found out that the conflict situation had indirect impacts on water quality of the lake through its influences on the surrounding human activities. First, it revealed relatively lower level of water degradation in 2013 to 2015 which was linked to the potential decrease in nutrient discharges brought about by population displacement, agricultural decline and the disruption of operations by the nearby fertilizer factory. Second, the study saw a degradation of water quality with the resumption of polluting activities around the lake following the government's regained strength and leverages in the war. The evidences of minimal changes in agricultural areas after 2012 led to a conclusion that agriculture has not been the main driver of the ups and downs in water quality. The limited knowledge on population movement made it difficult to assess the relative contributions of human settlements (i.e. runoffs, wastewater discharges). Some evidences pointed out that the fertilizer factory remained as the main driving factor of the apparent water quality changes. These include the disruption and continuation of operations during the war which aligned with spatial and temporal changes in algal concentration of the lake. However, increased operations of the factory since 2017 did not align with the decreasing trend in algal concentrations from 2017 to 2020. This led to a hypothesis that the recent water quality improvement could be linked to certain management strategies and rehabilitation efforts which are possibly related to the fertilizer factory.

This study has therefore successfully assessed water quality solely from satellite data and independent of in situ data and thus filled the current research gap on the state of Lake Qattinah during the war. The huge discrepancies in chlorophyll-a estimations from two different models showed potential inaccuracies of generated values and the need for in situ data collection to validate results. However, the consistency in the spatial and temporal patterns generated from the models supported the reliability of the methods performed and guided the interpretation of the results. The approach used in this study can be applied on other remote and inaccessible water bodies where no in situ data is available.

Although the actual algal concentrations in the lake remains unknown, this study has provided significant insights which can assist in the formulation of rehabilitation programs and management strategies. Additional information on the surrounding human activities is necessary to confirm the author's inferences on the factors driving the water quality changes. Integration of other relevant factors like changes in temperature, precipitation and other climatic conditions could significantly improve the interpretations in this study.

# References

Aljazeera. (2017, July 4). *Syria's 'de-escalation zones' explained.* https://www.aljazeera.com/news/2017/7/4/syrias-de-escalation-zones-explained

Allan, M. G., Hamilton, D. P., Hicks, B. J., & Brabyn, L. (2011). Landsat remote sensing of chlorophyll a concentrations in central North Island lakes of New Zealand. *International Journal of Remote Sensing*, *32*(7), 2037–2055. https://doi.org/10.1080/01431161003645840

Aminot, A., & Rey, F. (2002). Standard procedure for the determination of chlorophyll a by spectroscopic methods. *ICES: Techniques in Marine Environmental Sciences*, *28*.

Anderson, D. M., Glibert, P. M., & Burkholder, J. M. (2002). Harmful algal blooms and eutrophication: Nutrient sources, composition, and consequences. *Estuaries*, *25*(4), 704–726. https://doi.org/10.1007/BF02804901

Andrzej Urbanski, J., Wochna, A., Bubak, I., Grzybowski, W., Lukawska-Matuszewska, K., Łącka, M., Śliwińska, S., Wojtasiewicz, B., & Zajączkowski, M. (2016). Application of Landsat 8 imagery to regional-scale assessment of lake water quality. *International Journal of Applied Earth Observation and Geoinformation*, *51*, 28–36. https://doi.org/10.1016/j.jag.2016.04.004

Ansper, A., & Alikas, K. (2018). Retrieval of Chlorophyll a from Sentinel-2 MSI Data for the European Union Water Framework Directive Reporting Purposes. *Remote Sensing*, *11*(1), 64. https://doi.org/10.3390/rs11010064

Avisse, N., Tilmant, A., Müller, M. F., & Zhang, H. (2017). Monitoring small reservoirs' storage with satellite remote sensing in inaccessible areas. *Hydrol. Earth Syst. Sci.*, 15.

Barrett, E. C., & Curtis, L. F. (1999). *Introduction to Environmental Remote Sensing*. Stanley Thornes. https://books.google.se/books?id=WwU6BK3LlDEC

BBC News. (2019, January 14). Syria profile—Timeline. *BBC News*. https://www.bbc.com/news/world-middle-east-14703995

Bougarne, L., & Abbou, M. B. (2019). *Carlson's Index and OECD Classification for the Assessment of Trophic Status of Bab Louta Dam*. *10*(5), 4.

Bramich, J., Bolch, C. J. S., & Fischer, A. (2021). Improved red-edge chlorophyll-a detection for Sentinel 2. *Ecological Indicators*, *120*, 106876. https://doi.org/10.1016/j.ecolind.2020.106876

Brooks, B. W., Lazorchak, J. M., Howard, M. D. A., Johnson, M.-V. V., Morton, S. L., Perkins, D. A. K., Reavie, E. D., Scott, G. I., Smith, S. A., & Steevens, J. A. (2016). Are harmful algal blooms becoming the greatest inland water quality threat to public health and aquatic ecosystems? *Environmental Toxicology and Chemistry*, *35*(1), 6–13. https://doi.org/10.1002/etc.3220

Buma, W. G., & Lee, S.-I. (2020). Evaluation of Sentinel-2 and Landsat 8 Images for Estimating Chlorophyll-a Concentrations in Lake Chad, Africa. *Remote Sensing*, *12*(15), 2437. https://doi.org/10.3390/rs12152437

Campbell, J. B., & Wynne, R. H. (2011). *Introduction to Remote Sensing, Fifth Edition*. Guilford Press.

Carlson, R. E. (1977). A trophic state index for lakes1. *Limnology and Oceanography*, *22*(2), 361–369. https://doi.org/10.4319/lo.1977.22.2.0361

Carlson, R., & Simpson, J. (n.d.). *North American Lake Management Society February, 1996*. 92.

Cazzaniga, I., Bresciani, M., Colombo, R., Della Bella, V., Padula, R., & Giardino, C. (2019). A comparison of Sentinel-3-OLCI and Sentinel-2-MSI-derived Chlorophyll- *a* maps for two large Italian lakes. *Remote Sensing Letters*, *10*(10), 978–987. https://doi.org/10.1080/2150704X.2019.1634298

Cheng, X., & Li, S. (2006). An analysis on the evolvement processes of lake eutrophication and their characteristics of the typical lakes in the middle and lower reaches of Yangtze River. *Chinese Science Bulletin*, *51*(13), 1603–1613. https://doi.org/10.1007/s11434-006-2005-4

Conker, A., & Hussein, H. (2020). Hydropolitics and issue-linkage along the Orontes River Basin: An analysis of the Lebanon–Syria and Syria–Turkey hydropolitical relations. *International Environmental Agreements: Politics, Law and Economics*, *20*(1), 103–121. https://doi.org/10.1007/s10784-019-09462-7

Daher, J. (2019, September 4). *The Paradox of Syria's Reconstruction*. Carnegie Middle East Center. https://carnegie-mec.org/2019/09/04/paradox-of-syria-s-reconstruction-pub-79773

Dall'Olmo, G., & Gitelson, A. A. (2005). Effect of bio-optical parameter variability on the remote estimation of chlorophyll-a concentration in turbid productive waters: Experimental results. *Applied Optics*, *44*(3), 412–422. https://doi.org/10.1364/ao.44.000412

Dall'Olmo, G., Gitelson, A. A., & Rundquist, D. C. (2003). Towards a unified approach for remote estimation of chlorophyll-a in both terrestrial vegetation and turbid productive waters: UNIFIED APPROACH FOR CHLOROPHYLL ESTIMATION. *Geophysical Research Letters*, *30*(18). https://doi.org/10.1029/2003GL018065

Deutsch, E. S., Alameddine, I., & El-Fadel, M. (2018). Monitoring water quality in a hypereutrophic reservoir using Landsat ETM+ and OLI sensors: How transferable are the water quality algorithms? *Environmental Monitoring and Assessment*, *190*(3), 141. https://doi.org/10.1007/s10661-018-6506-9

Dillon, P. J., & Rigler, F. H. (2011). A Test of a Simple Nutrient Budget Model Predicting the Phosphorus Concentration in Lake Water. *Journal of the Fisheries Board of Canada*. https://doi.org/10.1139/f74-225

DLIFLC. (2019). *Country in Prespective: Syria*. Defense Language Institute Foreign Language Center (DLIFLC).

Dörnhöfer, K., & Oppelt, N. (2016). Remote sensing for lake research and monitoring – Recent advances. *Ecological Indicators*, *64*, 105–122. https://doi.org/10.1016/j.ecolind.2015.12.009

Enab Baladi. (2019, January). *Enab Baladi*. https://english.enabbaladi.net/archives/2019/01/general-fertilizers-company-from-syrian-stumbling-and-iranian-competition-to-russian-takeover/

EOS. (2017). *Sentinel-2: Satellite Imagery, Overview, And Characteristics*. https://eos.com/find-satellite/sentinel-2/

ESA. (n.d.-a). *Sentinel-2—Overview*. European Space Agency. Retrieved May 11, 2021, from https://sentinel.esa.int/web/sentinel/missions/sentinel-2/overview

ESA. (n.d.-b). *SNAP downloads*. Retrieved May 12, 2021, from https://www.esa.int/ESA_Multimedia/Images/2020/04/SNAP_downloads

ESA. (2006). *MERIS Product Handbook*. European Space Agency. https://earth.esa.int/eogateway/documents/20142/37627/MERIS-product-handbook.pdf

ESRI. (n.d.). *ArcGis Pro*. https://www.esri.com/en-us/arcgis/products/arcgis-pro/overview

Fanack Water. (n.d.). *Water Quality in Syria*. Fanack Water. Retrieved May 27, 2021, from https://water.fanack.com/syria/water-quality/

FAO. (2009). *AQUASTAT Transboundary River Basins—Asi-Orontes River Basin*. Food and Agriculture Organization of the United Nations (FAO).

FAO. (2017). *Counting the cost: Agriculture in Syria after six years of crisis*. Food and Agriculture Organization of the United Nations (FAO).

Ford, R. S. (2019). *The Syrian Civil War*.

Frumin, G. T., & Gildeeva, I. M. (2014). Eutrophication of water bodies—A global environmental problem. *Russian Journal of General Chemistry*, *84*(13), 2483–2488. https://doi.org/10.1134/S1070363214130015

Gaafar, R. (n.d.). *The Environmental Impact of Syria's Conflict: A Preliminary Survey of Issues*. 25.

Gholizadeh, M. H., Melesse, A. M., & Reddi, L. (2016). A Comprehensive Review on Water Quality Parameters Estimation Using Remote Sensing Techniques. *Sensors*, *16*(8), 1298. https://doi.org/10.3390/s16081298

Gilerson, A. A., Gitelson, A. A., Zhou, J., Gurlin, D., Moses, W., Ioannou, I., & Ahmed, S. A. (2010). Algorithms for remote estimation of chlorophyll-a in coastal and inland waters using red and near infrared bands. *Optics Express*, *18*(23), 24109. https://doi.org/10.1364/OE.18.024109

Gitelson, A. (1993). Nature of the peak near 700 nm on the radiance spectra and its application for remote estimation of phytoplankton pigments in inland waters. *8th Meeting on Optical Engineering in Israel: Optical Engineering and Remote Sensing*. https://www.academia.edu/2367218/Nature_of_the_peak_near_700_nm_on_the_radiance_spectra_and_its_application_for_remote_estimation_of_phytoplankton_pigments_in_inland_waters

Gitelson, A, Moses, W., Gurlin, D., & Rundquist, D. (2009). Estimating chlorophyll-a concentration in inland, estuarine and coastal waters: From lose range to satellite observations. In *Advances in Environmental Remote Sensing: Sensors, Algorithms, and Applications* (Qihao Weng). CRC Press.

Gitelson, Anatoly, Garbuzov, G., Szilágyi, F., MITTENZWEY, K.-H., Karnieli, A., & Kaiser, A. (1993). Quantitative Remote Sensing Methods for Real-Time Monitoring of Inland Waters Quality. *International Journal of Remote Sensing - INT J REMOTE SENS*, *14*, 1269–1295. https://doi.org/10.1080/01431169308953956

Glibert, P., Seitzinger, S., Heil, C., Burkholder, J., Parrow, M., Codispoti, L., & Kelly, V. (2005). The Role of Eutrophication in the Global Proliferation of Harmful Algal Blooms. *Oceanography*, *18*(2), 198–209. https://doi.org/10.5670/oceanog.2005.54

Gons, H. J. (1999). Optical Teledetection of Chlorophyll a in Turbid Inland Waters. *Environmental Science & Technology*, *33*(7), 1127–1132. https://doi.org/10.1021/es9809657

Google. (n.d.). *FAQ – Google Earth Engine*. Retrieved May 12, 2021, from https://earthengine.google.com/faq/

Gower, J., King, S., & Goncalves, P. (2008). Global monitoring of plankton blooms using MERIS MCI. *International Journal of Remote Sensing*, *29*(21), 6209–6216. https://doi.org/10.1080/01431160802178110

Grendaitė, D., Stonevičius, E., Karosienė, J., Savadova, K., & Kasperovičienė, J. (2018). Chlorophyll-a concentration retrieval in eutrophic lakes in Lithuania from Sentinel-2 data. *Geologija. Geografija*, *4*(1). https://doi.org/10.6001/geol-geogr.v4i1.3720

Gurlin, D., Gitelson, A. A., & Moses, W. J. (2011). Remote estimation of chl-a concentration in turbid productive waters—Return to a simple two-band NIR-red model? *Remote Sensing of Environment*, *115*(12), 3479–3490. https://doi.org/10.1016/j.rse.2011.08.011

Hadjimitsis, D. G., Hadjimitsis, M. G., Toulios, L., & Clayton, C. (2010). Use of space technology for assisting water quality assessment and monitoring of inland water bodies. *Bio-, Agro, and Urban Climatology*, *35*(1), 115–120. https://doi.org/10.1016/j.pce.2010.03.033

Haj Asaad, A., & Jaubert, R. (2014). Geostrategic stakes and the impact of the conflict in the Orontes River basin. *Confluences Méditerranée*, *N° 89*(2), 173. https://doi.org/10.3917/come.089.0173

Han, L. (1997). *Spectral Reflectance with Varying Suspended Sediment Concentrations in Clear and Algae-Laden Waters*. 5.

Hassan, S., Schmieder, K., & Böcker, R. (2010). Spatial patterns of submerged macrophytes and heavy metals in the hypertrophic, contaminated, shallow reservoir Lake Qattieneh/Syria. *Limnologica*, *40*(1), 54–60. https://doi.org/10.1016/j.limno.2009.01.002

Hollander, W. F. (2015). *Water as a political tool? Water management in Syria from the advent of Hafez al-Assad to the current Syrian crisis*. Leiden University.

Human Rights Watch. (2018). *World Report 2019: Rights Trends in Syria*. Human Rights Watch. https://www.hrw.org/world-report/2019/country-chapters/syria

IAMAT. (n.d.). *Syria: Climate Data | IAMAT*. International Association for Medical Assistance to Travellers. Retrieved May 31, 2021, from https://www.iamat.org/country/syria/climate-data

iMMAP. (n.d.). *Analysis Ready Data Cube*. https://immap.org/wp-content/uploads/2016/12/iMMAP-MENA-Ready-Data-Cube-A4-3.pdf

Internal Displacement Monitoring Centre. (2017). *Returnees in Syria: Sustainable Reintegration and Durable Soulutions, or a return to displacement?*

Jaafar, H. H., Zurayk, R., King, C., Ahmad, F., & Al-Outa, R. (2015). Impact of the Syrian conflict on irrigated agriculture in the Orontes Basin. *International Journal of Water Resources Development*, *31*(3), 436–449. https://doi.org/10.1080/07900627.2015.1023892

Johansen, R., Beck, R., Nowosad, J., Nietch, C., Xu, M., Shu, S., Yang, B., Liu, H., Emery, E., Reif, M., Harwood, J., Young, J., Macke, D., Martin, M., Stillings, G., Stumpf, R., & Su, H. (2018). Evaluating the portability of satellite derived chlorophyll-a algorithms for temperate inland lakes using airborne hyperspectral imagery and dense surface observations. *Harmful Algae*, *76*, 35–46. https://doi.org/10.1016/j.hal.2018.05.001

Khan, F., & Ansari, A. (2005). Eutrophication: An Ecological Vision. *Botanical Review*, *71*, 449–482. https://doi.org/10.1663/0006-8101(2005)071[0449:EAEV]2.0.CO;2

Kılıç, E. (2018). Impact of Syrian Civil War on Water Quality of Turkish Part of Orontes River. *Pollution*, *4*(3). https://doi.org/10.22059/poll.2018.250998.382

LAADS. (n.d.). *MEdium Resolution Imaging Spectrometer (MERIS)*. Retrieved May 11, 2021, from https://ladsweb.modaps.eosdis.nasa.gov/missions-and-measurements/meris/

Lubin, A., & Saleem, A. (2019). Remote sensing-based mapping of the destruction to Aleppo during the Syrian Civil War between 2011 and 2017. *Applied Geography*, *108*, 30–38. https://doi.org/10.1016/j.apgeog.2019.05.004

Manssour, K., & Al-Mufti, B. (2010). Influence of Industrial, Agricultural and Sewage Water Discharges on Eutrophication of Quttina Lake. *Jordan Journal of Civil Engineering*, *4*(4), 351–366.

Marx, A. J. (2016). Detecting urban destruction in Syria: A Landsat-based approach. *Remote Sensing Applications: Society and Environment*, *4*, 30–36. https://doi.org/10.1016/j.rsase.2016.04.005

Masocha, M., Dube, T., Nhiwatiwa, T., & Choruma, D. (2018). Testing utility of Landsat 8 for remote assessment of water quality in two subtropical African reservoirs with contrasting trophic states. *Geocarto International*, *33*(7), 667–680. https://doi.org/10.1080/10106049.2017.1289561

Matsushita, B., Yang, W., Chang, P., Yang, F., & Fukushima, T. (2012). A simple method for distinguishing global Case-1 and Case-2 waters using SeaWiFS measurements. *ISPRS Journal of Photogrammetry and Remote Sensing*, *69*, 74–87. https://doi.org/10.1016/j.isprsjprs.2012.02.008

Matthews, M. W. (2011). A current review of empirical procedures of remote sensing in inland and near-coastal transitional waters. *International Journal of Remote Sensing*, *32*(21), 6855–6899. https://doi.org/10.1080/01431161.2010.512947

Mishra, S., & Mishra, D. R. (2012). Normalized difference chlorophyll index: A novel model for remote estimation of chlorophyll-a concentration in turbid productive waters. *Remote Sensing of Environment*, *117*, 394–406. https://doi.org/10.1016/j.rse.2011.10.016

Mobley, C., Stramski, D., Bissett, W., & Boss, E. (2004). Optical Modeling of Ocean Waters: Is the Case 1 - Case 2 Classification Still Useful? *Oceanography (Washington D.C.)*, *17*. https://doi.org/10.5670/oceanog.2004.48

Mohamed, M. A., Anders, J., & Schneider, C. (2020). Monitoring of Changes in Land Use/Land Cover in Syria from 2010 to 2018 Using Multitemporal Landsat Imagery and GIS. *Land*, *9*(7), 226. https://doi.org/10.3390/land9070226

Mohammed, S. A., Alkerdi, A., Nagy, J., & Harsányi, E. (2020). Syrian crisis repercussions on the agricultural sector: Case study of wheat, cotton and olives. *Regional Science Policy & Practice*, *12*(3), 519–537. https://doi.org/10.1111/rsp3.12222

Moses, W. J., Gitelson, A. A., Berdnikov, S., & Povazhnyy, V. (2009). Satellite Estimation of Chlorophyll-$a$ Concentration Using the Red and NIR Bands of MERIS—The Azov Sea Case Study. *IEEE Geoscience and Remote Sensing Letters*, *6*(4), 845–849. https://doi.org/10.1109/LGRS.2009.2026657

NASA. (n.d.-a). *Landsat 8 Bands*. Retrieved May 11, 2021, from https://landsat.gsfc.nasa.gov/landsat-8/landsat-8-bands

NASA. (n.d.-b). *What is Remote Sensing? | Earthdata*. EarthData. Retrieved January 12, 2021, from https://earthdata.nasa.gov/learn/backgrounders/remote-sensing/

Navalgund, R. R., Jayaraman, V., & Roy, P. S. (2007). Remote sensing applications: An overview. *CURRENT SCIENCE*, *93*(12), 20.

Nojavan A., F., Kreakie, B. J., Hollister, J. W., & Qian, S. S. (2019). Rethinking the lake trophic state index. *PeerJ*, *7*, e7936. https://doi.org/10.7717/peerj.7936

Oki, K., & Yasuoka, Y. (2002). Estimation of chlorophyll concentration in lakes and inland seas with a field spectroradiometer above the water surface. *Applied Optics*, *41*(30), 6463–6469. https://doi.org/10.1364/ao.41.006463

Othman, I., & Al-Masri, M. S. (2007). Impact of phosphate industry on the environment: A case study. *Applied Radiation and Isotopes*, *65*(1), 131–141. https://doi.org/10.1016/j.apradiso.2006.06.014

Ouma, Y. O., Noor, K., & Herbert, K. (2020). Modelling Reservoir Chlorophyll- *a* , TSS, and Turbidity Using Sentinel-2A MSI and Landsat-8 OLI Satellite Sensors with Empirical Multivariate Regression. *Journal of Sensors*, *2020*, 1–21. https://doi.org/10.1155/2020/8858408

Peppa, M., Vasilakos, C., & Kavroudakis, D. (2020). Eutrophication Monitoring for Lake Pamvotis, Greece, Using Sentinel-2 Data. *ISPRS International Journal of Geo-Information*, *9*(3), 143. https://doi.org/10.3390/ijgi9030143

Qaddour, J. (n.d.). *Homs, a Divided Incarnation of Syria's Unresolved Conflict - Contentious Politics in the Syrian Conflict: Opposition, Representation, and Resistance*. Carnegie Middle East Center. Retrieved April 15, 2021, from https://carnegie-mec.org/2020/05/15/homs-divided-incarnation-of-syria-s-unresolved-conflict-pub-81804

SEOS. (n.d.). *Harmful Algal Blooms*. Retrieved May 5, 2021, from https://seos-project.eu/marinepollution/marinepollution-c03-p05.html

Sharma, A. (2021, January 1). *Getting Started with SNAP Toolbox in Python*. Medium. https://towardsdatascience.com/getting-started-with-snap-toolbox-in-python-89e33594fa04

Smith, V. H., & Schindler, D. W. (2009). Eutrophication science: Where do we go from here? *Trends in Ecology & Evolution*, *24*(4), 201–207. https://doi.org/10.1016/j.tree.2008.11.009

Sòria-Perpinyà, X., Vicente, E., Urrego, P., Pereira-Sandoval, M., Tenjo, C., Ruíz-Verdú, A., Delegido, J., Soria, J. M., Peña, R., & Moreno, J. (2021). Validation of Water Quality Monitoring Algorithms for Sentinel-2 and Sentinel-3 in Mediterranean Inland Waters with In Situ Reflectance Data. *Water*, *13*(5), 686. https://doi.org/10.3390/w13050686

The Syria Institute. (n.d.). *No Return to Homs*. The Syria Institute.

UN-ESCWA and BGR. (2013). *Inventory of Shared Water Resources in Western Asia*. United Nations Economic and Social Commision; Bundesanstalt für Geowissenschaften und Rohstoffe. https://waterinventory.org/surface_water/orontes-river-basin

USGS. (n.d.). *Landsat 5*. USGS. Retrieved May 5, 2021, from https://www.usgs.gov/core-science-systems/nli/landsat/landsat-5?qt-science_support_page_related_con=0#qt-science_support_page_related_con

USGS. (2013). Landsat 8. In *Landsat 8* (USGS Numbered Series No. 2013–3060; Fact Sheet, Vols. 2013–3060). U.S. Geological Survey. https://doi.org/10.3133/fs20133060

Walker, K. (2021, March 2). *Environmental Ruin Could Make Postwar Syria Unlivable*. World Politics Review. https://www.worldpoliticsreview.com/articles/29462/an-overlooked-casualty-of-the-syria-civil-war-its-environment

Watanabe, F., Alcantara, E., Rodrigues, T., Imai, N., Barbosa, C., & Rotta, L. (2015). Estimation of Chlorophyll-a Concentration and the Trophic State of the Barra Bonita Hydroelectric Reservoir Using OLI/Landsat-8 Images. *International Journal of Environmental Research and Public Health*, *12*, 10391–10417. https://doi.org/10.3390/ijerph120910391

Yacobi, Y. Z., Moses, W. J., Kaganovsky, S., Sulimani, B., Leavitt, B. C., & Gitelson, A. A. (2011). NIR-red reflectance-based algorithms for chlorophyll-a estimation in mesotrophic inland and coastal waters: Lake Kinneret case study. *Water Research*, *45*(7), 2428–2436. https://doi.org/10.1016/j.watres.2011.02.002

Zimba, P. V., & Gitelson, A. (2006). Remote estimation of chlorophyll concentration in hyper-eutrophic aquatic systems: Model tuning and accuracy optimization. *Aquaculture*, *256*(1–4), 272–286. https://doi.org/10.1016/j.aquaculture.2006.02.038

Zwijnenburg, W. (2019, December 3). *In Syria, the Environmental Toll of War Beginning to Emerge | Planetary Security Initiative*. Fanack.Com. https://www.planetarysecurityinitiative.org/news/syria-environmental-toll-war-beginning-emerge